DEPARTMENT OF VETERINARY MEDICINE

PhD in Animal Health and Zoonosis

XXXVII cycle

Scientific Disciplinary Sector: MVET-02/B

Non-thermal processing technologies and viral viability assays: Key approaches for studying human norovirus (HuNoV) in foods

PhD student

Annamaria PANDISCIA

Coordinator:

Prof. **Maria TEMPESTA**

Tutor:

Prof. **Valentina TERIO**

Co-tutor:

Prof. **Angela DIPINTO**

Final exam 2024/2025

INDEX

Non-thermal processing technologies and viral viability assays: Key approaches for studying human norovirus (HuNoV) in foods

Abstract

Human noroviruses (HuNoVs) are the leading cause of foodborne and waterborne viral gastroenteritis globally. To mitigate the risks posed by this enteric virus, it is essential to identify effective non-thermal technologies for inactivating HuNoV, alongside reliable methods to assess viral infectivity. This dual approach, combining viral inactivation technologies with infectivity assays, will help the food industry and regulatory authorities in ensuring public health. The aim of this PhD thesis is to evaluate the efficacy of two non-thermal technologies, High Pressure Processing (HPP) and Plasma-Activated Seawater (PASW), for inactivating HuNoV and its surrogates in high-risk food items such as berries and shellfish. The study employs RT-qPCR and viability RT-qPCR assays, in addition to traditional and advanced cell culture techniques such as the novel Human Intestinal Enteroid (HIE) system, to assess HuNoV viral inactivation and infectivity.

Riassunto

I Norovirus umani (HuNoV) sono la principale causa di gastroenterite virale di origine alimentare a livello globale. Per mitigare i rischi posti da questo virus enterico, è essenziale identificare tecnologie non termiche capaci di inattivarlo, insieme a metodi affidabili per valutare la sua infettività. Questo approccio combinato, che unisce le tecnologie di inattivazione virale con saggi di infettività, aiuterà l'industria alimentare e le autorità regolatorie a garantire la salute pubblica. L'obiettivo di questa tesi di dottorato è valutare l'efficacia di due tecnologie non termiche ossia Alte pressioni (HPP) e Acqua di mare attivata al plasma (PASW) nell'inattivare HuNoV e i suoi

surrogati in alimenti ad alto rischio, come fragole e molluschi bivalvi. Lo studio si basa su saggi di RT-qPCR e RT-qPCR di vitalità, insieme a tecniche di coltura cellulare tradizionali e avanzate, tra cui il nuovo sistema di enteroidi intestinali umani, HIE, per valutare l'inattivazione virale e l'infettività dell'HuNoV.

1. INTRODUCTION

Foodborne viruses are increasingly recognized as one of the most common causes of human acute gastroenteritis (AGE) outbreaks worldwide [1,2].

Most of the water or foodborne viral outbreaks are caused by human norovirus (HuNoV), hepatitis A (HAV) and E (HEV) viruses, rotavirus (RV), astrovirus (HAstV), adenovirus (HAdV), and sapovirus (SaV) [3,4]. After the successful implementation of RV and HAV vaccines, HuNoVs have become the leading cause of viral gastroenteritis in the US and other high-income countries [5,6]. The European Rapid Alert System for Food and Feed (RASFF) portal recorded 188 notifications of food matrices contaminated by foodborne viruses over the last decade. Among these, HuNoV was linked to more than 150 alerts, while hepatitis A was reported in 12 alerts, and no other foodborne viruses were notified [7]. These viruses spread through the fecal-oral route and are, therefore, referred to as "enteric viruses" throughout this PhD thesis. The transmission of enteric viruses to humans depends on several factors, including virus stability, food processing methods (where food matrices may protect viral particles), and host susceptibility [6]. Additionally, the infectious dose of foodborne viruses is typically low, meaning even a small amount can cause foodborne illnesses [8].

Viral contamination can occur during both pre-harvest and post-harvest activities. Oysters, mussels, clams, lettuce, green onions, other leafy vegetables, raspberries, and strawberries may become contaminated during pre-harvest stages due to environmental factors such as fecal pollution in seawater and irrigation water, improper use of organic waste as fertilizer on agricultural land, or direct contamination by livestock, wild animals, and birds [9,10]. Conversely, most post-harvest

contaminations are caused using improper food handling practices of ready-to-eat (RTE) foods such as sandwiches, cold cuts and pastries [11].

Unlike bacteria, viruses cannot replicate in food but can remain viable during food processing and storage, maintaining their infectivity [8].

Today, ensuring the microbiological safety and quality of high-risk foods is a critical concern in the food industry. Consumers increasingly demand minimally processed and ready-to-eat products, which are at risk of contamination by foodborne viruses and can lead to outbreaks.

Viral contamination of food can be prevented implementing specific controls for raw materials and food production, adopting robust food safety management systems such as Good Agricultural Practices (GAP) and Good Manufacturing Practices (GMP) throughout the supply chain, providing food-handling education, ensuring effective sanitation measures, promoting proper hand hygiene, and developing appropriate strategies for managing ill workers [3]. Moreover, food preservation technologies are essential for safeguarding the microbiological safety of high-risk foods.

Especially, thermal processing methods can prevent microbial hazards related to their consumption but, unfortunately, they can adversely affect both the nutrient contents and sensory characteristics of food matrices [12]. On the other hand, non-thermal technologies, including high-pressure processing (HPP) treatments, cold plasma (CAP) and Plasma-activated water (PAW), represent a promising and sustainable tool to develop a robust viral control strategy. To face this challenge, it's essential to integrate effective non-thermal inactivation methods with reliable and accurate infectivity assays.

The current gold standard for detecting and quantifying enteric viruses in food matrices is reverse transcription quantitative real time PCR (RT-qPCR) [13,14]. However,

while this technique is highly sensitive, it cannot distinguish between infectious and inactivated viral particles, limiting its ability to conduct proper risk assessments, an essential aspect of developing effective control strategies in the food industry [9]. Therefore, in addition to identifying the most effective non-thermal technologies for inactivating enteric viruses, it is also crucial to determine the best methods for assessing viral infectivity post-treatment.

Viability RT-qPCR which involves pre-treating samples with viability markers like propidium monoazide (PMA), has been proposed to address the RT-qPCR limitations [15,16]. Moreover, based on the lack of cell culture system for HuNoV, murine norovirus (MNV), feline calicivirus (FCV), and Tulane virus (TV) have been employed as cultivable viral surrogate for studying HuNoV survival and stability. Recently, a 3D cell culture model using human intestinal enteroids (HIEs) has been developed as a more effective in vitro system for cultivating HuNoV [17].

2. OBJECTIVE OF THE PhD THESIS

The dual approach combining advanced viral inactivation technologies with infectivity assays will help the food industry and regulatory authorities to mitigate the risks of enteric viral contamination and ensure public health protection. Therefore, the aim of this PhD thesis is to evaluate the efficacy of two non-thermal technologies such as HPP and Plasma-activated seawater (PASW), for inactivating HuNoV and its surrogates in high-risk food items such as berries and shellfish. Moreover, both traditional and advanced cell culture techniques, along with molecular approaches, will be evaluated in these high-risk foods to identify the most effective viability assays for predicting HuNoV infectivity. Firstly, the feature of HuNoVs, current non-thermal treatments, HPP and PAW technologies will be described in brief. Subsequently, this

PhD thesis will include four original research articles focusing on viral viability assays, HIEs system and the antiviral efficacy of HPP and PASW. These scientific studies will represent a significant advancement in identifying the most effective non-thermal technologies and viability assays for controlling the microbiological hazards posed by HuNoV, providing valuable data to address the challenges faced by the food industry.

3. NOROVIRUS

3.1 Structure and genotypes of Noroviruses

Noroviruses (NoVs) belong to the *Caliciviridae* family and are classified under the *Norovirus* genus [18]. NoVs particles are 27–30 nm in diameter, no-enveloped, small round structured, with a linear, positive-sense, single-stranded RNA genome of about 7.5 kb in length. NoV was originally referred to as Norwalk or Norwalk-like virus since the first NoV outbreak was reported at an elementary school in Norwalk, Ohio in 1968 [19]. Subsequently, in 1972, the first clinical samples were isolated from an infectious stool filtrate [20]. NoVs can infect a wide range of mammalian host species that include humans, dogs, cats, pigs, mice, sheep and cattle and several new unclassified NoVs have recently been detected in bats, sea lions and harbor porpoise and in non-human primates [21–30].

The NoV genome is organized into three open reading frames (ORFs) with the exception of murine noroviruses (MNVs) containing a fourth ORF [30,31] (Figure 1). ORF1 encodes a polyprotein that is cleaved, after the viral genome RNA translation, into six nonstructural mature proteins (NS) including NS7, the viral RNA-dependent RNA polymerase (RdRp) [32].

ORF2 encodes the major capsid protein (VP1) which consists of 90 dimers that constitute a shell domain (S) and a protruding (P) domain divided into P1 and P2

subdomains. The P2 subdomain is highly variable, contains potential neutralizing antibody epitopes and interacts with the putative HuNoV cellular receptors called histoblood group antigens (HBGA) represented by a complex terminal carbohydrates that can be both cell-associated (e.g., red blood cells and mucosal epithelium) and non-cell-associated which serve as binding ligands for virus facilitating the HuNoV entry [33,34].

However, there are some HuNoV strains which don't bind any HBGA ligand, suggesting potential additional cofactors [35].

Despite the lack of a complete understanding of HuNoV entry in the host cells[36], it is supposed that NoV enters by endocytosis and, after the viral uncoating, the viral genome is released into the host cytoplasm and viral genome is replicated. New proteins are produced, and the assembled virions are released upon cell lysis[37].

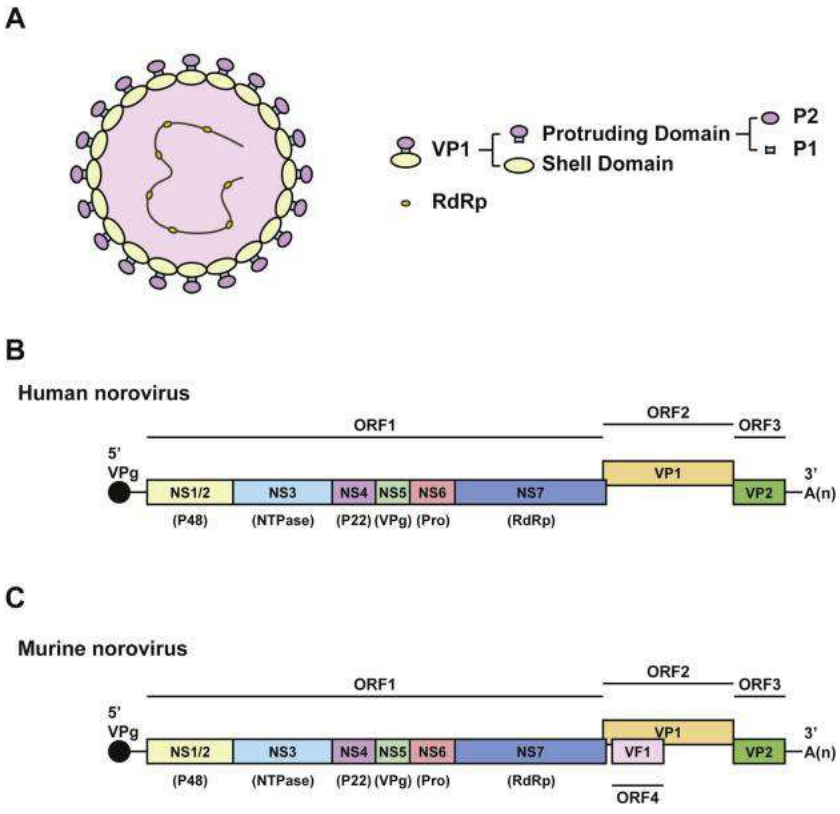

Figure 1: *Schematic of the structure of HuNoVs [38]*

NoV evolution is driven by recombination as well as point mutations. Especially, recombination at the ORF1/ORF2 junction is increasingly recognized as an important mechanism of NoV evolution since novel combinations of capsid and polymerase genotypes can be exchanged impacting NoV pathogenesis, fitness, and immune evasion [39]. Additionally, the same capsid may be associated with different polymerase genotypes, potentially providing an advantage by altering the efficiency of viral replication[40].

Therefore, based on the differences of the VP1 amino acid sequences, NoVs are currently classified into ten genogroups (G), subdivided into 49 different genotypes. Moreover, based on nucleotide diversity of the RdRp region, NoVs can be subdivided also into 60 P (polymerase)-types. Hence, dual typing of noroviruses has become more common, with the genotype listed first, followed by the P-type in brackets (e.g., GII.4 [P16])[41].

GI, GII, GIV, GVIII and GIX genogroups have been described in humans [30,42]. Despite the high genetic diversity of NoVs, HuNoV Genogroup II, genotype 4 (GII.4) has been recognized as the most prevalent in humans worldwide and new variants have been detected rapidly due to its high genetic variability caused by antigenic drift in VP1 and genetic recombination between circulating norovirus strains [43,44]. GII.4 genotypes are categorized into distinct epidemiologically significant variants, each named with the place where the first strain with a complete capsid sequence was submitted to GenBank (e.g., GII.4 Sydney) [45]. GII.4 genotypes are primarily related to person-to-person transmission and AGE outbreaks in closed environments such as schools, nursing homes, and summer camps [46]. On the other hand, non-GII.4 genotypes, such as GI.3, GI.6, GI.7, GII.3, GII.6, and GII.12, are more commonly spread through foodborne and waterborne route [40,47].

3.2 Public health implication of HuNoV

HuNoVs are responsible for an overall estimated 684 million cases of AGE, worldwide, leading to societal costs of around $60 billion [48,49]. In the United States, an estimated 21 million HuNoV gastroenteritis cases, more than 109,000 hospitalizations and 900 deaths are reported every year [50]. In Europe, HuNoV is reported as the third most frequently causative agent of foodborne outbreaks in 2022 after *Salmonella* spp and bacterial toxins and it involved the highest number of human cases (n= 7305) [2]. Diarrhea, vomiting, nausea, stomach pain, low-grade fever, headache and body aches are the symptoms mostly described in patients with HuNoV disease although HuNoV infections are generally short and self-limited [51].

HuNoV infection can affect individuals of all ages, but young children and the elderly are particularly at higher risk for developing severe illness. When people have been exposed to HuNoV, they start to develop symptoms within 12 to 48 hours and healthy individuals infected by HuNoV often get better in 1-3 days [52,53].

HuNoV is highly infectious, and it has been estimated that a range of 10 up to 100 HuNoV viral particles are sufficient to develop an infection [54].

Symptomatic individuals shed high amounts of virus in the feces, mainly during the first 24 to 48 hours after the onset of symptoms, with a peak of viral shedding ranging from 0.5–1.640 $\times 10^9$ gc/g of feces but HuNoV viral particles can lasts until four weeks in stool [55]. Furthermore, HuNoV viral particles has been detected also in the vomit of infected individuals [55]. It has been demonstrated that asymptomatic individuals can shed viral particles as well as symptomatic patients although the risk of HuNoV transmission from asymptomatic people is less frequent [56]. Additionally, immunity to HuNoV can persist between 2 and 6 months after the infection and, consequently,

it is considered that a range of three to eight episodes of HuNoV illness can occur during lifetime, with at least one coming up before the age of 5 [57].

3.3 HuNoV transmission

HuNoV is highly transmissible and can be mainly transmitted through the fecal–oral route, which can occur firstly via direct person-to-person contact and aerosolized particles and secondly, after the consumption of contaminated food or water [3,58]. Atmar et al. demonstrated that the 50% of HuNoV human infectious dose ranges between 1320 and 2800 genome equivalents (g/eq) [59]. HuNoV infectious viral particles can be released by diarrheal and/or vomiting episodes representing the main route of HuNoV transmission in closed environments such as nursing homes, long-term care and healthcare facilities, concerts, events, and cruise-ships [60].

Moreover, HuNoV viral particles can contaminate environmental waters through direct discharge, the release of inadequately treated sewage from wastewater treatment plants or discharges from vessels and urban runoff [60].

HuNoV can survive in several environmental conditions from freezing until heating at 60 °C, on food and surfaces [61]. They can persist on berries, vegetables, and fruit but also on carpets, formica, stainless steel, polyvinyl chloride, and ceramic surfaces[62]. Moreover, it shows a high resistance against common sanitizers and disinfectants such as chlorine bleach, quaternary ammonium compounds, ethyl alcohol [63]. It has been demonstrated that about 10 ppm of chlorine can inactivate HuNoV but these high levels are not permitted in drinking water systems [54].

Contamination of food items can occur at any point of food processing, from farm to fork. Infected food handlers, food service workers, sewage treatment workers can

increase the risk to develop HuNoV outbreaks typically transfer the virus to food products[51].

HuNoV infections after consumption of bivalve shellfish, leafy vegetables and fresh produce such as soft berries are commonly reported [9,58]. Berries have been involved in several HuNoV outbreaks worldwide and they were considered to have a higher risk to be contaminated with HuNoV than other food items [64]. It has been suggested that the high prevalence of HuNoV in berries is linked to their surface characteristics, which provide more attachment points for HuNoV. Blackberries, raspberries, and strawberries, being aggregate fruits, have irregular, bumpy surfaces[65].

Between 1983 and 2018, HuNoV contamination in berries was linked to 46 foodborne outbreaks, resulting in over 15,000 reported cases globally [66]. In Europe, especially in Italy, most HuNoV outbreaks have been associated with the consumption of raw or undercooked bivalve mollusks in the last years [2,67]. In Italy, a 6 year-survey (from January 2014 to December 2019) on HAV and HuNoV in berries, drinking water, processed foods and leafy greens conducted by Pavoni et al. evidenced that HuNoV is the most common viral pathogen involved in shellfish-borne viral outbreaks together with HAV whereas the other food categories showed a lower HuNoV rate of contamination [68].

3.4 HuNoV viral surrogates

Based on the lack of reproducible cell culture systems to cultivate HuNoVs in vitro, RT-qPCR remains the gold standard method for NoV detection. However, as described above, RT-qPCR cannot provide information between infectious and non-infectious virus particles. Significative efforts have been made to develop a cell culture model for assessing HuNoV infectivity but, this goal has not yet been obtained.

In the last decade cultivable surrogates such as Feline Calicivirus (FCV) F9 strain (FCV-F9), Murine Norovirus-1 (MNV-1), Tulane Virus (TV), and Coliphage MS2 and PhiX174, were employed as an useful tool to study HuNoV survival and inactivation although they still represent an indirect HuNoV estimation and can provide biased data [69–71].

MNV-1 belongs to genogroup GV of NoV with a genetic and structural similarity with the HuNoV GII strains and it was the first norovirus successfully propagated in cell culture [72].

MNV causes more serious symptoms than HuNoV such as hepatitis, pneumonia, and nervous system inflammation in mice. Nevertheless, as HuNoV, it is an enteric virus, transmitted via the fecal-oral route, replicating in the intestine, and shows a similar resilience to low pH levels, better than FCV that has been demonstrated to be less resilient [73]. MNV-1 grows and replicate in the murine macrophage cell line RAW 264.7 that has been employed to carry out HuNoV plaque assay and represent the first HuNoV cell culture system [74].

Another HuNoV potential animal surrogate model is the Tulane virus (TV), a rhesus monkey calicivirus belonging to *Recovirus* genus within *Caliciviridae* family [75]. TV can replicate in vitro in rhesus monkey kidney (LLC-MK2) cells causing cytopathic effects as well as MNV-1[76]. Moreover, in contrast with MNV-1 and FCV-F9, TV can recognize HBGA receptors [77].

FCV-F9 belongs to *Caliciviridae* family and shares similarities with HuNoV although causes respiratory illness in cats [69].

Coliphages are viruses that infect *E. coli* and are commonly found in human fecal waste. F-specific (e.g., MS2) and somatic (e.g., φ174) bacteriophages have been commonly used as viral surrogates for viral inactivation and as indicators of fecal

contamination in Europe and the USA because their structure and persistence in the environment resemble those of human enteric viruses, and they show a similar response to treatment processes [78,79]. Somatic coliphages are DNA viruses that infect *E. coli* via its outer membrane, while F-specific DNA or RNA coliphages infect *E. coli* through a F pilus (a specific appendage used for bacterial conjugation)[80,81]. They can be measured using a simple and cost-effective method such as the plaque-forming unit (PFU) assay [80].

It is only in recent years that significant progress has been made in culturing human noroviruses in vitro, thanks to the development of a stem cell-derived human intestinal enteroid (HIE) culture system that has been shown to support replication of several HuNoV strains, including GII.4 and GII.3 [82]. However, further improvements are needed to enhance its reproducibility and infection efficiency.

4. CURRENT NON-THERMAL TREATMENTS AND WATER-ASSISTED SYSTEMS FOR FOODBORNE VIRUSES INACTIVATION

4.1 Common non-thermal treatments against foodborne viruses

The risk of microbial contamination has been addressed by the employment of several non-thermal technologies such as irradiation, ultraviolet (UV) light and ultrasound treatments that have been shown to be more effective against bacterial than foodborne viral pathogens [83]. For all these non-thermal treatments, damages of viral capsid and nucleic acid are the main mechanism of viral inactivation [84,85].

Enteric viruses have been described as highly resistant to irradiation (gamma, e-beam, X-rays). Despite the U.S. FDA approved the use of gamma irradiation up to 4.0 kiloGray (kGy) to control foodborne pathogens in fresh iceberg lettuce and spinach, this dose range has been demonstrated to not effectively inactivate MNV-1 with only a 1.7 to 2.4 $\log_{10}$ PFU/ml virus reduction in fresh produce at the dose of 5.6 kGy [86] and a maximum reduction of 2.21 $\log_{10}$ PFU/mL at 12 kGy on strawberries [87].

TV seems to be more sensitive to e-beam irradiation than MNV-1 with a reduction of 1.4 $\log_{10}$ PFU/mL at 3.9 kGy on strawberries [88]. Therefore, as suggested by Praveen et al., e-beam irradiation can represent a useful treatment together with other non-thermal technology to ensure the virological inactivation on food [83,89].

As well as irradiation, the solely employment of High-Intensity ultrasound (HIUS) is not suitable to inactivate foodborne viruses [90]. Su et al. demonstrated that HIUS treatment of 20 kHz reduced of 1.55 log MNV-1 inoculated in orange juice after 30-min exposure to ultrasound treatment [90].

Furthermore, the employment of ultraviolet (UV) light represents a successful technology to inactivate foodborne viruses on food matrices, food surfaces and water. Recent studies have demonstrated the UV efficacy against MNV-1, HAV, FCV and MS2 bacteriophage from different food matrices such as chocolate, pistachos, cornflakes, fresh chicken breast, skim milk and coconut water [91–95]. However, one limitation of UV treatment on liquid foods is represented by the loss of it efficacy with turbidity and suspended solids absorbing or scattering the light before reaching the viral particles [84].

4.2 Water-assisted systems for foodborne viruses inactivation

The risk of microbial contamination has been also addressed by the employment of water-assisted non-thermal technologies based on chemical and physical sanitizing treatments in the food industry harnessing water to deliver antimicrobial effects while maintaining the food's nutritional and sensory qualities. These systems have been developed to prevent cross-contamination and reduce the microbial load in food matrices contaminated with bacterial pathogens such us *Listeria monocytogenes, Escherichia coli,* and *Salmonella* spp. in the food industry [96]. Moreover, they also showed a microbicidal activity against foodborne viral pathogens or their surrogates[97–99].

Chlorine-based sanitizers are inexpensive disinfectants with a broad microbicidal spectrum and demonstrated antiviral activities [99]. After destroying the viral capsid, free chlorine can enter the virus particles and inhibit virus replication damaging the viral RNA. [100]. However, corrosive and potential surface staining or irritant properties occur at high chlorine concentrations. Chlorine can react with organic

substances to form trihalomethanes, which are potential carcinogens and may pose health risks to humans [101].

Moreover, toxic residues can remain in the wastewater and cause waste disposal problems [102].

On the other hand, peroxyacids, sanitizers formed through the equilibrium reaction between a short chain organic acid and hydrogen peroxide, do not release toxic compounds into the environment [103,104]. Vimont et al. carried out a scientific study about the virucidal effect of peroxyacids against MNV-1, a HuNoV surrogate, demonstrating that they can be employed for safe inactivation of HuNoV in water or on food surfaces [97].

Electrolyzed water technology has garnered significant attention due to its ability to produce strong oxidative disinfectants with cost-effectiveness and minimal environmental impact. This technology is based on electrolysis of a dilute salt solution, such as sodium chloride, that is electrolyzed in water with the production of pH-dependent aqueous chlorine oxidants, including chlorine gas, hypochlorous acid, and hypochlorite ions. Electrolyzed water has been assessed for various food safety applications in the food industry, such as to wash surfaces in food preparation areas and directly on food surfaces of fresh produce. Together with the already reported antibacterial efficacy, electrolyzed water demonstrated also antiviral activities [105]. Moorman et al. reported that electrolyzed water inactivates HuNoV GII.4 Sydney and cultivable HuNoV surrogates, for example, and murine norovirus in suspension and on stainless steel surfaces by destruction of viral capsid [98]. Few downsides can affect the efficacy of this technology such as the initial expensive costs of the equipment installation and treatment-times that could affect the its overall efficacy and adoption in food industry [106].

Another alternative to chlorine sanitizers is the ozone that doesn't develop any hazardous waste during its use and with a stronger antimicrobial activity [107]. The antiviral activity of ozone depends on its concentration and the typology of food matrices [108].

All these virucidal technologies can be employed alone or in combination. However, they show some issues such as residual chemical traces affecting environmental and human health but also food quality, variable viral inactivation efficacy and elevated costs. Therefore, novel sustainable water-assisted technologies with strong antimicrobial activity are surging in order to ensure food safety of minimally processed foods.

5. HIGH-PRESSURE PROCESSING (HPP)

5.1 Core concepts of HPP

High pressure treatments, often referred to as High Pressure Processing (HPP), represent an innovative, sustainable and promising non-thermal food preservation technology with an effective microbicidal activity [109]. The HPP method applies uniform instantaneous hydrostatic pressure, commonly ranging from 300 up to 600 MPa (megapascals) at refrigeration or mild process temperatures (< 45°C) to solid foods, packaged or unpackaged, placed in a pressure vessel (Figure 2) [110,111].

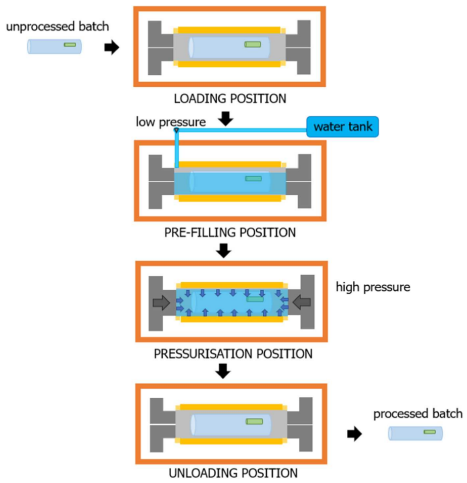

Figure 2: Rapresentation of a traditional HPP system[111]

HPP can be generated using an external pump, a moving piston, or by heating the pressure-transmitting fluid within a sealed chamber. In batch systems, water is a low-compressibility medium to transmit pressure. There are three different stages occurring during the HPP treatments with different time intervals (Figure 3):

a) Pressure build up or CUT (Come up Time): the pressure is gradually increased by pumping the liquid medium into the pressure chamber using pumps and pressure intensifiers.

b) Holding Time: once the desired pressure is reached, the product is maintained at the target pressure for the chosen period.

c) Pressure Release or CDT (Come-down Time): this is the final stage where the pressure rapidly decreases because the chamber is depressurized.

CUT and CDT times are determined by the capabilities of the equipment used.

Each stage plays a crucial role in the overall process and determines the effectiveness of pressure application [111].

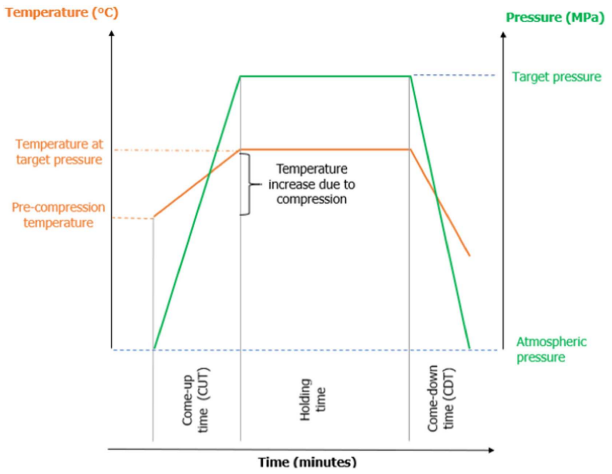

Figure 3: Representation of temperature and pressure profile of a food during a HPP treatment[111]

The target pressure, holding time, and initial fluid temperature in HPP are process parameters depending on the food matrix and the desired microbial inactivation outcomes. To achieve the desired processing temperature, the system can be either chilled or heated using supplementary equipment or by maintaining the pressure-transmitting fluid at a specific temperature.

In the food industry, HPP pressures typically reach up to 600 MPa although 1400 MPa can be employed through laboratory equipment integrating cooling or heating system [111].

During the HPP process, the temperature of the food can increase slightly due to the compression of fluids, but it typically remains below 40°C in most applications. The high pressures employed in HPP treatments are responsible of the microbial inactivation caused by the mechanical disruption of cellular structures [112]. Under pressure, the volume of foods typically decreases, while it increases during decompression. In packaged foods subjected to HPP, the risk of post-process contamination is minimized because foods remain in their final packaging throughout the process [113]. The first high-pressure-processed products were sold in Japan in 1990 and included jams, fruit jellies, sauces, and fruit juices. Over the past two

decades, a major and increasingly successful industrial application of HPP has been the non-thermal pasteurization of food to extend the shelf life of foods [114].

To date, several pressure-processed foods are commercialized in many countries such as fresh bivalve mollusks, ready-to-eat meat products, vegetable products, juices, beverages, salsa, jams, and drinkable yogurt [115,116]. HPP treatments can induce some expected or unexpected chemical reactions affecting directly or indirectly food quality and safety. Further scientific research is needed to better improve the knowledge about the mechanisms and kinetics of food stability when they are subjected to extreme pressure and temperature conditions. This goal will be crucial for comparing HPP treatment with traditional methods such as pasteurization and sterilization at atmospheric pressure, as well as for developing or improving food regulations.

Safety criteria for HPP-treated foods and their labeling have been established in many countries around the world.

In Europe, there aren't specific regulations about HPP. However, standalone facilities performing HPP on food products of animal origin must be approved based on the EU REG 852/2004 [111,117] and foods treated with HPP must be properly labeled and comply with the requirements outlined in Regulation (EC) No. 2017/2470 and Regulation (EU) 2015/2283 for the marketing of novel foods[118,119].

5.2 The Impact of HPP on food quality

HPP treatments can affect the physical and chemical proprieties of food with advantages and disadvantages.

Despite structural changes can occur in larger macromolecules, such as carbohydrates and proteins during HPP treatment, this process does not break covalent bonds, and

smaller molecules like vitamins and aroma compounds remain unaffected [110]. This HPP characteristic has been suggested to be responsible of the preservation of biological activity of functional compounds, such as ascorbic acid, folates, antioxidants, anthocyanins, lycopene and conjugated linoleic acid [115]. Moreover, based on the capacity of HPP to modify the protein structures, it can alter the functionality of enzymes in foods commonly involved in ripening or spoilage processes or it can destroy allergenic proteins [120].

HPP can modify the chemical bonds of carbohydrates causing starch swelling and potentially gelatinization, a process similar to thermal gelation, where starch granules absorb water, swell, and form a gel-like consistency potentially altering the texture of food, especially in starchy products [121].

HPP can cause lipid crystallization, which may alter the physical state of fats or oils in the food accelerating oxidation, particularly in foods with a high lipid content (e.g., nuts, seeds, or oily foods) thus producing off-flavors or spoilage. For example, the application of HPP to meat and meat products results in a modification of quality parameters such as color, texture and water holding capacity [122].

HPP has been proposed not only as a food preservation method but also as a technology to enhance the bioactive compound content in foods and improve their extraction. It promotes their release from the intracellular compartments incrementing their bio accessibility [123].

Studies have shown that pressurized foods often contain higher levels of functional compounds, such as phenolics, compared to untreated products[124]. For example, the antioxidant activity of HPP-treated blackberry and strawberry puree was higher than those of the thermally processed one [125].

5.3 Antimicrobial activity of HPP

The antimicrobial efficacy of HPP has been investigated for several years and it was highly demonstrated that bacterial pathogens are inactivated at room temperatures with HPP in the range of 200 up to 600 MPa[116]. HPP treatments have been shown to reduce vegetative bacterial cells of *Salmonella enteritidis* from sliced vacuum-packaged dry-cured ham[126], *Enterobacteriaceae* from chicken nuggets [127], *L. monocytogenes* and *E. coli* spp. from smoked rainbow trout fillets and fresh European catfish fillets [128], yeast and mold from mango pulp[129] and *E. coli* O157: H7 and *Staphylococcus aureus* from carrot juice [130], all with at least 3 $\log_{10}$ of reduction[131]. However, bacterial endospores exhibit significantly higher resistance to HPP compared to vegetative cells. Spores of *Clostridium* spp. and *Bacillus* spp., can withstand pressure treatments exceeding 1000 MPa at room temperature [116].

HPP can also disrupt bacterial membrane integrity by inducing phase changes in lipid bilayers, but this effect is not relevant for enteric viruses since they are non-enveloped without lipid bilayers [132].

Despite being few scientific studies that assess the virucidal efficacy of HPP, in the most cases it has been shown that enteric viruses can be inactivated with lower HPP pressures than spores or vegetative cells. For example, Aganovic et al. reported that 400 MPa for 5 minutes at 4 °C proved to be effective for reducing viruses of at least 4 $\log_{10}$ [116].

The inactivation of enteric viruses in foods through HPP technology is influenced by several parameters related to HPP treatments (e.g. pressure, temperature,and duration of pressure treatment*)* or to virus type, composition of food matrix, water activity (aw), salt concentration and pH of foods [110]. The increment of pressure levels intensifies the virus inactivation although a "tailing effect", referred to as a decrement

of the microbial inactivation rate when the time of treatment is extended, has been reported [133,134]. This phenomenon is generally caused by microbial resistance, protective factors, or physical limitations of the pressure treatment process [114]. Regarding HPP temperature, enteric viruses have been shown different inactivation results [134].

MNV-1 inactivation has been described as inversely proportional to temperature increase [135], especially, it was more efficient at 4 °C than at 20 °C in fresh iceberg lettuce and strawberries [136] while HAV was highly reduced when subjected to elevated HPP pressure and temperature (>30°C) in Dulbecco's modified Eagle medium (DMEM) with 10% fetal bovine serum (FBS) [137]. The pH value during HPP treatments influenced the virus inactivation based on the distinct virus species[110]. HuNoV is more sensitive to HPP inactivation carried out at neutral pH [138] while an easier inactivation of HAV can be obtained at low pH values [134].

Moreover, the a_w and NaCl content can affect the efficacy of HPP viral inactivation since the enteric viruses show a better stability in foods with high a_w than in the low moisture foods and NaCl can protect viral particles against HPP treatments [139,140]. Finally, the inactivation of viruses by HPP is influenced by the food matrix since lipids, protein and carbohydrates can enhance or reduce the HPP efficacy [111].

Most scientific studies focused only about a limited range of pressure, temperature, and time combinations. To overcome this drawback, several predictive models have been developed aiming to predict virus reduction across a wide range of different parameter combinations.

6. PLASMA ACTIVATED WATER (PAW)

6.1 Core concepts of non-thermal plasma

Plasma is recognized as “the fourth state of matter” in addition to solid, liquid and gas. It consists of complete or partly ionized gases with a range of charged and neutral reactive species and, during the plasma generation, radiations are emitted across the ultraviolet (UV), visible, and near-infrared regions. Based on the temperature of particles, there are two categories of plasma: equilibrium, or thermal plasma and non-equilibrium or non-thermal plasma, named also “Cold plasma” (CAP). In the thermal plasma, particles are in thermal equilibrium and reach extremely high temperatures such as thousands or millions of degrees Celsius [141].

Cold plasma is generated at room-temperature through an high-voltage electrical discharge process across a gas (e.g., air, oxygen (O_2),Argon (Ar), Helium (He)) which is ionized leading to the production of several reactive species such as reactive oxygen and nitrogen species (RONS) including nitrate (NO_3^-)and nitrite ions (NO_2^-), radical species (peroxyl ($^{\bullet}ROO$), hydroxyl radicals ($^{\bullet}OH$), superoxide anion ($O_2^{\bullet-}$) and non-radical species (ozone (O_3), OH^- ion, singlet oxygen ($^1O_2$), and hydrogen peroxide (H_2O_2) [142], all involved in the CAP microbicidal activity[143].

There are several studies confirming the CAP antimicrobial effects on foods[143] but color loss, alterations in surface topography and degradation of bioactive compounds after the CAP treatments, have been observed [144,145].

Plasma activated water (PAW) is generated when CAP is applied to water, to medium or to other aqueous solutions. The interaction between the water sample and the active particles produced by CAP leads to PAW solutions that represent alternative methods to overcome the CAP drawbacks (Figure 4) [99,146]. The electric discharge can be

triggered directly in the water or in the air above the water to be treated and the chemistry and reaction products can differ [145].

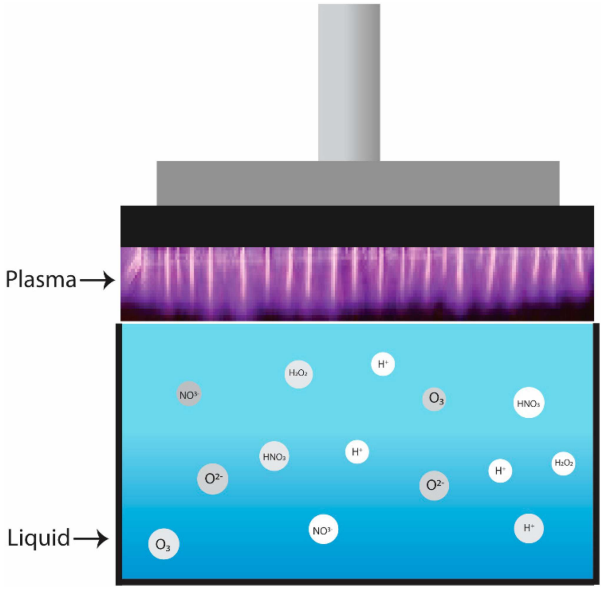

Figure 4: PAW generation [147]

Different methods are commonly employed to generate PAW such as glow discharge, spark discharge, corona discharge, arc discharge, gliding arc discharge and dielectric barrier discharge (DBD) but Plasma jet and DBD-based configurations are the most widely employed in food research since they are easier to develop and perform [148]. In DBD system, an electric field is created between two electrodes separated by a dielectric barrier, where an inert or neutral gas (air, O_2, Ar, He) is ionized to produce plasma. A dielectric material (e.g. glass or quartz) is placed between the two electrodes and represents the insulating material that allow the formation of an electric field. It creates a barrier that limits the amount of current that can pass through the discharge gap, forcing the discharge to occur in a non-thermal such as cold plasma state and avoiding arcing and sparking responsibles of plasma instability (Figure 5) [149]. DBD can be carried out through alternating or direct current across a broad range of gas pressures (typically between 10^4 and 10^6 Pa) and frequencies (ranging from 0.05 to

500 kHz)[150]. Several parameters such as operating voltage, the working gas, the distance between the electrodes and the treatment time, can affect the production of reactive species in PAW. DBD can operate at atmospheric or even higher pressure producing several chemically reactive species during the PAW treatment showing antimicrobial activity and, a large and homogeneous discharge area is produced [151]. Therefore, it is particularly effective as a plasma source for treating large surface areas [152].

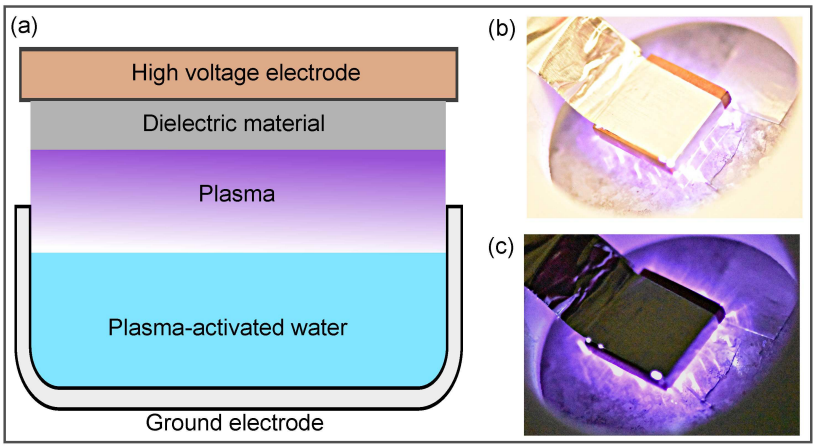

***Figure 5**: a)Typical Setup for DBD Generation in PAW.*

b,c) *Common DBD generation employing glass as dielectric material [149]*

In plasma jet systems, helium or argon (as gas carrier) flows at varying speeds across two parallel electrodes. Different plasma jet devices have been developed for the stable generation of non-thermal plasmas based on DBD configuration. Radio frequency (RF) excitation is commonly used to generate plasma jets or flames at atmospheric pressure. The excited species are expelled through a small nozzle or hole near the electrode's terminal, assisted by the carrier gas. Plasma jets are employed for direct, localized treatments, making them suitable for applications in small areas.

Nevertheless, the high costs related to the employment of gas make them unsuitable for large-scale food processing [152,153].

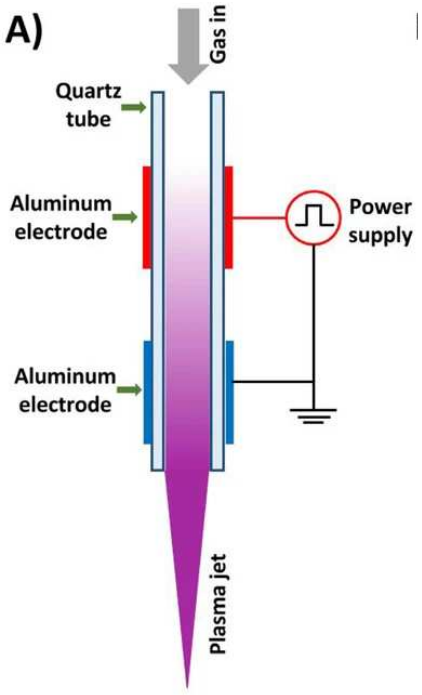

Figure 6: *Typical Setup for plasma jet system generation in PAW[154]*

During PAW generation, several phenomena occur such as a pH reduction, an increment of the oxidation-reduction potential (ORP) and of the electrical conductivity (EC) of the treated water solution [148].

Furthermore, short-lived species ($^{\bullet}OH$, $^{\bullet}NO_2$, $^{\bullet}NO$ radicals) and long-lived species (O_3, H_2O_2, NO_3^-, NO_2^-) are generated. After the treatment, the latter can also interact with each other or with water molecules, leading to the formation of new reactive species as secondary products [149].

O_3 is generated when the working gas is air or O_2 and, as well as atomic oxygen, it can dissolve in water generating $^{\bullet}OH$ [155]. Moreover, the interaction between nitric oxide (NO) and superoxide (O_2^-) generates peroxynitrite ($ONOO^-$), a highly short-lived

reactive compound with a high antiviral activity as well as peroxynitrous acid (ONOOH) produced from $ONOO^-$ under acidic conditions [156–158].

It was reported that increased plasma discharge time leads to an increment in the concentration of NO_2^-, NO_3^- and H_2O_2, a lower pH value and higher ORP [159].

The stability of reactive species generated during PAW treatments is a significant parameter to assess the effectiveness and shelf-life of PAWs. Scientific studies obtained divergent results about the stability of PAW depending on the storage temperature. Traylor et al. reported that PAW retained its antimicrobial properties for seven days when stored at room or refrigerated temperatures while Tsoukou et al. observed a PAW antimicrobial activity after 18 months when stored at −80 °C [160,161]. Guo et al. reported that PAW stored at room temperature (22°C) for up to ten days exhibited similar antiviral activity against MS2 and Φ174 bacteriophages than the freshly prepared PAW [162]. Other authors highlighted that chemistry of long-lived chemical species are stable for at least three weeks of storage [161,163].

6.2 Antimicrobial activity of PAW

The antibacterial efficacy of PAW has already been well established [145,148], but it is only in the past decade that scientific research has increasingly focused on exploring its antiviral activity [164].

Several scientific studies have demonstrated that PAW can successfully inactivate bacteriophages (Φ174, MS2) [162], FCV [165], MNV-1 [166], severe acute respiratory syndrome coronavirus-2 (SARS-CoV-2), and human coronavirus 229E [167,168].

In this context, RONS are considered as a chaotic system involved in numerous chemical reactions that plays a key role in the biological effects induced by PAW

[169]. It was suggested that they can lead to viral protein degradation or function losing via oxidation [162,166,167,170].

Wang et al. confirmed this evidence reporting that long-lived RONS species such as H_2O_2 and NO_3^- and short-lived species such as OH• represented crucial factors in inactivating MNV-1 by PAW, prepared by plasma discharge with Ar, O_2, or O_2-Ar mixture gas, potentially damaging viral proteins with consequent destruction of the viral capsid [166].

The same authors performed a morphological analysis of MNV-1 treated with PAW, at 22 °C for 1h, through a transmission electron microscopy (TEM) analysis. They observed two different morphologies of MNV-1 viral particles such as broken and structurally intact virus particles suggesting that PAW might inactivate MNV-1 by disrupting the viral structure and making the intact viral particle non-infectious.

$ONOO^-$and ONOOH have been involved in FCV inactivation by damaging viral genomic RNA during DBD plasma torch treatment[157].

Furthermore, Guo et al. demonstrated that $^1O_2$ inactivated bacteriophages Φ174, and MS2 by destroying nucleic acid and protein [162]. However, the virucidal role of UV radiation and ozone (O_3), generally generated in a small amount during plasma treatments, is considered negligible [171].

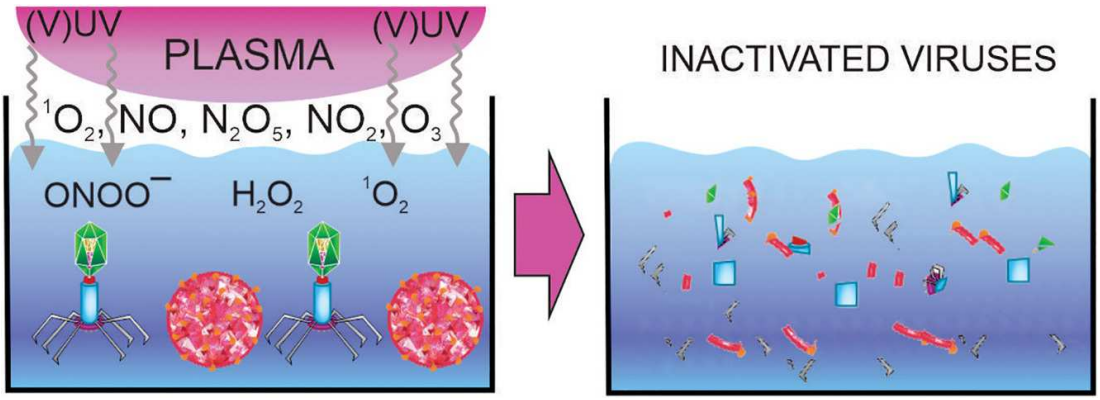

Figure 7: *Chemical species involved in viral inactivation mediated by PAW [164]*

7. CHALLENGES FOR ESTIMATING HUMAN NOROVIRUS INFECTIVITY BY VIABILITY RT-qPCR AS COMPARED TO REPLICATION IN HUMAN INTESTINAL ENTEROIDS

The food industry frequently faces various challenges related to the management of enteric virus contamination in food matrices due to several factors, some of which are linked to their detection and quantification [172].

RT-qPCR represents a robust, cost-efficient, sensitive, and specific biomolecular gold standard method that is faster than culture-based assays for the detection and quantification of foodborne viruses [173]. However, its main drawback is related to the overestimation of the number of infectious viral particles detected in food or water samples (as aforementioned) [173]. Several approaches have been developed to quantify viral infectivity of HuNoV such as 1) an enzimatic pretreatment with nucleases and/or proteolytic enzymes which allow to digest noninfectious virus particle [174]; 2) Selective recovery of potentially infectious HuNoVs from foods using porcine gastric mucin (PGM) [175]; 3) Full-length or long-range RT-PCR used to estimate genomic integrity and reduce the detection of inactivated HuNoV and fragmented HuNoV RNA [176]; 4) Pretreatment with intercalating HuNoV nucleic acid dyes ((Viability PCR Crosslinker Kit (CL), ethidium monoazide (EMA), propidium monoazide (PMAxx™), and platinum chloride ($PtCl_4$)) [177]. Markers such as CL, PMAxx^{TM} and EMA penetrate damaged or destroyed viral capsids and covalently bind to RNA after being exposed to strong visible light, thereby inhibiting DNA amplification. In contrast, intact viral particles remain unaffected by PMAxx, and their RNA can still be amplified via RT-qPCR [9]. Intercalating dyes such as PMAxx™, CL and EMA could provide false positive results. Leifels et al. confirmed

the limitations of these dye treatments in distinguishing between native and non-infectious viral particles after UV irradiation [178].

Correlating the results obtained from viability RT-qPCR with those from HuNoV in vitro cell culture models provides a more comprehensive understanding of HuNoV viability and infectivity. Therefore, we conducted a scientific study aimed to evaluate the efficacy of molecular viability assays as rapid, reliable alternatives to cell culture systems for predicting viral inactivation in high-risk food matrices such as strawberry puree.

We tested the effectiveness of three different viability markers ((Viability PCR Crosslinker Kit (CL), propidium monoazide (PMAxx™) and platinum chloride ($PtCl_4$)) to assess the sensitivity and reliability of RT-qPCR for estimating HuNoV infectivity.

We compared results from HIE model with viability molecular assays using infectious HuNoV genotypes and TV as HuNoV surrogate. Moreover, a nearly full-length genomic assay combined with PMAxx™ was employed to evaluate HuNoV thermal inactivation.

Finally, the performance of the viability RT-qPCR was compared to HuNoV replication in HIE model to predict the viral inactivation in strawberry puree after HPP treatments.

Article adapted for printing of the PhD thesis. Available online on International Journal of Food Microbiology, ELSEVIER, https://doi.org/10.1016/j.ijfoodmicro.2023.110507

Challenges for estimating human norovirus infectivity by viability RT-qPCR as compared to replication in human intestinal enteroids

Samantha Q. Wales[a], Annamaria Pandiscia[b,c], Michael Kulka [a], Gloria Sánchez[b], Walter Randazzo[b,*]

[a]Center for Food Safety and Applied Nutrition, Food and Drug Administration, Laurel, MD, United States

[b]Department of Preservation and Food Safety Technologies,Institute of Agrochemistry and Food Technology, IATA-CSIC, Avda. Catedrático Agustín Escardino 7, Valencia, Paterna 46980, Spain

[c]Department of Veterinary Medicine, University of Bari, Provincial Road to Casamassima Km 3, Bari, Valenzano 70010, Italy

Highlights

•Viability RT-qPCR and replication in human intestinal enteroids (HIE) were compared using human norovirus (HuNoV).

•Platinum chloride ($PtCl_4$), as viability marker, affected HuNoV infectivity.

•Viability RT-qPCRs detected HuNoV inactivation at extreme thermal and pressure conditions only.

•Replication in HIE was a more robust assay than viability RT-qPCRs to infer HuNoV infectivity.

Abstract

Viability RT-qPCR, a molecular detection method combining viability marker pre-treatment with RT-qPCR, has been proposed to infer infectivity of viruses which is particularly relevant for non-culturable viruses or sophisticated cell culture systems. Being human noroviruses (HuNoV) most frequently associated with foodborne outbreaks, this study compared different viability techniques and infectivity in human intestinal enteroids (HIE) to ultimately determine whether the molecular approaches could serve as rapid assays to predict HuNoV inactivation in high-risk food. To this end, the performance of three viability RT-qPCR assays with different intercalating markers ((Viability PCR Crosslinker Kit (CL), propidium monoazide (PMAxx™), and platinum chloride ($PtCl_4$)) in estimating survival of HuNoV exposed to thermal and high pressure (HPP) treatments was compared to replication tested in the HIE cell culture model. A nearly full-length genomic molecular assay coupled with PMAxx™ to infer HuNoV thermal inactivation was also assessed. The experimental design included HuNoV genogroup I.3 [P13], GII.4 Sydney [P16], GII.6 [P7], along with Tulane virus (TV) serving as surrogate. Finally, viability RT-qPCR was tested in HPP-treated strawberry puree, selected as a food matrix with high viral contamination risk. PMAxx™ and CL performed evenly, while $PtCl_4$ affected HuNoV infectivity. Taking all experimental data together, viability RT-qPCR was demonstrated to be an improved method over direct RT-qPCR to estimate viral inactivation at extreme thermal (95 °C) and HPP (450 MPa) exposures, but not under milder conditions as amplification signals were detected. Despite its complexity and limitations, the HIE demonstrated a more robust model than viability RT-qPCR to assess HuNoV infectivity.

Keywords

Molecular methods; Cell culture; Food safety

DOI: https://doi.org/10.1016/j.ijfoodmicro.2023.110507

1. Introduction

Human noroviruses (HuNoV) are the leading cause of acute viral gastroenteritis in both children and adults (Koopmans, 2008). These non-enveloped viruses are primarily transmitted through the faecal–oral route, either via direct person-to-person contact, contact with contaminated fomite or the consumption of contaminated food and water. In order to prevent infections, food safety agencies have implemented regulations that utilize standardized molecular techniques, such as quantitative reverse transcription polymerase chain reaction (RT-qPCR), to assess the levels of HuNoV contamination (ISO 15216-1, 2017; Williams-Woods et al., 2022). Although standardized RT-qPCR provides homogenized data to determine the presence of HuNoV contamination, it is unable to distinguish between infectious and non-infectious viral particles, posing a significant limitation for comprehensive risk assessments. Culture-based methods for virus replication are considered the gold standard for assessing infectivity, but such methods have historically been lacking for HuNoV (Estes et al., 2019; Ettayebi et al., 2016). As a result, the evaluation of HuNoV survival and stability has traditionally relied on the use of cultivable surrogate viruses like murine norovirus (MNV), feline calicivirus (FCV), or Tulane virus (TV) (Cromeans et al., 2014). Alternatively, the use of viability RT-qPCR has been proposed to overcome RT-qPCR limitation (Parshionikar et al., 2010; Randazzo et al., 2016). This technique involves pre-treating the sample with a viability marker (also known as intercalating dye), such as propidium monoazide (PMA) or platinum (IV)

chloride. After pre- treatment, viral RNA is purified and quantified using RT-qPCR. The viability markers specifically bind to free and accessible RNA from capsid-compromised viruses and prevent their amplification. By comparing the quantitation of viability treated and untreated samples, a difference in results indicates that the virus capsid was compromised and therefore noninfectious (Leifels et al., 2020). As an alternative measurement of infectivity, the assessment of genome integrity using nearly full-length genomic molecular assays has been proposed, although its robustness and sensitivity have not always been confirmed (Ho et al., 2016). Recently, a novel three-dimensional (3D) cell culture technique utilizing non-transformed stem cell-derived human intestinal enteroids (HIEs) has been implemented as a robust and reproducible in vitro cultivation system for HuNoV (Costantini et al., 2018; Ettayebi et al., 2016). Despite its utility, it still suffers from limitations due to technical difficulty, expense, a relative lack of strain susceptibility and the necessity of high virus titer for successful replication, which can be a challenge for application in the food safety arena (Estes et al., 2019). In order to comprehensively evaluate the effectiveness of viability RT-qPCR in estimating HuNoV infectivity, we conducted a series of experiments comparing the results obtained from the complex HIE model and viability molecular approaches. In detail, we examined different viability RT-qPCR using infectious HuNoV genotypes and TV, and assessed several thermal and high pressure inactivation conditions. Additionally, we investigated the performance of a nearly full-length genomic molecular assay combined with PMAxx™ to infer HuNoV thermal inactivation. Finally, we compared HIE replication and viability RT-qPCR using three viability markers to determine if these molecular approaches could serve as rapid assays to predict viral inactivation in strawberry puree, a high-risk food matrix for viral contamination.

2. Material and methods

2.1. Virus strains, clinical samples, cell lines, and infectivity assays

Human genogroup I (GI.3[P13]) and II (GII.4 Sydney [P16], and GII.6[P7]) norovirus-positive faecal samples were suspended in phosphate-buffered saline (PBS) to a final 10 % (wt/vol) suspension. Clarified stool suspensions were prepared by passing through serial filters (5, 1, 0.45, and 0.22 μm) as described previously (Costantini et al., 2018) and stored at -80 ◦C in aliquots. TV was used as HuNoV surrogate and tested by cell culture as detailed hereafter. TV provided by Prof. Farkas (Louisiana State University, LA, US) was grown and assayed in LLC-MK2 cell line (ATCC CCL-7) cultured in Opti- MEM (Gibco Life Technologies) supplemented with 2 % of heat-inactivated fetal bovine serum (FBS; GE Healthcare Bio-Sciences) and 2 % of an antibiotic cocktail of penicillin and streptomycin (Cromeans et al., 2014; Esseili et al., 2018). The LLC-MK2 cells were cultured in T75 flasks at 37 ◦C in a 5 % CO2 incubator. TV infectivity was calculated by determining the 50 % tissue culture infectious dose ($TCID_{50}$) in 96-well plates using the Spearman-Karber method after visual inspection of cells for presence of cytopathic effect (CPE) at 96-hour post infection (hpi). Briefly, ten-fold serial dilutions of TV were prepared in PBS and 20 μL per well were inoculated on a total of eight wells. After 1 h post infection 150 μL of Opti-MEM were added to each well and plates were incubated at 37 ◦C in a 5 % CO_2 incubator and monitored for CPEs (Randazzo et al., 2020).

2.2. Human intestinal enteroids model for norovirus infectivity

HuNoV infectivity was tested using the HIE model. Undifferentiated 3D HIEs and differentiated monolayers were maintained and produced using commercial

IntestiCult™ Organoid Medium Human media (STEMCELL Technologies Inc.), as described in (Carmona and Randazzo, 2023). Differentiated HIE monolayers were typically 100 % confluent after five- to seven-days and used for HuNoV infections. Two sets of 96- well plates with 100 % confluent differentiated HIE monolayers were inoculated in triplicate with 100 µL of each HuNoV sample diluted at 1:10 in Complete Media without Growth Factors (CMGF-) supplemented with 500 µM sodium glycochenodeoxycholate. After 1 h incubation at 37 °C, the inoculum was removed, monolayers were washed twice with CMGF-, and 100 µL of Organoid Differentiation Medium (ODM) was added to each well. For each set of infections, one 96-well plate was immediately frozen at -80 °C (1 hpi) and the second plate was incubated at 37 °C and 5 % CO_2 for 48 h (48 hpi) and then frozen. Finally, RT-qPCR was used to determine the amount of HuNoV RNA from HIE monolayers at 1 and 48 hpi to evaluate HuNoV replication. Specific cut-off criteria were adopted to designate a sample as infectious: (i) no cytotoxic effect on monolayers at 48 hpi, (ii) at least a 3-fold RNA/ DNA increase in HIEs culture (Desdouits et al., 2022), and (iii) quantifiable viral load at both 1 hpi and 48 hpi with statistically significant difference between time points.

2.3. Purification, detection and quantification of viral RNA by RT-qPCR

Viral RNA was extracted using the Maxwell® RSC Instrument (Promega) according to the manufacturer's instructions. Then, it was detected in duplicate by TaqMan RT-qPCR using the RNA UltraSense One-Step quantitative RT-PCR system (Invitrogen) on a LightCycler 480 instrument (Roche Diagnostics). The primers and probe used for detecting HuNoV GI and GII, and TV have been previously described (Chhabra et al., 2017; ISO 15216-1, 2017). Ten-fold serial dilutions of synthetic gBlock gene

fragments (IDT) were used to build an external standard curve and HuNoV RNA quantified as genome equivalents (HuNoV GI: y = -3.5106x + 37.329, R = 0.999; HuNoV GII: y = -3.56x + 40.664, R = 0.997). Standard curve for TV quantification was generated by serial end-point dilution, amplifying 10-fold RNA dilutions obtained from cell culture stock (y = - 3.287x + 41.187, R = 0. 987). In some experiments (Fig. 3), viral RNA was extracted using TRI Reagent®, followed by the Direct-zol RNA Miniprep extraction kit (Zymo Research) according to manufacturer's instructions. Viral RNA was detected using the Quantitect® _Probe RT-PCR kit (Qiagen) on the Applied Biosystems 7500 Fast instrument (CA) using the primer pair and probe COG2R/ QNIF2d/QNIFS as described (Ettayebi et al., 2016), using an in-house full-length GII.4 transcript to generate a standard curve and quantify genome copies (Yu et al., 2016). Positive and negative amplification controls were included in each RT-qPCR run, along with inhibitory amplification control consisting of a 10-fold diluted RNA for each sample.

2.4. Assessment of intercalating markers for viability RT-qPCR

The performance of three intercalating markers to be coupled to RT-qPCR for viability RT-qPCR was screened. Specifically, the photoactivable dye PMAxx™ (Biotium), the metal compound platinum (IV) chloride ($PtCl_4$; Acros Organics) and the Viability PCR Crosslinker Kit (CL; Promega) were included in the study. Stock solutions were prepared as follow: PMAxx™ was dissolved in water at 4 mM, $PtCl_4$ was dissolved in dimethyl sulfoxide (DMSO, Sigma-Aldrich) at 50 mM, and CL was dissolved in DMSO at 100 μM. All reagents were stored at -20 °C and protected from light. Viability pre-treatments were performed in DNA LoBind tubes (Eppendorf Iberica, Madrid, Spain) as follows: (I) incubation with 100 μM PMAxx™ photoactivatable dye

and 0.5 % Triton 100X (Fisher-Scientific) at room temperature (RT) for 10 min at 150 rpm in an orbital shaker and 15 min photoactivation using a photo-activation system (Led-Active Blue, GenIUL) (Chen et al., 2020); alternatively (II) incubation with 500 µM $PtCl_4$ at RT for 30 min at 150 rpm in an orbital shaker (Chen et al., 2020); and (III) incubation with 2.5 to 50 µM CL at 37 °C for 30 min, a vortex step to mix followed by additional 30 min at 37 °C incubation. Finally, 20 µL of neutralization buffer included in CL kit was added and the sample was incubated at RT for 15 min. Once viability pre-treatments were completed, the samples were extracted and RNA quantified, or set aside for infection of the HIE (Section 2.5). Initially, the three intercalating markers were preliminarily tested on TV, HuNoV GI.3[P13] and GII.4 Sydney [P16] purified RNA. Each experiment included a purified RNA sample without viability marker as a positive control. After viability pre-treatments, viral RNA was re-extracted and quantified by RT-qPCR. The three intercalating markers were also tested on TV, HuNoV GI.3 [P13] and GII.4 Sydney [P16] viral suspensions inactivated at 99 °C for 10 min. To this end, 100 µL of heat-treated viral suspensions were incubated in DNA LoBind tubes with 100 µM PMAxx™, 500 µM PtCl4, and 2.5 to 50 µM CL final concentrations. Viability treatments were carried out as mentioned above. Finally, viral RNA was extracted and quantified. Each experiment included an infectious (no heat-treated) control sample and a heat treated (at 99 °C for 10 min) sample processed without viability markers (RT-qPCR alone). Finally, to specifically investigate the performance of PMAxx™ RT-qPCR, two genetically diverse HuNoV suspensions, GII.4[P16] and GII.6[P7] were either heat treated at 60 and 95 °C for 10 min or kept on ice (infectious control sample). The 60 °C treatment was selected as shown effective for viral inactivation (Ettayebi et al., 2016). Additionally, a mixed sample was produced by mixing 95 ◦C heat treated and control samples at 1:1 *v*/v ratio.

These conditions were tested to gauge the sensitivity of the assay in attenuated inactivation mimicking real-life scenarios. For each set of experiments, heat-treated and control samples were further subjected to infectivity assay on HIE model, RT-qPCR, and 200 µM PMAxx™ RT-qPCR, as described above.

2.5. Assessment of norovirus infectivity by full-length RT-PCR A PMAxx™

A pre-treatment coupled with full-length RT-PCR was investigated as an alternative for examining GII.4[P16] and GII.6[P7] infectivity. The nearly full-length complementary DNA sequences were synthesized as previously described (Parra et al., 2017). Samples were either incubated at 60 or 95 ◦C for 10 min, or kept on ice (control samples), and 200 µM PMAxx™ pre-treated or not. The TX30SXN primer (Katayama et al., 2002) at 5 µM final concentration, and the Maxima H Minus First Strand cDNA Synthesis Kit (Thermo Fisher Scientific) were used for cDNA synthesis. Amplification of the full-length genome was performed using 5 µL of the RT reaction, primers TX30SXN and GII1-35 (5′ GTGAATGAAGATGGCGTCTAACGACGCTTCCGCTG 3′, targeting the conserved region at the 5′-end of GII), and the SequalPrep Long PCR Kit (Invitrogen) following manufacturer's recommendations. Amplicons were visualized following agarose gel electrophoresis of samples in precast 1 % agarose gel/TAE/ethidium bromide gels (BioRad).

2.6. Assessment of intercalating markers on viral infectivity

To assess potential effect of intercalating markers on viral infectivity, TV (6.1 ± 0.2 $\log_{10}$ $TCID_{50}$/mL) and HuNoV GII.4 Sydney [P16] (6.1 ± 0.2 $\log_{10}$ gc/100 µL) infectious suspensions were exposed to viability pre-treatments as in Section 2.3.

Then, viral replication was assessed by cell culture on LCC-MK2 and HIEs as described above. In addition, to exclude any potential cytotoxicity effect on LLC-MK2 cells and HIEs, cell monolayers were visually inspected by using a Zeiss Axiovert microscope at 1 and 48 hpi. A sample without viability treatment was included as control for each virus.

2.7. High-pressure processing assays

HPP treatments were performed in a pilot scale unit (High-Pressure Food Processor, EPSI NV, Belgium) with a vessel operating volume of 2.35 L and a maximum treatment pressure of 600 MPa. The pressure transmitting fluid was a mixture of water and ethylene glycol (70:30, v: v). HPP was applied in samples distributed in 300 μL PCR tubes, placed in polyethylene bags and heat-sealed (MULTIVAC Thermosealer). A constant holding temperature of 22 ± 1 °C was maintained during HPP as the pressure transmitting fluid was automatically and continually refrigerated. After completing the treatment, the samples were immediately stored at -80 °C. Two different sets of experiments were carried out. Initially, TV and HuNoV GII.4 Sydney [P16] suspensions were mixed with PBS (ratio 1:30) and exposed to 0 (infectious control), 300, 400 and 500 MPa for 5 min. Viral inactivation was determined by cell culture and viability RT-qPCR as described above. Then, the inactivation of HuNoV GI.3[P13] and GII.4 Sydney [P16] suspensions in PBS and strawberry puree (both inoculated at ratio 1:30) was investigated for 5 min HPP at 350, 400, and 450 MPa. Fresh strawberries were purchased from a local market and puree obtained using an electric blender. After the treatment, samples were stored at -80 °C until testing. To avoid cytotoxicity, PBS and strawberry puree samples inoculated with HuNoV GI.3[P13] and GII.4 Sydney [P16] were further diluted 1:100 in Complete Media

without Growth Factors (CMGF-) supplemented with 500 µM sodium glycochenodeoxycholate. The diluted aliquot was used for infection on HIE model, RT-qPCR and viability RT-qPCR as represented in Fig. 1.

2.8. Statistical analysis

All data were compiled from at least three independent experiments with three technical replicates for each variable. Significant differences in mean infectivity were determined by the analysis of variance (ANOVA) followed by Dunnett's multiple comparisons test. Differences in means were considered significant when the p was <0.05. GraphPad Prism version 8 (GraphPad Software, USA) software was used for statistical analyses and data representation.

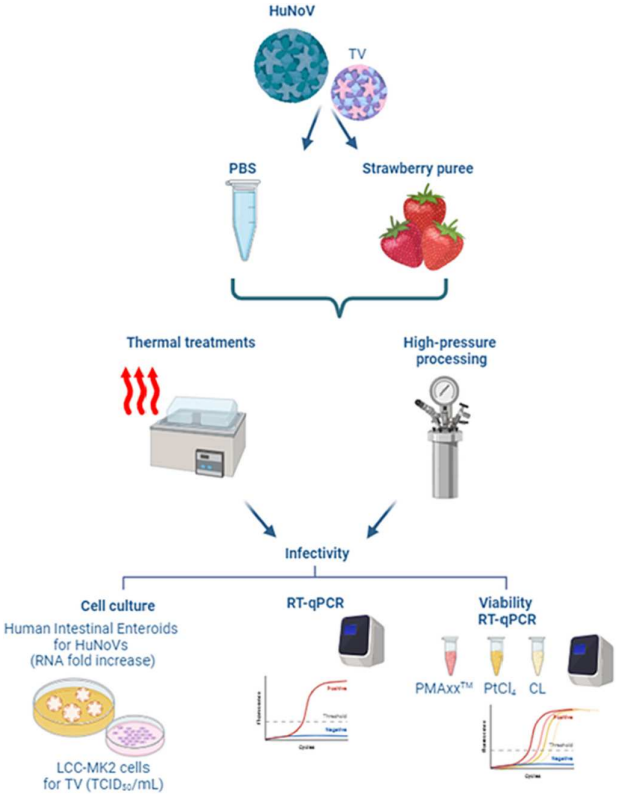

Fig. 1. Workflow followed to compare the viral infectivity assessed by replication on cell culture, RT-qPCR, and viability RT-qPCR using three viability markers.

3. Results

3.1. Screening of intercalating markers and performance of viability RT-qPCR for heat-treated HuNoV and TV suspensions

3.1.1. Performance of viability RT-qPCR on purified viral RNA

PMAxx™ and $PtCl_4$ viability markers were initially evaluated on purified HuNoV GII.4 Sydney [P16] and TV RNA at specific concentrations selected from previous studies (Chen et al., 2020; Fraisse et al., 2018; Randazzo et al., 2018, 2016). CL viability marker was tested on viral RNA at 50 µM, the maximum concentration recommended by the supplier. HuNoV GII.4 Sydney [P16] and TV RNA were purified from 4.1 ± 0.2 $\log_{10}$ $TCID_{50}$/mL and 4.7 ± 0.3 $\log_{10}$ gc/mL infectious virus suspensions resulting in 30.4 ± 0.2 and 30.1 ± 0.1 cycle thresholds (Ct), respectively. Pre-treatment of extracted viral RNA with 100 µM PMAxx™ resulted in an average reduction of 3.3 and 2.4 Ct for HuNoV GII.4 Sydney [P16] and TV respectively, compared to controls. In contrast, 500 µM $PtCl_4$ and 50 µM CL completely eliminated the amplification signals for both viral RNAs. Additionally, the inhibition of the amplification reaction due to the presence of viability markers in the reaction mixture was excluded by testing in parallel 10-fold RNA dilutions (data not shown).

3.1.2. Effect of viability markers on viral replication

Replication of HuNoV GII.4 Sydney [P16] and TV suspensions pre-treated with viability markers and cultivated in HIE and LCC-MK2 as receptive cell systems showed that 500 µM $PtCl_4$ significantly reduced by 2.88 $\log_{10}$ (p= 0.0019) the infectivity of HuNoV GII.4 Sydney [P16]. A 0.4 $\log_{10}$ reduction in TV infectivity was also observed, although it was not statistically significant (p= 0.6633) (Table 1). Pre-

treatment with 100 µM PMAxx™ reduced the infectivity of HuNoV GII.4 Sydney [P16] by 1.12 log_{10} (p = 0.0143) but had no effect on TV. CL viability pre-treatment at 50 µM did not affect viral infectivity of either virus. Microscopic examination of HIE and LCC-MK2 monolayers infected with pre-treated viral suspensions confirmed the absence of cytotoxic effects caused by any of the tested viability markers.

3.1.3. Performance of viability RT-qPCR for heat-treated viral suspensions

In the next step, we evaluated the performance of different viability RT-qPCR methods using infectious and thermally inactivated (99 °C for 5 min) samples of HuNoV GI.3[P13], HuNoV GII.4 Sydney [P16], and TV. The samples with initial titers of 7.3 ± 0.0, 7.3 ± 0.1, and 9.0 ± 0.2 log_{10} gc/100 µL, respectively, were pre-treated with 100 µM PMAxx™, 500 µM $PtCl_4$, and 2.5 to 50 µM CL before RNA extraction and quantification. No significant differences were observed between infectious and inactivated controls for both HuNoV genotypes. However, the thermally inactivated TV suspension showed a 1.1 log_{10} lower titer compared to its infectious counterpart (Fig.2). All the viability pre-treatments of thermally inactivated viral suspensions resulted in reduced amplification signals, enabling a lower estimation of viral infectivity, which is desirable for accurate infectivity assessment. The detection of the three inactivated viruses using CL viability RT-qPCR was inversely proportional to the concentration of the marker.

Table 1. Effect of viability markers on TV and HuNoV GII.4 Sydney [P16] replication assayed in LCC-MK2 and HIE cell-cultures.

	TV				HuNoV GII.4 Sydney [P16]				
	Titer		Log_{10} reduction	p-Value	Titer		Log_{10} reduction	Fold viral RNA increase	p-Value
	(log_{10} $TCID_{50}$/mL ± SD)				(log_{10} gc/100 µL ± SD)				
Untreated	6.07	±0.18			7.74	±0.30		590.97	
50 µM CL	5.95	±0.18	0.13	0.9733	7.47	±0.14	0.27	532.70	0.8995
100 µM PMAxx™	6.14	±0.09	−0.06	0.9963	6.62	±0.42	1.12	122.71	0.0143
500 µM $PtCl_4$	5.70	±0.71	0.38	0.6633	4.86	±0.09	2.88	1.30	0.0019

Abbreviations: TV, Tulane virus; HuNoV, human norovirus; CL, viability PCR Crosslinker Kit; PMAxx™, propidium monoazide viability marker; $PtCl_4$, platinum (IV) chloride viability marker.

Specifically, a concentration of 50 µM CL completely prevented the amplification of 3 out of 4 replicates of inactivated HuNoV GI.3[P13] (resulting in a mean reduction of 2.6 log_{10} gc/100 µL compared to control), and 2 out of 4 replicates of inactivated HuNoV GII.4 Sydney [P16] (with a mean reduction of 3.0 log_{10} gc/100 µL). The 50 µM CL assay reduced TV amplification by 2.4 gc/100 µL. Comparing the thermal inactivation of HuNoV and TV, different patterns were observed for PMAxx™ and $PtCl_4$. PMAxx™ reduced the amplification signals of TV (with a mean reduction of 1.6 log_{10} gc/100 µL) more than HuNoV GI.3[P13] (with a mean reduction of 1.1 log_{10} gc/ 100 µL) and HuNoV GII.4 Sydney [P16] (with a mean reduction of 0.6 log_{10} gc/100 µL). On the other hand, $PtCl_4$ pre-treatment resulted in a reduction of 0.5, 3.5 and 2.2 log_{10} gc/100 µL for TV, HuNoV GI.3[P13] and HuNoV GII.4 Sydney [P16], respectively. Moreover, only 1 out of 4 replicates of HuNoV GI.3[P13] showed amplification (Fig. 2). Additionally, the performance of PMAxx™ RT-qPCR was evaluated on HuNoV GII.4[P16] and GII.6[P7] exposed to temperatures of 60 and 95 °C (Fig. 3). The results were compared to replication on HIE, which was previously reported to be prevented under both thermal exposures (Costantini et al., 2018; Ettayebi et al., 2016). In these experiments, given the preliminary findings presented in Fig. 2, the concentration of the viability marker was increased to 200 µM PMAxx™, in line with recommendations from prior research (Chen et al., 2020; Fraisse et al., 2018; Randazzo et al., 2016). At 60 °C, the inactivation of HuNoV, as evidenced by the absence of detectable replication (RNA fold-increase) in HIE, was not accurately mirrored by the PMAxx™ assay. Additionally, the RNA levels measured by RT-qPCR indicated no degradative impact on the nucleic acid at the tested temperature. It was,

however, able to statistically differentiate between infectious and inactivated HuNoV when exposed to 95 °C for both tested genotypes. Interestingly, RT-qPCR alone also detected a significantly lower amount of RNA, suggesting that that high temperature was impacting the integrity of the genetic material. The mixed samples containing both infectious and 95 °C heat-inactivated viruses exhibited replication on HIE to a similar extent as samples with only infectious virus. As well, PMAxx™ RT-qPCR assays performed similarly in mixed and infectious samples. Thus, both HIE and PMAxx™ RT-qPCR assays revealed the level of infectious viruses, while the inactivated portion was not discerned. Although these findings could advocate a conservative approach in the context of risk assessment analyses, the efficiency of the techniques in discriminating infectious and inactivated viruses has not been confirmed in these experiments. As an alternative approach to infer the concentration of infectious and inactivated HuNoV, nearly full-length was used as approximation for RNA integrity. Thus, the performance of PMAxx™ was further investigated through visualization of nearly full-length genome sequences following treatment with the viability marker (Fig. 4). A reduced signal of PMAxx™ treated HuNoV GII.4[P16] was observed in both untreated and 60 °C heated samples. However, despite the prevention of viral replication with 60 °C treatment, a clear band was still detected for the PMAxx™ treated sample. Full-length amplification was completely inhibited in samples exposed to 95 °C, both with and without PMAxx™ treatment, which aligns with the infectivity data, as well as the viability RT-qPCR for the GII.4 [P16] strain.

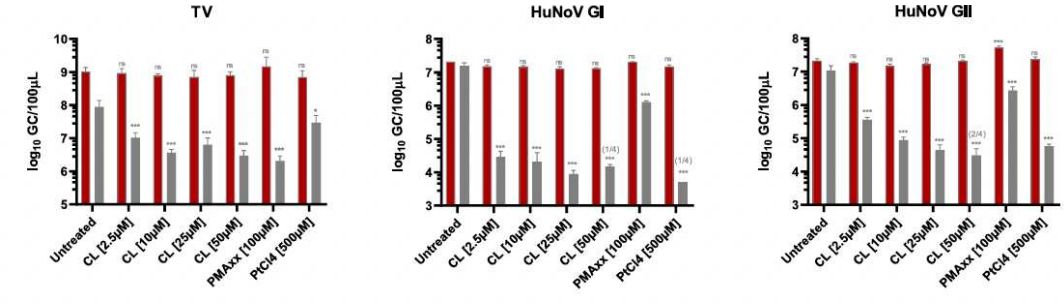

Fig. 2. Screening of viability markers on infectious (red bars) and thermally inactivated (5 min at 99 °C, grey bars) Tulane virus (TV), human norovirus genogroup I (HuNoV GI.3[P13]), and GII (HuNoV GII.4 Sydney [P16]). Error bars indicate SDs; asterisks indicate significant difference from untreated control: *$p < 0.05$; ***$p < 0.001$; ns, no significant difference; numbers in parenthesis indicate the positive/total number of samples analysed, when not specified all replicates (4 out of 4) showed viability RT-qPCR amplification signals.

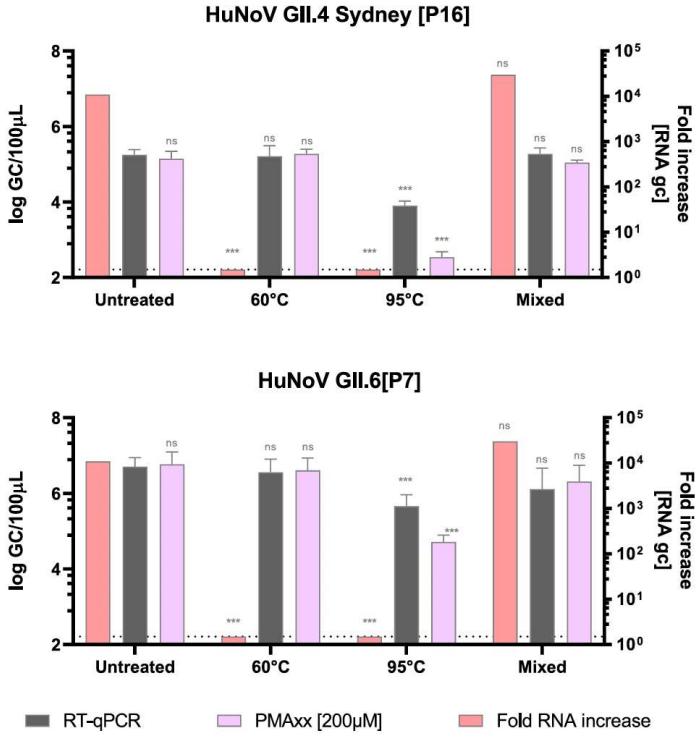

Fig. 3. Performance of cell culture (viral RNA fold increase), RT-qPCR, and 200 µM PMAxx™ RT-qPCR to discriminate between infectious and thermally inactivated (60, and 95 °C, 10 min) HuNoV GII.4 Sydney [P16], and HuNoV GII.6 [P7]. Error bars indicate SDs; asterisks indicate significant difference from untreated control: ***$p < 0.001$; ns, no significant difference; dashed line indicates the lower limit of viral replication in HIE model.

3.2. Screening of intercalating markers and performance of viability RT-qPCR for HPP-treated TV and HuNoV suspensions

The performance of viability RT-qPCR was further tested on HPP-treated TV and HuNoV GII.4 Sydney [P16]. The viral suspensions were prepared in PBS, treated at 300, 400, and 500 MPa for 5 min, and the viral titers estimated using RT-qPCR, viability RT-qPCR, and cell culture (Fig. 5). The initial infectious titer of TV (6.2 ± 0.1 $\log_{10}$ $TCID_{50}$/ mL) exposed to 300 MPa was reduced to 2.8 ± 0.1 $\log_{10}$ $TCID_{50}$/mL, resulting in a 3.4 $\log_{10}$ inactivation. Treatments at 400 and 500 MPa resulted in complete inactivation of TV. Using RT-qPCR, TV RNA was detected at 8.8 ± 0.1 $\log_{10}$ gc/100 µL in the untreated sample, while HPP-treated samples showed decreases ranging from 1.1 to 1.8 $\log_{10}$ (Fig. 5). Compared to direct RT-qPCR, viability RT-qPCR using 50 µM CL showed no statistically significant differences in TV titers for both 300 (p = 0.0628) and 400 (p = 0.1220) MPa HPP-treated conditions, though signals were reduced by 0.7 $\log_{10}$. However, amplification signals were significantly ($p < 0.001$) reduced in samples exposed to 500 MPa. Infectious HuNoV GII.4 Sydney [P16] was not inactivated at 300 MPa (637 RNA gc fold-increases), partially inactivated at 400 MPa (131 RNA gc fold-increases), and completely inactivated at 500 MPa as confirmed by replication in HIE. When assessing RNA titers by RT-qPCR, a mean reduction of 1.4 $\log_{10}$ gc/100 µL was observed at 400 and 500 MPa compared to the control. Differences between viability RT-qPCRs and direct RT-qPCRs for infectious and 300 MPa treated samples were not significant ($p \geq 0.8988$), indicating the detection of infectious virus. However, following exposure to 400 MPa, viability RT-qPCRs overestimated viral infectivity compared to replication in HIE. Upon further increasing the pressure to 500 MPa, complete inactivation was detected by replication in HIE and viability RT-qPCRs, but not by RT-qPCR alone. Overall, 50

μM CL, 100 μM PMAxx™, and 500 μM $PtCl_4$ performed similarly for HPP-treated HuNoV GII.4 Sydney [P16] (Fig. 5).

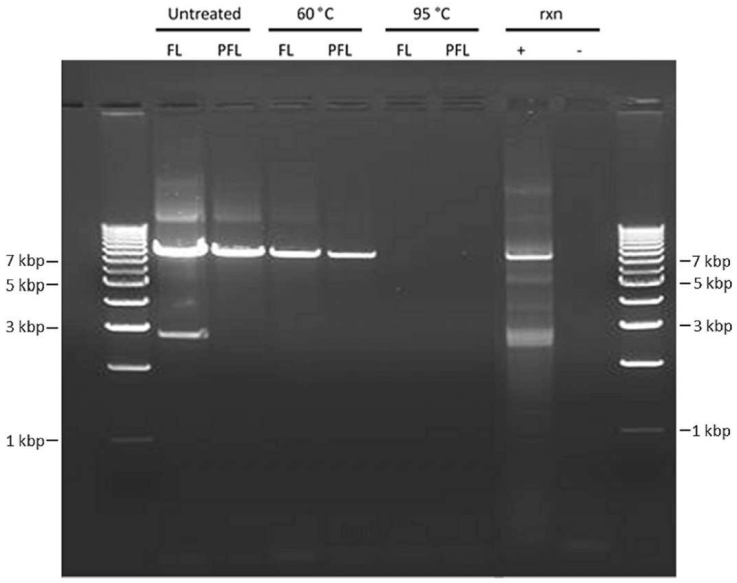

Fig. 4. Performance of full-length RT-PCR, and PMAxx™ full-length RT-PCR to discriminate between infectious (untreated) and thermally inactivated (60, and 95 °C, 10 min) HuNoV GII.4 Sydney [P16]. A one kilobase-pair (kbp) dsDNA ladder was run in the first and last lanes of the gel; selected marker lengths are identified on the figure. The 2 major amplicons (bands) observed, e.g., in the untreated/FL lane, are of estimated lengths 7.5 kbp and 2.6 kbp.

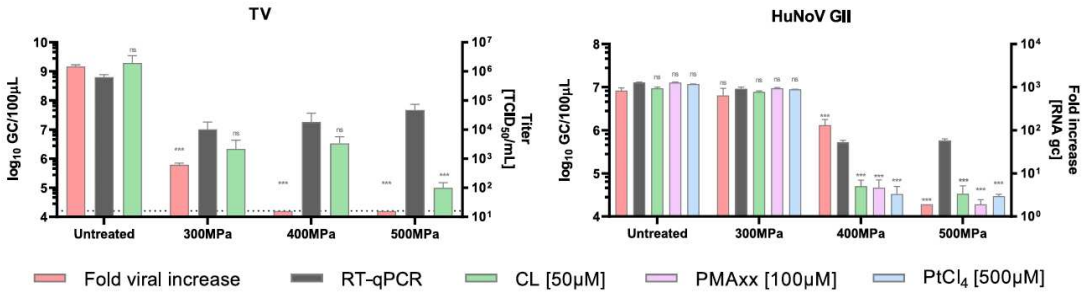

Fig. 5. Performance of cell culture ($TCID_{50}$ or viral RNA fold increase), RT-qPCR, and viability RT-qPCR to discriminate between infectious and high pressure inactivated (5 min) Tulane virus (TV), and human norovirus genogroup II (HuNoV GII.4 Sydney [P16]) in PBS. Error bars indicate SDs; asterisks indicate significant difference from untreated control: ***$p < 0.001$; ns, no significant difference; dashed line indicates the limit of quantification of $TCID_{50}$/mL assay.

3.3. Performance of viability RT-qPCR versus replication in HIE to assess human norovirus inactivation by HPP in strawberry puree

The performance of viability RT-qPCR for inferring HuNoV infectivity was further evaluated in PBS and strawberry puree samples exposed to HPP treatments at 350, 400, and 450 MPa for 5 min. The quantification of HuNoV GI.3[P13] and HuNoV GII.4 Sydney [P16] was performed by direct RT-qPCR, viability RT-qPCR with 50 µM CL, 100 µM PMAxx™, or 500 µM $PtCl_4$, and infectivity in HIE (Fig. 6). Overall, the results from all three viability RT-qPCRs lacked correlation with the loss of infectivity of HuNoV GI.3[P13] after HPP treatments in PBS and strawberry puree (Fig. 6A and C). The differences in titers determined by viability RT-qPCR were not statistically significant compared to RT-qPCR alone for all tested conditions, except for the virus treated at 450 MPa in strawberry puree (Fig. 6C). In the case of the virus treated at 450 MPa in strawberry puree, HuNoV GI.3[P13] showed 1.8- fold RNA increase in HIE, which did not comply with the cut-off criteria adopted in this study for deeming a sample as infectious. Comparing PMAxx™ viability RT-qPCR to RT-qPCR, a mean reduction of 2.16 $\log_{10}$ gc/100 µL was observed, while CL and $PtCl_4$ completely prevented RNA amplification, indicating no infectivity (Fig. 6C). For GII.4 Sydney [P16], the viability RT-qPCRs detected significant reductions in samples exposed to 400 and 450 MPa in either PBS (Fig. 6B) or strawberry puree (Fig. 6D). The reductions measured were >2 $\log_{10}$ in PBS and >0.9 $\log_{10}$ gc/100 µL in strawberry puree, regardless of the viability marker used. There was an absence of correlation between molecular assays and viral infectivity since HuNoV GII.4 Sydney [P16] from 350 MPa treated samples replicated in HIE while significant differences were obtained comparing RT-qPCR and viability RT-qPCRs. As well, samples exposed to >400 MPa retained RT-qPCR signals yet did not replicate. Also, significant differences were

observed between viability RT-qPCR and RT-qPCR signals regardless of the replication rates resulting from HIE infections (e.g., 350 MPa vs. 400 MPa). In summary, despite the significant reductions compared to RT-qPCR, none of the viability RT-qPCRs assays completely prevented the amplification of RNA from HuNoV GI.3[P13] and HuNoV GII.4 Sydney [P16] samples that failed to replicate in HIE.

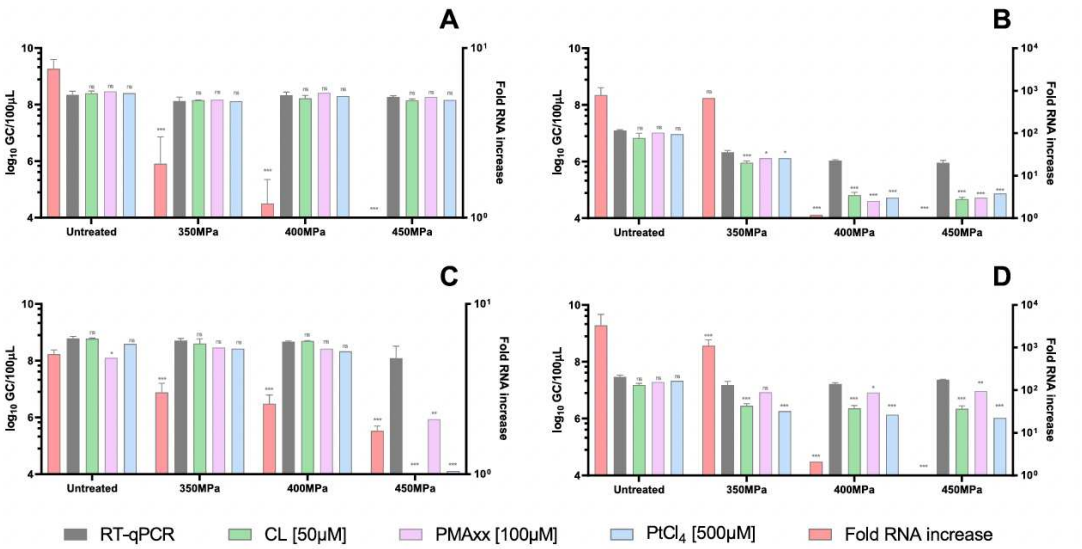

Fig. 6. Performance of viability RT-qPCR to discriminate between infectious and high pressure inactivated human norovirus genogroup I (HuNoV GI.3[P13], panel A and C) and HuNoV GII.4 Sydney [P16] (panel B and D) compared to RT-qPCR and cell culture (viral RNA increase on human intestinal enteroids) in PBS (panel A and B) and strawberry puree (C and D). Error bars indicate SDs; asterisks indicate significant difference from untreated control: ***p < 0.001; **p < 0.01; *p < 0.1; ns, no significant difference.

4. Discussion

The use of viability RT-qPCR has been proposed as a method to infer viral infectivity in complex environmental and food samples (Leifels et al., 2019). However, a comprehensive assessment of viability molecular techniques for estimating HuNoV infectivity in comparison to cell culture methods has not yet been reported. In this

study, our objective was to investigate the relationship between HuNoV infectivity and viral RNA levels, which were measured by both direct RT-qPCR and viability RT-qPCR, including the latter as a rapid molecular estimation for viral infectivity. We specifically focused on evaluating different viability RT-qPCR approaches to determine the patterns of inactivation for HuNoV following exposure to thermal and HPP treatments. These results were directly compared with the replication of the virus in the HIE system. Because it has been used as a cultivable surrogate for HuNoV, TV was also selected for comparison purposes in this study (Cromeans et al., 2014). Our findings provide evidence that viability RT-qPCR can be used to determine the inactivation of HuNoV suspensions following extreme thermal (99 °C for 5 min) and pressure (500 MPa for 5 min) treatments, despite the presence of residual amplification signals. Among the viability markers tested, CL showed consistent performance for all three viruses examined, namely HuNoV GII.4 Sydney [P16], HuNoV GI.3 [P13] and TV. However, divergent results were observed for PMAxx™ and $PtCl_4$.

$PtCl_4$ exhibited superior performance compared to PMAxx™ for detecting inactivation of HuNoV GI.3[P13] and HuNoV GII.4 Sydney [P16], while the opposite trend was observed for TV. This discrepancy could be attributed to variations in the amplicon length and the presence of secondary structures in the targeted RNA, which may influence the binding of viability markers. Similar observations have been reported in previous studies investigating different combinations of markers and viruses (Puente et al., 2020; Randazzo et al., 2018). Our results align with a study by Fraisse (Fraisse et al., 2018), where the superior performance of $PtCl_4$ over PMAxx™ in discriminating infectious and heat-inactivated HuNoV was also demonstrated. However, it is worth emphasizing that $PtCl_4$ pre-treatment had a significant impact on viral infectivity (2.88 $\log_{10}$ reduction for HuNoV GII.4 Sydney [P16]), which deems

it less plausible as a viability marker, as compared to CL (no reduction) or PMAxx™ (1.12 $\log_{10}$ reduction) (Table 1). Full-length or long-range RT-PCR has been used to estimate genomic integrity reducing the detection of inactivated HuNoV and fragmented RNA (Pecson et al., 2011; Raymond et al., 2023). Our study revealed that full-length RT-PCR and PMAxx™ full-length RT-PCR provided reduced signals for 60 °C heated samples, indicating an improved ability to distinguish infectious and inactivated viruses compared to the smaller amplicons generated by RT-qPCR with or without viability pre-treatment as in Fig. 3. However, infectivity data at 60 °C demonstrated that full-length RT-PCR either with and without PMAxx™ viability pretreatment was not successful in estimating the thermal inactivation of HuNoV GII.4 Sydney [P16]. The full-length RT-PCR revealed amplification loss concomitant with loss of infectivity after sample exposure to 95 °C. However, amplification efficiency decreases with fragment size, making amplification of full-length genomic RNA relatively insensitive. Thus, this technique itself may prove less practical for application to routine analyses of food and environmental samples in comparison to RT-qPCR. To validate our findings, we conducted additional experiments using HPP-treated strawberry puree, as strawberries continue to be linked to HuNoV outbreaks around the globe (Bozkurt et al., 2021). We previously reported that 100 μM PMAxx™ pretreatment with a double photoactivation step was able to significantly reduce HuNoV GI and HuNoV GII PCR signals in thermally treated strawberries (1.22–2.09 $\log_{10}$ reduction as compared with RT-qPCR) (Chen et al., 2020). In this study, the PMAxx™ pretreatment with a single photoactivation step prevented the amplification of samples exposed to extreme HPP conditions only. The discrepancies between the studies could be attributed to several factors, including the specimen used for inoculation (not tested for infectivity in the previous study) and their preparation

steps (e.g., filtration, initial concentration), the variations in pretreatment conditions, and the exposure to different inactivation technologies (thermal vs. HPP). It is interesting to note that for HuNoV GI.3[P13], the strawberry puree matrix appears to have conferred some protection from HPP in infectivity as compared to HPP performed in the presence of PBS alone. These factors can introduce variability and limitations in the efficacy of the protocols employed (Leifels et al., 2019). Our data further support the conclusion that RT-qPCR alone is not a reliable indicator of HuNoV infectivity, regardless of whether the viruses were subjected to heat or HPP treatments. This finding aligns with previous reports that have compared treated and untreated samples by direct RT-qPCR (Cromeans et al., 2014; Knight et al., 2013; Li et al., 2012; Sánchez et al., 2011). Ultimately, our findings provide support for the use of viability approaches, such as viability RT-qPCR, as an improved method for inferring the inactivation of HuNoV, but only under extreme thermal and high HPP conditions. By incorporating viability markers, these approaches have the potential to enhance the accuracy and reliability of standardized molecular quantification methods by reducing at least false-positive signals. However, it is important to note that viability RT-qPCR may not be fully successful in distinguishing viruses that have been inactivated due to the loss of cell-attaching ability or damage to nucleic acids while the intact capsid remains (Leifels et al., 2019). Because such conditions are commonly encountered in environmental and food samples, overestimation of infectious HuNoV by viability RT-qPCR may occur, which is coherent with the adoption of a conservative approach in risk assessments (Ceuppens et al., 2014). PMAxx™ demonstrated to be unable to discriminate infectious virus inactivated at lower temperatures (Fig. 3) and returned lower Ct values compared to both 50 μM CL and 500 μM $PtCl_4$ (Fig. 2). Thus, it can be argued that PMAxx™ is the least effective

viability marker of those tested in this study, and caution should be used when interpreting results utilizing it in viability assays for HuNoV (Table 1). While the main focus of the study was to evaluate viability RT-PCR, significant insights into HuNoV infectivity and persistence were gained using the HIE model. Two different strains of HuNoV GII, namely GII.4 Sydney [P16] and HuNoV GII.6 [P7], were completely inactivated after heating at 60 °C for 10 min (Fig. 3). Exposing HuNoV to HPP, differing levels of resistance to inactivation were observed between the two genotypes depending on the medium. Specifically, HuNoV GI was more prone to inactivation by HPP than GII in PBS, but it was more resistant to inactivation in strawberry puree (Fig. 6). This finding represents the inaugural comparative analysis of the behaviour of different HuNoV genotypes under various conditions, shedding light on the complex interplay between viral strains and food matrices in the face of food processing. Using RT-qPCR, Cromeans et al. (2014) compared the reductions of HuNoV GI.5 and GII.13 suspensions exposed to increasing HPP pressures for 1 min, concluding that GI was more sensitive than GII. In the same study, TV was the most resistant cultivable surrogate virus among many tested, being completely inactivated at 600 MPa. Regrettably, the reductions in TV RNA levels were not correlated with TV infectivity and did not align with the decrease observed in HuNoV RNA. Consequently, a definitive conclusion regarding HuNoV inactivation could not be reached. Based on infectivity data, our results interestingly support HuNoV GII as more resistant than TV to HPP in PBS (Fig. 5). Similar conclusions were reported for thermal inactivation estimating HuNoV infectivity by capsid integrity assays (Bartsch et al., 2019). Taking these findings together, the choice of a surrogate virus when assessing inactivation treatments need caution given the public health implications. Our infectivity data in HIE are consistent with the survival patterns measured for HuNoV using porcine

gastric mucin (PGM)-conjugated magnetic beads coupled with RT-qPCR as an expedient assay for assessing viral infectivity (Huang et al., 2016; Li et al., 2013; Ye et al., 2014). The authors reported that receptor-binding ability of HuNoV was completely lost following HPP treatments at ≥500 MPa for 2 min in blueberries and strawberries. Moreover, our results revealed distinct sensitivities of the two tested HuNoV genogroups to HPP treatments, with HuNoV GI.3[P13] displaying greater resistance compared to HuNoV GII.4 Sydney [P16], which is in agreement with literature (Huang et al., 2016; Li et al., 2013; Ye et al., 2014). This differential pressure resistance of HuNoV strains may be attributed to the inherent nature of the virus (e.g., thermodynamic stability, protein structure, and isoelectric point), even though experimental evidence is required to confirm such hypotheses. In conclusion, the viability RT-qPCR cannot fill the gap in knowledge around the inactivation of infectious HuNoV with absolute certainty. Our data further support the conclusion that RT-qPCR alone is not a reliable indicator of HuNoV infectivity, regardless of whether the viruses were subjected to heat or HPP treatments. This finding aligns with previous reports that have compared treated and untreated samples by direct RT-qPCR (Cromeans et al., 2014; Knight et al., 2013; Li et al., 2012; Sánchez et al., 2011). Our results from individual experiments and across replicates are largely consistent. However, occasional discrepancies were noted, such as the partial or complete inactivation of HuNoV GII at 400 MPa in PBS (Figs. 5 and 6), prompting concerns regarding the variable replication rates within the HIE model. In this sense, the limit of detection of the HIE assay ($10^{3–4}$ GC/well) restricts the interpretation of samples where no replication is observed. This does not necessarily confirm a non-infectious sample, as undetected infectious viral particles could still be present. Besides that, the HIE system has significant value as it remains one of the few robust options (e.g.,

zebra fish, and salivary glands) (Ghosh et al., 2022; Tan et al., 2023; Van Dycke et al., 2019) for specifically identifying infectious HuNoV, despite the extensive efforts needed and multiple methodological hurdles, which are still pending to be overcome.

Funding This research was supported by "PREVISION" _(PID2019-105509RJ-I00, MCIN/AEI/10.13039/501100011033) project funded to WR. AM is supported by a predoctoral research grant funded by University of Bari "A. Moro" _(Italy). IATA-CSIC is a Centre of Excellence Severo Ochoa (CEX2021-001189-S MCIN/AEI/10.13039/501100011033). SQW and MK are supported by the U.S. Food and Drug Administration. The findings and conclusions in this article are those of the authors and do not necessarily represent those of the U.S. Food and Drug Administration. The funding sources had no role in the study design, data collection, analysis of data, writing, or in the decision to publish.

CRediT authorship contribution statement Samantha Q. Wales: Conceptualization, Investigation, Methodology, Writing – review & editing. **Annamaria Pandiscia:** Investigation, Methodology. **Michael Kulka:** Investigation, Methodology, Writing – review & editing. **Gloria Sánchez:** Writing – review & editing. **Walter Randazzo:** Conceptualization, Data curation, Formal analysis, Funding acquisition, Project administration, Resources, Supervision, Writing – original draft, Writing – review & editing.

Declaration of competing interest

The authors declare that they have no known competing financial interests or personal relationships that could have appeared to influence the work reported in this paper.

Data availability

Data will be made available on request.

Acknowledgements Authors would like to thank Dr. Mary K. Estes (Baylor College of Medicine, Houston, TX) and Prof. Javier Buesa (Department of Microbiology, School of Medicine, University of Valencia, Valencia, Spain) for providing secretor positive HIEs (J2 cell line), and human norovirus-positive faecal samples, respectively. Also, Dr. A. Martinez Lopez and M. D. Rodrigo Aliaga (IATA-CSIC) are acknowledged for providing access to high pressure equipment and assisting in HPP experiments. Authors also acknowledge PROMEGA for providing Viability PCR Crosslinker Kit (CL, cat. CS333003).

References

Bartsch, C., Plaza-Rodriguez, C., Trojnar, E., Filter, M., Johne, R., 2019. Predictive models for thermal inactivation of human norovirus and surrogates in strawberry puree. Food Control 96, 87–97. https://doi.org/10.1016/j.foodcont.2018.08.031.

Bozkurt, H., Phan-Thien, K.-Y., van Ogtrop, F., Bell, T., McConchie, R., 2021. Outbreaks, occurrence, and control of norovirus and hepatitis a virus contamination in berries: a review. Crit. Rev. Food Sci. Nutr. 61, 116–138. https://doi.org/10.1080/ 10408398.2020.1719383.

Carmona, N., Randazzo, W., 2023. Passaging human intestinal organoids and monolayers set up. Protoc. Exch. https://doi.org/10.21203/rs.3.pex-2221/v1.

Ceuppens, S., Li, D., Uyttendaele, M., Renault, P., Ross, P., Ranst, M.V., Cocolin, L., Donaghy, J., 2014. Molecular methods in food safety microbiology: interpretation and implications of nucleic acid detection. Compr. Rev. Food Sci. Food Saf. 13, 551–577. https://doi.org/10.1111/1541-4337.12072.

Chen, J., Wu, X., Sánchez, G., Randazzo, W., 2020. Viability RT-qPCR to detect potentially infectious enteric viruses on heat-processed berries. Food Control 107, 106818.

https://doi.org/10.1016/j.foodcont.2019.106818.

Chhabra, P., Ranjan, P., Cromeans, T., Sambhara, S., Vinj´e, J., 2017. Critical role of RIG-I and MDA5 in early and late stages of tulane virus infection. J. Gen. Virol. 98, 1016–1026. https://doi.org/10.1099/jgv.0.000769.

Costantini, V., Morantz, E.K., Browne, H., Ettayebi, K., Zeng, X.-L., Atmar, R.L., Estes, M. K., Vinj´e, J., 2018. Human norovirus replication in human intestinal enteroids as model to evaluate virus inactivation. Emerg. Infect. Dis. 24, 1453–1464. https://doi. org/10.3201/eid2408.180126.

Cromeans, T., Park, G.W., Costantini, V., Lee, D., Wang, Q., Farkas, T., Lee, A., Vinj´e, J., 2014. Comprehensive comparison of cultivable norovirus surrogates in response to different inactivation and disinfection treatments. Appl. Environ. Microbiol. 80, 5743–5751. https://doi.org/10.1128/AEM.01532-14.

Desdouits, M., Polo, D., Le Mennec, C., Strubbia, S., Zeng, X.L., Ettayebi, K., Atmar, R.L., Estes, M.K., Le Guyader, F.S., 2022. Use of human intestinal enteroids to evaluate persistence of infectious human norovirus in seawater. Emerg. Infect. Dis. 28, 1475–1479. https://doi.org/10.3201/EID2807.220219.

Esseili, M.A., Meulia, T., Saif, L.J., Wang, Q., 2018. Tissue distribution and visualization of internalized human norovirus in leafy greens. Appl. Environ. Microbiol. 84 https://doi.org/10.1128/AEM.00292-18.

Estes, M.K., Ettayebi, K., Tenge, V.R., Murakami, K., Karandikar, U., Lin, S.C., Ayyar, B. V., Cortes-Penfield, N.W., Haga, K., Neill, F.H., Opekun, A.R., Broughman, J.R., Zeng, X.L., Blutt, S.E., Crawford, S.E., Ramani, S., Graham, D.Y., Atmar, R.L., 2019. Human norovirus cultivation in nontransformed stem cell-derived human intestinal enteroid cultures: success and challenges. Viruses 11. https://doi.org/10.3390/ v11070638.

Ettayebi, K., Crawford, S.E., Murakami, K., Broughman, J.R., Karandikar, U., Tenge, V.R., Neill, F.H., Blutt, S.E., Zeng, X.L., Qu, L., Kou, B., Opekun, A.R., Burrin, D., Graham, D.Y., Ramani, S., Atmar, R.L., Estes, M.K., 2016. Replication of human noroviruses in stem cell-derived human enteroids. Science 353, 1387–1393. https:// doi.org/10.1126/SCIENCE.AAF5211.

Fraisse, A., Niveau, F., Hennechart-Collette, C., Coudray-Meunier, C., Martin-Latil, S., Perelle, S., 2018. Discrimination of infectious and heat-treated norovirus by combining platinum compounds and real-time RT-PCR. Int. J. Food Microbiol. 269, 64–74.

https://doi.org/10.1016/J.IJFOODMICRO.2018.01.015.

Ghosh, S., Kumar, M., Santiana, M., Mishra, A., Zhang, M., Labayo, H., Chibly, A.M., Nakamura, H., Tanaka, T., Henderson, W., Lewis, E., Voss, O., Su, Y., Belkaid, Y., Chiorini, J.A., Hoffman, M.P., Altan-Bonnet, N., 2022. Enteric viruses replicate in salivary glands and infect through saliva. Nature 607, 345–350. https://doi.org/ 10.1038/s41586-022-04895-8.

Ho, J., Seidel, M., Niessner, R., Eggers, J., Tiehm, A., 2016. Long amplicon (LA)-qPCR for the discrimination of infectious and noninfectious phix174 bacteriophages after UV inactivation. Water Res. 103, 141–148. https://doi.org/10.1016/j. watres.2016.07.032.

Huang, R., Ye, M., Li, X., Ji, L., Karwe, M., Chen, H., 2016. Evaluation of high hydrostatic pressure inactivation of human norovirus on strawberries, blueberries, raspberries and in their purees. Int. J. Food Microbiol. 223, 17–24. https://doi.org/10.1016/J. IJFOODMICRO.2016.02.002.

ISO 15216-1, 2017. Microbiology of food and animal feed—Horizontal method for determination of Hepatitis A Virus and norovirus in food using real-time RT-PCR—Part 1. Method Quantif.

Katayama, K., Shirato-Horikoshi, H., Kojima, S., Kageyama, T., Oka, T., Hoshino, F.B., Fukushi, S., Shinohara, M., Uchida, K., Suzuki, Y., Gojobori, T., Takeda, N., 2002. Phylogenetic analysis of the complete genome of 18 norwalk-like viruses. Virology 299, 225–239. https://doi.org/10.1006/viro.2002.1568.

Knight, A., Li, D., Uyttendaele, M., Jaykus, L.-A., 2013. A critical review of methods for detecting human noroviruses and predicting their infectivity. Crit. Rev. Microbiol. 39, 295–309. https://doi.org/10.3109/1040841X.2012.709820.

Koopmans, M., 2008. Progress in understanding norovirus epidemiology. Curr. Opin. Infect. Dis. 21, 544–552. https://doi.org/10.1097/QCO.0B013E3283108965.

Leifels, M., Shoults, D., Wiedemeyer, A., Ashbolt, N.J., Sozzi, E., Hagemeier, A., Jurzik, L., 2019. Capsid integrity qPCR—an azo-dye based and culture-independent approach to estimate adenovirus infectivity after disinfection and in the aquatic environment. Water. https://doi.org/10.3390/w11061196.

Leifels, M., Dan, C., Sozzi, E., Shoults, D.C., Wuertz, S., Mongkolsuk, S., Sirikanchana, K., 2020. Capsid integrity quantitative PCR to determine virus infectivity in environmental and food applications – _a systematic review. Water Res. X 11, 100080. https://doi.org/10.1016/j.wroa.2020.100080.

Li, D., Baert, L., Xia, M., Zhong, W., Van Coillie, E., Jiang, X., Uyttendaele, M., 2012. Evaluation of methods measuring the capsid integrity and/or functions of noroviruses by heat inactivation. J. Virol. Methods 181, 1–5. https://doi.org/ 10.1016/j.jviromet.2012.01.001.

Li, X., Chen, H., Kingsley, D.H., 2013. The influence of temperature, pH, and water immersion on the high hydrostatic pressure inactivation of GI.1 and GII.4 human noroviruses. Int. J. Food Microbiol. 167, 138–143. https://doi.org/10.1016/j. ijfoodmicro.2013.08.020.

Parra, G.I., Squires, R.B., Karangwa, C.K., Johnson, J.A., Lepore, C.J., Sosnovtsev, S.V., Green, K.Y., 2017. Static and evolving norovirus genotypes: implications for epidemiology and immunity. PLoS Pathog. 13, e1006136 https://doi.org/10.1371/ journal.ppat.1006136.

Parshionikar, S., Laseke, I., Fout, G.S., 2010. Use of propidium monoazide in reverse transcriptase PCR to distinguish between infectious and noninfectious enteric viruses in water samples. Appl. Environ. Microbiol. 76, 4318–4326. https://doi.org/ 10.1128/AEM.02800-09.

Pecson, B.M., Ackermann, M., Kohn, T., 2011. Framework for using quantitative PCR as a nonculture based method to estimate virus infectivity. Environ. Sci. Technol. 45, 2257–2263. https://doi.org/10.1021/es103488e.

Puente, H., Randazzo, W., Falco, I., Carvajal, A., Sánchez, G., 2020. Rapid selective detection of potentially infectious porcine epidemic diarrhea coronavirus exposed to heat treatments using viability RT-qPCR. Front. Microbiol. 11, 1911.

Randazzo, W., Lopez-Galvez, F., Allende, A., Aznar, R., Sánchez, G., 2016. Evaluation of viability PCR performance for assessing norovirus infectivity in fresh-cut vegetables and irrigation water. Int. J. Food Microbiol. 229, 1–6. https://doi.org/10.1016/j. ijfoodmicro.2016.04.010.

Randazzo, W., Khezri, M., Ollivier, J., Le Guyader, F.S., Rodríguez-Díaz, J., Aznar, R., Sánchez, G., 2018. Optimization of PMAxx pretreatment to distinguish between human norovirus with intact and altered capsids in shellfish and sewage samples. Int. J. Food Microbiol. 266 https://doi.org/10.1016/j.ijfoodmicro.2017.11.011.

Randazzo, W., Costantini, V., Morantz, E.K., Vinjé, J., 2020. Human intestinal enteroids to evaluate human norovirus GII.4 inactivation by aged-green tea. Front. Microbiol. 11, 1917. https://doi.org/10.3389/fmicb.2020.01917.

Raymond, P., Paul, S., Guy, R.A., 2023. Impact of capsid and genomic integrity tests on norovirus extraction recovery rates. Foods (Basel, Switzerland) 12. https://doi.org/ 10.3390/foods12040826.

Sánchez, G., Aznar, R., Martínez, A., Rodrigo, D., 2011. Inactivation of human and murine norovirus by high-pressure processing. Foodborne Pathog. Dis. 8, 249–253. https://doi.org/10.1089/fpd.2010.0667.

Tan, M.T.H., Gong, Z., Li, D., 2023. Use of zebrafish embryos to reproduce human norovirus and to evaluate human norovirus infectivity decay after UV treatment. Appl. Environ. Microbiol. 89, e0011523 https://doi.org/10.1128/aem.00115-23.

Van Dycke, J., Ny, A., Conceiç˜ao-Neto, N., Maes, J., Hosmillo, M., Cuvry, A., Goodfellow, I., Nogueira, T.C., Verbeken, E., Matthijnssens, J., de Witte, P., Neyts, J., Rocha-Pereira, J., 2019. A robust human norovirus replication model in zebrafish larvae. PLoS Pathog. 15, e1008009.

Williams-Woods, J., Rodriguez, R., Marchant, J., Gail Swinford, A., Burkhardt, W., 2022. FDA BAM Chapter 26: Concentration, Extraction and Detection of Enteric Viruses from Food, in: Bacteriological Analytical Manual (BAM).

Ye, M., Li, X., Kingsley, D.H., Jiang, X., Chen, H., 2014. Inactivation of human norovirus in contaminated oysters and clams by high hydrostatic pressure. Appl. Environ. Microbiol. 80, 2248–2253. https://doi.org/10.1128/AEM.04260-13.

Yu, C., Wales, S.Q., Mammel, M.K., Hida, K., Kulka, M., 2016. Optimizing a custom tiling microarray for low input detection and identification of unamplified virus targets. J. Virol. Methods 234, 54–64. https://doi.org/10.1016/j.jviromet.2016.03.013.á

8. SURVIVAL MODELLING OF INFECTIOUS HUMAN NOROVIRUS AND SURROGATES FOR HIGH-PRESSURE INACTIVATION IN STRAWBERRY PUREE

A comprehensive risk assessment aimed at developing preventive strategies in the food industry (e.g., postharvest processing interventions) have been hindered by the lack of a permissive cell line to assess HuNoV infectivity [179,180].

Nowadays, the European standard ISO 15216-1:2017, based on RT-qPCR methodology, is employed for detection and quantification of HuNoV RNA in high-risk foods, such as berries, vegetables, shellfish, and ready-to-eat products that are susceptible to viral contamination [181]. However, this standardized method doesn't provide information about the structural integrity and infectivity of HuNoV viral as demonstrated in previous scientific works [9,16]. Therefore, novel strategies have been introduced to evaluate the most effective methods for testing viral infectivity and to assess the efficacy of non-thermal technologies in inactivating enteric viruses, particularly HuNoV, due to its significant role in foodborne illness.

Based on the promising features of HPP as preservation technology to control HuNoV contamination in food matrices (as already described in chapter 3 and 5), we conducted a scientific study testing the efficacy of HPP in inactivating MNV-1, TV and HuNoV in strawberry puree and validating the operational parameters (e.g., holding pressure and exposure time) for HPP, using infectivity data obtained with the novel HIE system. Furthermore, the results obtained were used to propose mathematical models and to define the kinetic constants for developing suitable HPP processes to control HuNoV contamination in strawberry puree since mathematical models help to evaluate the efficacy of processing variables on microorganisms subjected to thermal or non-

thermal processes and predict the kinetic inactivation of foodborne pathogens providing predictive data about their inactivation/survival [180].

Article adapted for printing of the PhD thesis. Available online on Innovative Food Science and Emerging Technologies, ELSEVIER, https://doi.org/10.1016/j.ifset.2024.103702

Survival modelling of infectious human norovirus and surrogates for high-pressure inactivation in strawberry puree

Annamaria Pandiscia [a,b], Irene Falcó[a,c], Valentina Terio [b], Antonio Martínez [a], Gloria Sánchez [a], Dolores Rodrigo [a], Walter Randazzo [a,*]

[a]*Department of Preservation and Food Safety Technologies, Institute of Agrochemistry and Food Technology, IATA-CSIC, Avda. Catedrático Agustín Escardino 7, Valencia, Paterna 46980, Spain*

[b]*Department of Veterinary Medicine, University of Bari, Provincial Road to Casamassima Km 3, Bari, Valenzano 70010, Italy*

[c] *Department of Microbiology and Ecology, University of Valencia, Av. Dr. Moliner, 50, Burjassot 46100, Valencia, Spain*

DOI: https://doi.org/10.1016/j.ifset.2024.103702

Highlights

•The HIE model can be used to assess HuNoV infectivity in berry purees.

•Tulane virus resulted more resistant than murine norovirus to HPP.

•Weibull distribution function described virus survival for HPP inactivation.

•Treatments at 450 MPa for 5 min control virus contamination in strawberry puree.

Abstract

Berries contaminated with human norovirus (HuNoV) have been frequently identified as a cause of foodborne gastroenteritis. To prevent virus transmission while preserving sensory and quality parameters, non-thermal treatments, such as high-pressure processing (HPP), can be applied to the berries and products thereof. Here, strawberry purees contaminated with HuNoV genogroup I (GI.3[P13]) and II (GII.4 Sydney [P16]), along with murine norovirus (MNV) and Tulane virus (TV) serving as surrogates, were exposed to HPP at several pressure-time combinations. Virus inactivation was assessed by cell culture, including the novel human intestinal enteroids (HIE) model for HuNoVs. The infectivity results showed TV more resistant than MNV to HPP, as also confirmed by kinetic mathematical modelling. Results indicated that a holding pressure of 450 MPa and an exposure time of ≥5 min are reliable operational conditions for HPP process to successfully control viral contamination. In addition, the inactivation models deduced from MNV and TV viruses were challenged with experimental HuNoV GII.4 infectivity resulting in bias factors <1 for all treatment conditions. This finding validates the proposed models for the conservative estimation of HuNoV inactivation. Our work offers a blueprint for moving forward with inactivation studies using the HIE system, which provides useful practical information on optimum treatments for the best public health outcomes.

Keywords: Human intestinal enteroids; Cell culture; Food safety; Viral pathogens ;Risk assessment

1. Introduction

Berries are an essential component of a healthy diet and their consumption has been increasing worldwide as either fresh fruit, frozen products to be used in several culinary preparations, or as smoothies or purees (Vahapoglu, Erskine, Subasi, & Capanoglu, 2021). However, human norovirus (HuNoV) has been reported as one of the most common pathogens linked to the consumption of berries representing a serious public health threat (Bozkurt, Phan-Thien, van Ogtrop, Bell, & McConchie, 2021; Nasheri, Vester, & Petronella, 2019). To date, fresh and frozen berries have been globally involved in sixty-eight viral foodborne disease outbreaks, with forty-six caused by HuNoV and resulting in 15,000 notified cases (Bozkurt et al., 2021; FDA, 2022). In Europe, more than ten notifications of frozen berries contaminated by HuNoV have been reported in the Rapid Alert System for Food and Feed (RASFF) portal over the last three years (2020 to 2023). Based on the epidemiological data, the World Health Organization (WHO) included HuNoV as one of the food-borne pathogens of concern for both fresh and frozen berries (JEMRA, 2023, 2024). HuNoVs are members of the family *Caliciviridae* and considered the main cause of acute virus gastroenteritis in children and adults (Koopmans, 2008). HuNoVs are non-enveloped viruses which are typically transmitted by the faecal–oral route either in person-to-person and food contaminated scenarios. Berries can be contaminated by irrigation water, fertilizers or infected harvesters and food handlers (Codex Alimentarius, 2012). Moreover, they are manually collected, and post-harvest sanitizing wash is not commonly applied as it reduces their shelf life (Bower, 2007). In addition, several studies showed that infectious HuNoV can persist for at least seven days in frozen berries (Bartsch et al., 2016; Butot, Putallaz, & Sánchez, 2008;

Li, Butot, Zuber, & Uyttendaele, 2018; Verhaelen, Bouwknegt, Lodder-Verschoor, Rutjes, & de Roda Husman, 2012).

Thermal processing methods can prevent microbial hazards linked with the consumption of berries but, unfortunately, they severely affect the nutritional and sensorial quality of food (Aadil, Madni, Roobab, Rahman, & Zeng, 2019). Nowadays, high hydrostatic pressure processing (HPP) represents one of the most promising non-thermal food processing techniques to overcome this problem. Moreover, HPP does not significantly affect the physical properties, visual appearance, aroma, colour and overall acceptability of strawberry puree (Huang et al., 2016; Huang, Ye, & Chen, 2013). Several studies applied HPP against bacterial pathogens in different food products, while information on the susceptibility of infectious HuNoV has been inferred using molecular methods or cultivable surrogates, such as murine norovirus (MNV), feline calicivirus (FCV) and Tulane virus (TV) (Cannon et al., 2006; Chen, Hoover, & Kingsley, 2005; Cromeans et al., 2014; DiCaprio, Ye, Chen, & Li, 2019; Govaris & Pexara, 2021; Huang et al., 2016; Jones et al., 2014; Kingsley, Holliman, Calci, Chen, & Flick, 2007; Li, Chen, & Kingsley, 2013; Pan, Buenconsejo, Reineke, & Shieh, 2016; Sánchez, Aznar, Martínez, & Rodrigo, 2011). However, molecular methods do not inform on virus infectivity, and surrogates provide biased data and still represent an indirect estimation for the actual human virus pathogen (Li, Chen, & Kingsley, 2013; Wales, Pandiscia, Kulka, Sánchez, & Randazzo, 2024). Alternatively, approaches based on capsid integrity coupled with quantitative reverse transcription real-time PCR (RT-qPCR) have been reported for HuNoV, including porcine gastric mucine (PGM) assays or viability RT-qPCR (Dancho, Chen, & Kingsley, 2012; Tong et al., 2023). All these previous findings collectively cover a broad range of pressures (from 300 to 600 MPa) that ensure virus inactivation. Discrepancies result also from

the outcomes of clinical trial studies (Leon et al., 2011) and gnotobiotic pig models (Fangfei et al., 2015), in which pressure effective treatments for oysters were identified at 600 or 350 MPa, respectively. These variations are a consequence of diverse experimental designs, including the tested virus, temperature, holding pressure time, time exposure, pH, matrix/suspension, testing method, among other factors. Recently, a novel three-dimensional (3D) cell culture technique based on non-transformed stem cell-derived human intestinal enteroids (HIEs) which recapitulate the complexity and cell diversity of the gastrointestinal tract, was used to assess the HuNoV infection (Costantini et al., 2018; Ettayebi et al., 2016). Actually, a handful of studies assessed HuNoV persistence and susceptibility in food and environment by using the complex and demanding HIE system (Allende et al., 2024; Desdouits et al., 2022; Escudero-Abarca et al., 2020; Irene Falcóet al., 2023; Overbey, Zachos, Coulter, & Schwab, 2021; Overbey, Zachos, Coulter, Jacangelo, & Schwab, 2021; Randazzo, Costantini, Morantz, & Vinje, 2020). In a recent study, we showed that 500 MPa HPP treatment completely inhibits HuNoV GII.4 infectivity in the HIE model, while lower pressure of 400 MPa reduced the infectious virus titer but cell infection was not fully prevented (Falcóet al., 2023). Treatments at 450 MPa for 5 min inactivated HuNoV GII.4 in PBS and strawberry puree (Wales et al., 2024), while HuNoV GI.3 was inactivated in PBS only. Taking all these results together, pressures in the 450–600 MPa range are suggested to be targeted for the complete inactivation of infectious HuNoV (Huang et al., 2016; Li et al., 2013; Ye, Li, Kingsley, Jiang, & Chen, 2014; Falcó et al., 2023; Wales et al., 2024; Leon et al., 2011). However, due to the different experimental designs and techniques adopted in previous studies, resulting in diverse patterns of virus inactivation, a definitive conclusion regarding HuNoV pressure inactivation could not be reached. The main objective of this study was to validate the operational

parameters for HPP processing as an effective intervention for controlling HuNoV contamination in berry puree using infectivity data obtained with the novel HIE system. Moreover, to investigate the kinetic inactivation and generate predictive models, suboptimal pressure treatments have been included in the experimental design to target residual virus infectivity. To this end, we evaluated HPP at different combinations of pressure (300, 400 and 450 MPa) and exposure time on MNV, TV and HuNoV infectivity in strawberries puree using cell culture methods. The resulting dataset was used to propose mathematical models and to define the kinetic constants for developing suitable HPP processes to control HuNoV contamination in strawberry puree.

2. Material and methods

2.1. Virus strains, clinical samples, cell lines, and infectivity assays

Human genogroup I (GI.3[P13]) and II (GII.4 Sydney [P16]) norovirus-positive faecal samples were selected as successfully tested to replicate in the HIE model. Faecal samples were suspended in phosphate-buffered saline (PBS) to a final 10% (wt/vol) suspension. Clarified stool suspensions were prepared by passing through serial filters (5, 1, 0.45, and 0.22 μm) as described previously (Costantini et al., 2018) and stored at -80 °C in aliquots. TV and MNV were used as HuNoV surrogates and tested by cell culture as detailed hereafter. TV provided by Prof. Farkas (Louisiana State University, LA, US) was grown and assayed in LLC-MK2 cell line (ATCC CCL-7) cultured in Opti-MEM (Gibco Life Technologies, Grand Island, NY) supplemented with 2% of heat-inactivated fetal bovine serum (FBS; GE Healthcare Bio-Sciences, Austria) and 2% of an antibiotic cocktail of penicillin and streptomycin. MNV-1 was propagated and assayed in RAW 264.7 (ATCC TIB-71) cultured in Dulbecco's Modified Eagle's

Medium (DMEM; Biowest, Nuaill´e, France) supplemented with 10% FBS, 1% of an antibiotic cocktail of penicillin and streptomycin, 1% of L-glutamine and 1% of Hepes. The LLC-MK2 and RAW 264.7 cells were cultured in T75 flasks at 37 °C in a 5% CO2 incubator. MNV and TV infectivity was calculated by determining the 50% tissue culture infectious dose ($TCID_{50}$) using the Spearman-Karber method after visual inspection of cells for presence of cytopathic effect (CPE) after 48 and 96 h post infection (hpi), respectively. Briefly, ten-fold serial dilutions of MNV and TV were prepared in PBS and 20 µl per well were inoculated on a total of eight wells. After 1 h post infection 150 µl of post-infection media, DMEM supplemented with 2% of FBS or Opti-MEM, were added to each well and plates were incubated at 37 çC in a 5% CO2 incubator and monitored for CPEs (Falcó et al., 2017; Randazzo et al., 2020).

2.2. Maintenance, differentiation and infection of human intestinal enteroids

Secretor positive HIEs derived from human jejunal biopsy (J2 cell line) were provided by Prof. Mary K. Estes (Baylor College of Medicine, Houston, TX). Undifferentiated 3D HIEs and differentiated monolayers were maintained and produced using commercial IntestiCult™ _Organoid Medium Human media (STEMCELL Technologies Inc.) following the optimized protocol described in (Carmona & Randazzo, 2023). In brief, HIE cultures were maintained and propagated as undifferentiated 3D cultures embedded in Matrigel using Organoid Growth Media (OGM), prepared by mixing equal volumes of components A and B, and supplemented with 10 mM ROCK inhibitor Y-27632. After 7 days, highly dense 3D cultures were dissociated into a single cell suspension and plated as undifferentiated monolayers. To this end, domes were broken and cells resuspended in Gentle Cell Dissociation Reagent (STEMCELL Technologies Inc.). After 10 min incubation on a rocking

platform, dissociated cells were pelleted for 5 min at 200 ×*g*, resuspended in OGM, and seeded onto a 96-well plate previously coated with collagen IV. After 24 h at 37 ◦C in 5% CO2, OGM was replaced with differentiation medium (ODM), to induce monolayer differentiation. ODM was prepared by mixing an equal volume of component A and CMGF- medium (consisted of advanced DMEM–F-12 medium supplemented with 100 U/ml penicillin-streptomycin, 10 mM HEPES buffer, and 1 × _GlutaMAX). HIE cell monolayers resulted differentiated and 100% confluent after five- to seven-days and used for HuNoV infections as described hereafter. Two sets of 96-well plates with 100% confluent differentiated HIE monolayers were inoculated in triplicate with 100 µl of each HuNoV sample and incubated at 37 ◦C for 1 h. After the inoculum was removed, monolayers were washed twice with CMGF-, and 100 µl of ODM was added to each well. For each set of infections, one 96-well plate was immediately frozen at -80 °C (1 hpi) and the second plate was incubated at 37 °C and 5% CO_2 for 48 h (48 hpi) and then frozen. Finally, RT-qPCR was used to determine the amount of HuNoV RNA from HIE monolayers at 1 and 48 hpi to evaluate HuNoV replication. Virus RNA was detected and quantified as described in Section 2.6.

2.3. Inoculation of berry purees and infectivity titration

Fresh strawberries, blueberries, and raspberries were purchased from a local market and purees obtained using an electric blender. Resulted purees were characterized for total soluble solids (TSS), and total titratable acidity (TA) using a PAL-BX/ACID1 (ATAGO, Tokyo, Japan) digital refractometer, and pH was determined by an accumet AE150 (Fisher Scientific, Madrid, Spain) instrument. As a preliminary step, potential cytopathic effects and virus replications were assessed by titrating MNV, TV, HuNoV GI.3[P13] and HuNoV GII.4 Sydney [P16] spiked in strawberries, blueberries, and

raspberries purees, either undiluted or diluted to 1:10, and 1:100 in corresponding postinfection media.

2.4. High-pressure processing assays

HPP were performed in a pilot scale unit (High-Pressure Food Processor, EPSI NV, Belgium) with a vessel operating pressure of 2.35 l and a maximum treatment pressure of 600 MPa. The pressure transmitting fluid was a mixture of water and ethylene glycol (70:30, v:v). HPP was applied in samples distributed in 300 µl PCR tubes, placed in polyethylene bags and heat-sealed (MULTIVAC Thermosealer). A constant holding temperature of 22 ± 1 °C was maintained during HPP as the pressure transmitting fluid was automatically and continually refrigerated. After completing the treatment, the samples were immediately stored at -80 °C. The kinetic inactivation of MNV, TV, HuNoV GI.3[P13] and GII.4 Sydney [P16] suspensions in PBS and strawberry puree inoculated at ratio 1:30 was investigated for HPP at 350, 400, and 450 MPa for increasing pressurization times. After the treatment, samples were stored at -80 °C until tested for virus infectivity by infection on cell cultures. PBS and strawberry puree samples inoculated with HuNoV GI.3 [P13] and GII.4 Sydney [P16] were diluted in CMGF- to 1:1000 final dilution to be used for HIE monolayers inoculation. Similarly, MNV and TV were diluted 1:10 in post infection media previous to monolayer infection.

2.5. Purification, detection and quantification of virus RNA by RT-qPCR

Virus RNA was extracted using the Maxwell® RSC Instrument (Promega) according to the manufacturer's instructions. Then, it was detected in duplicate by TaqMan RT-qPCR using the RNA UltraSense One-Step quantitative RT-PCR system (Invitrogen)

on a LightCycler 480 instrument (Roche Diagnostics, Germany). The set of primers and probe included in the ISO 15216-1 (2017) was used for detecting HuNoV GI.3 [P13] and GII.4 Sydney [P16]. Ten-fold serial dilutions of synthetic gBlock gene fragments (IDT) were included to quantify the HuNoV RNA into genome equivalents (HuNoV GI: y = -3.5106× + 37.329, R = 0.999; HuNoV GII: y = - 3.56× + 40.664, R = 0.997). Positive and negative amplification controls were included in each run.

2.6. Data modelling and assessment of models performance

Infectivity data for MNV, TV, and HuNoV GII.4 [P16]) exposed to HPP in strawberry purees were used for survival modelling. A data preprocessing step was applied to identify and remove outliers from experimental dataset for each virus, pressure and time exposure combination. Thereafter, the applicability of Weibull distribution function (Eq. 1) to fit the log10 -transformed experimental data was assessed by using GInaFiT software (Geeraerd, Valdramidis, & Van Impe, 2005).

(Eq. 1)

$$log_{10}(N) = log_{10}(N_0) - (\frac{t}{\delta})^p$$

where N ($TCID_{50}$/mL) represents the final concentration of virus; N0 ($TCID_{50}$/mL) is the initial concentration of virus; t is the time exposure during HHP treatment (min); δ _is the scale parameter; p is the shape parameter, which corresponds to a concave upward curve if $p < 1$, a downward convex curve if $p > 1$, and if $p = 1$ it describes a linear behavior. Defined the scale parameter (δ), its correlation to pressure was analyzed to represent the secondary model, finally informing on the reliability of our kinetic data (Fig. S1-S2). Fitting parameters are reported in the manuscript (Table 2, and Tables S1-S6). This secondary model should be able to predict virus scale

parameter (δ) at a pressure not tested experimentally. The models deduced for MNV and TV viruses were used to evaluate the performance of these viruses as surrogates by assessing the ability to predict HuNoV GII.4 inactivation using the Bias factor (Bf) (Ross, 1996) defined in Eq. 2 (Eq. 2) as follows:

(Eq. 2)

$$B_f = 10^{\frac{\Sigma\left[Log_{10}\left(\frac{X_{predicted}}{X_{observed}}\right)\right]}{n}}$$

where $X_{predicted}$ is the survival fraction predicted by the models deduced for MNV or TV, and $X_{observed}$ is the survival fraction obtained experimentally. B_f indicates whether the predicted data are numerically above or below the experimental data, thus indicating a structural deviation of the model. A bias factor with a value less than or equal to 1 indicates a conservative model, i.e. the estimated predictions are safe.

2.7. Statistical analysis

All data were compiled from at least three independent experiments with three technical replicates for each variable. Significant differences in mean infectivity were determined by the analysis of variance (ANOVA) followed by Dunnett's multiple comparisons test. Differences in means were considered significant when the p was <0.05. GraphPad Prism version 8 (GraphPad Software, USA) software was used for statistical analyses and data representation.

3.Results

3.1 Inoculation of berry purees and infectivity titration

Strawberry, blueberry and raspberry purees were physico-chemically characterized and pH, TSS, TA, and sugar/acid ratio determined (Table 1). RAW, LCC-MK2 and

HIE monolayers when infected with undiluted spiked strawberry, blueberry, and raspberry samples showed a cytotoxic effect, likely because of the acidity of the purees. Thus, 10- and 100-fold dilutions of samples in post infectious media were used to infect surrogates and HuNoVs, respectively. This allowed the successful replication of MNV, TV, and HuNoVs in berry purees showing 5–6 $\log_{10}$ $TCID_{50}$/mL titer

Table 1. Physico-chemical characterization of strawberry, blueberry and raspberry purees.

Berry puree	**pH**	**TSS[a]**	**TA[b]**	**Sugar/acid ratio**
Strawberry	3.45	6.0	0.52	11.5
Blueberry	2.87	12.4	1.75	7.09
Raspberry	3.46	14.7	0.84	17.5

[a]TSS, total soluble solids, (°Brix); [b]TA, total titratable acidity, (%w/w of citric acid).

for surrogates, and ≈1 and ≈3 $\log_{10}$ increase between 1 and 48 hpi for HuNoV GI.3[P13] and GII.4 Sydney [P16], respectively. These increases were consistent to those observed in PBS (Fig. 1).

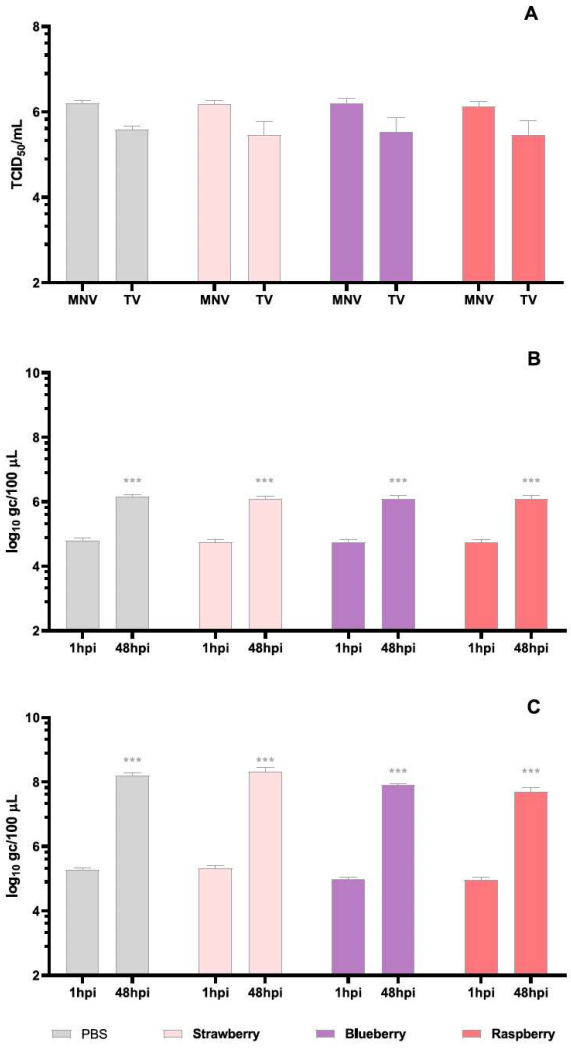

Fig. 1. Infectivity of MNV (Panel A), TV (Panel A), HuNoV GI.3[P13] (Panel B) and HuNoV GII.4 Sydney [P16] (Panel C) inoculated in PBS, strawberry, blueberry, and raspberry purees, diluted 1:10 (MNV, and TV) or 1:100 (HuNoV) and tested by cell culture. Error bars indicate SDs. Significant differences between 1 and 48 hpi were observed for all purees (***, $p < 0.001$).

3.2. Inactivation of MNV, TV, and infectious HuNoV exposed to HPP in buffer and strawberry puree

To comprehensively study the response of HuNoV to HPP in food matrices, strawberry puree was artificially contaminated with MNV, TV, HuNoV GI.3[P13] and HuNoV GII.4 Sydney [P16] and subjected to 350, 400 and 450 MPa for increasing time intervals. However, the limited amount of HuNoV GI.3[P13] faecal filtrate restricted

the HPP conditions to be tested, which were representatively selected (Fig. 2). The kinetic inactivation of infectious HuNoV and surrogates exposed to different combinations of pressure and time are shown in Fig. 2. Overall, either matrix (PBS vs strawberry puree), pressure (350, 400, or 450 MPa) and time exposure variables were significant to explain the differences observed for virus inactivation. Specifically, HPP at 350 MPa did not prevented the replication of surrogates in neither PBS nor strawberry puree. However, a time exposure-dependent decrease of their infectious titer was observed. Replication of HuNoVs exposed to 350 MPa was detected in strawberry puree for all exposure time tested, while it was prevented in PBS solution after 7.5 min for HuNoV GII.4 Sydney [P16] or 10 min treatments for HuNoV GII.4 Sydney [P16] and HuNoV GI.3[P13], respectively. Increasing the pressure to 400 MPa, TV and MNV in PBS were inactivated after 5 and 7.5 min, respectively, while residual infectivity was detected for both surrogates in strawberry puree for all the exposure time tested. HuNoV GII.4 Sydney [P16] was completely inactivated in 2.5 min in PBS, and in 7.5 min in strawberry puree. Residual HuNoV GII.4 Sydney [P16] infectivity was observed in strawberry puree for shorter time exposures. HuNoV GI.3[P13] treated at 400 MPa for 5 min resulted completely inactivated in PBS, but not in strawberry puree. HPP treatment at 450 MPa resulted in complete inactivation of MNV within 1 min, and both TV and HuNoV GII.4 Sydney [P16] within 5 min, whether in PBS or strawberry puree. The only exception was observed in strawberry puree inoculated with MNV, where the virus remained infectious after 1 min while it lost infectivity after 2.5 min. HuNoV GI.3 [P13] inactivation data at 450 MPa resulted discrepant, as infectious virus was observed in either PBS and strawberry puree after 5 min, which was the longer exposure time tested at that pressure. We observed a

baroprotective effect of the strawberry matrix, as infectious viruses were detected in the puree but not in PBS for several combinations of time and pressure exposure.

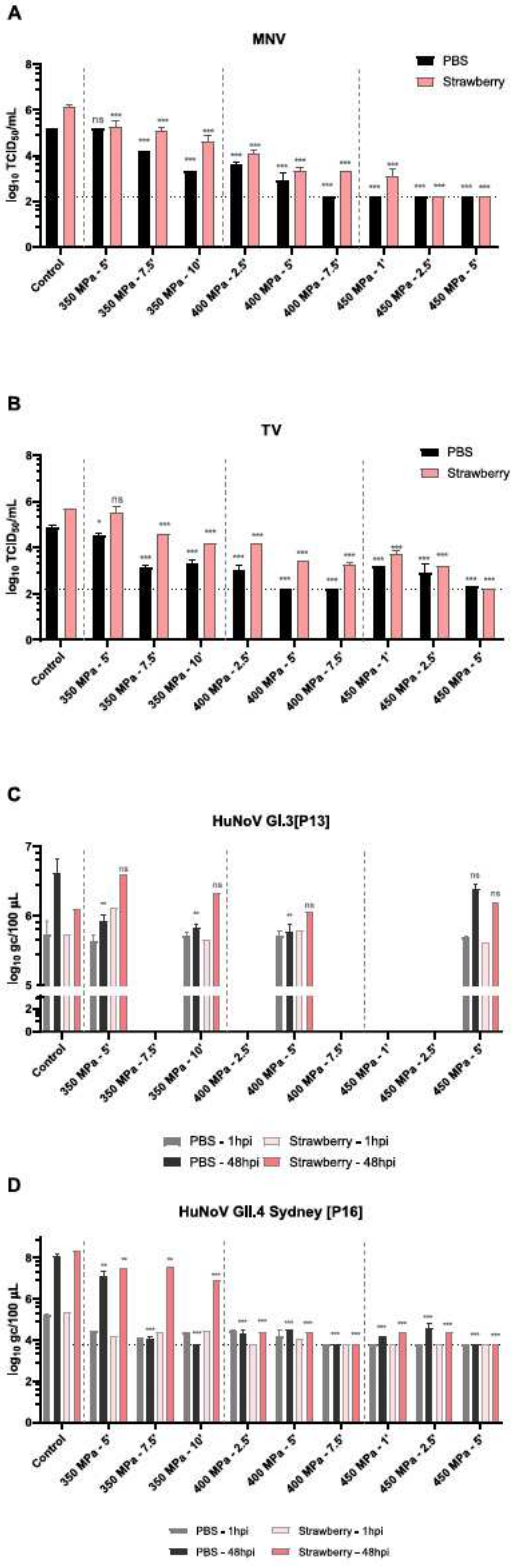

Fig. 2. Inactivation of murine norovirus (MNV, Panel A), Tulane virus (TV, Panel B), human norovirus genogroup I (HuNoV GI.3[P13], Panel C) and HuNoV GII.4 Sydney [P16] (Panel D) by high pressure

in PBS and strawberry puree as determined by cell culture ($TCID_{50}$ for surrogates, or virus RNA increase on human intestinal enteroids for HuNoV). Error bars indicate SDs. Asterisks indicate significant difference from untreated PBS or puree controls: ***p < 0.001; **p < 0.01; ns, no significant difference; dashed line indicates the limit of quantification of $TCID_{50}$ (MNV and TV) or HIE/RT-qPCR (HuNoV) assays.

3.3. Predictive models for HuNoV infectivity

Experimental data for each combination of virus, pressure and exposure time were initially curated. We chose to model the survival curves in strawberry puree due to the food safety significance of the pathogen in this specific food matrix. Additionally, the number of suitable data points for PBS samples was restricted by the complete inactivation of viruses observed for various HPP treatments in buffered solution (PBS). Infectivity data of MNV and TV in strawberry purees were successfully modelled (Fig. 3, Table 2, and Tables S1-S6). MNV and TV inactivation curves for 350, 400, and 450 MPa HPP never followed a straight line; thus they could not be analyzed by using a log-linear model. Among all the models tested, the Weibull distribution function (Eq. 1) showed the best fit for the survival curves of MNV and TV at the tested pressure levels. According to these results (Tables S1-S6), the low root mean square errors (RMSE) indicate the good fit of the Weibull distribution function, which can be used to describe the virus inactivation curves in strawberry puree. According to Table 2, TV was more resistant to pressure than the MNV, since the scale parameter (δ), which is the kinetic equivalent, was greater for each of the pressures in the study. Additionally, a secondary model was deduced to correlate primary parameter with pressure for both viruses modelled. In all cases a good square correlation coefficient was obtained (Figs. S1 and S2). Moreover, the models deduced for MNV and TV were challenged with experimental HuNoV GII.4 inactivation data

to test their ability to predict the inactivation of the human virus pathogen by means of the bias factor (Eq. 2). For all the studied conditions, inactivation rates predicted were lower than the ones experimentally observed for HuNoV GII.4. Specifically, bias factors ranged between 0.60 and 0.93. Therefore, given that bias factors were lower than 1 for all treatment conditions, the use of the proposed inactivation models based on surrogates represents a conservative approach as it guarantees the food safety.

Table 2. Parameter of scale and shape of the Weibull survival function used in fitting the survival curves.

Virus	350 MPa			400 MPa			450 MPa		
	δ	**p**	**RMSSE**	**δ**	**p**	**RMSSE**	**δ**	**p**	**RMSSE**
MNV	4.47	0.68	0.3721	0.36	0.32	0.2630	0.01	0.21	0.9369
TV	7.82	2.13	0.4418	1.06	0.49	0.1555	0.23	0.40	0.1393

MNV, murine norovirus; TV, Tulane virus; δ, scale parameter (min-1); p, shape parameter; RMSSE, root mean sum of squared error.

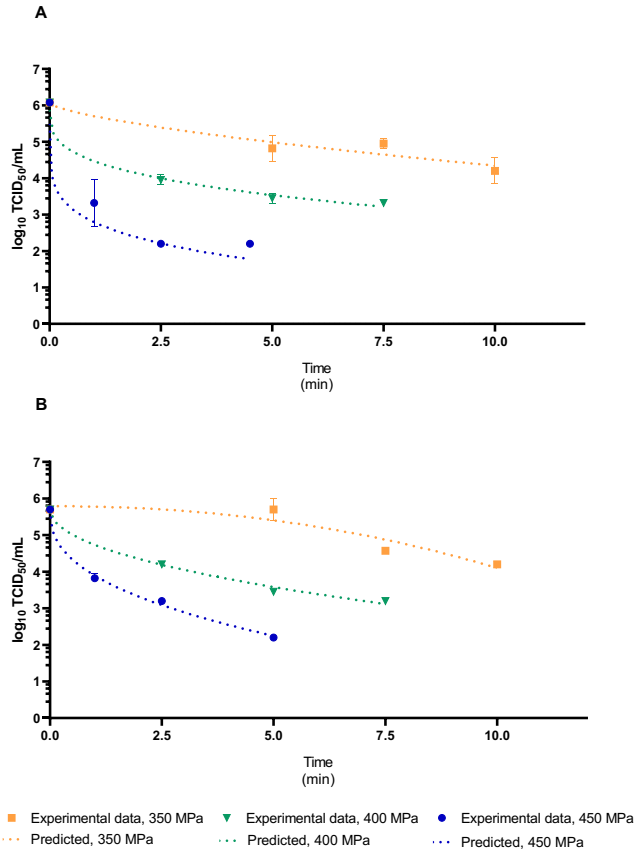

Fig. 3. Inactivation of murine norovirus (A) and Tulane virus (B) virus in strawberry puree HPP treated at 350, 400 and 450 MPa as compared to Weibull survival functions.

4. Discussion

Monitoring programmes have been implemented worldwide by national food safety agencies to determine HuNoV contamination levels using standardized molecular methodologies targeting virus RNA (ISO 15216-1, 2017; Williams-Woods, Rodriguez, Marchant, Gail Swinford, & Burkhardt, 2022). While standardized methods help providing homogenized data to define the occurrence of HuNoV RNA contamination in berries, comprehensive risk assessments focused on preventive strategies in food industry (e.g., postharvest processing interventions) have been impaired by the lack of a permissive cell line to estimate its infectivity (Estes et al., 2019). The main objective of this study was to validate the operational parameters

(e.g., holding pressure and exposure time) for HPP processing as an effective intervention for controlling HuNoV contamination in berry puree using infectivity data obtained with the novel HIE system. We demonstrate that the HIE model can be used to evaluate the effectiveness of preservation technologies, such as HPP, against HuNoV in complex high-risk food matrix (e.g., strawberry puree). Specifically, our data proven that HuNoV GI.3[P13] and HuNoV GII.4 Sydney [P16] can be experimentally spiked in berry purees, HPP treated under different pressure and time exposure conditions, and inactivation patterns defined using replication in HIE cell culture. In a previous work, we determined the inactivation of infectious HuNoV GII.4 Sydney [P16] buffered suspension exposed to HPP (Falcó et al., 2023). By testing several HPP conditions (e.g., pressure and exposure time) in PBS and strawberry puree contaminated with HuNoV GI.3[P13], HuNoV GII.4 Sydney [P16], MNV and TV, our experimental setup expands the knowledge on virus infectivity reduction by HPP. Strawberry puree was selected for being the soft fruit most commonly associated to HuNoV infections among the ones included in this study. We observed that 5.7 ± 0.0 and 5.8 ± 0.2 $\log_{10}$ gc/100 µl HuNoV GI.3[P13], and 4.2 ± 0.3 and 4.2 ± 0.5 HuNoV GII.4 Sydney [P16] must be present in PBS and strawberry puree to successfully replicate in HIE. Even though those values are consistent with previous reports, they also indicate the limited sensitivity of the HIE system to detect infectious HuNoV in real scenarios (Costantini et al., 2018; Estes et al., 2019; Ettayebi et al., 2016; Overbey, Zachos, Coulter, & Schwab, 2021; Wales, Kulka, Keinard, Ngo, & Papafragkou, 2023). Indeed, high virus concentrations in artificial contaminations were used to allow the assessment of inactivation data over a large range of different pressure regimes. Overall, treatments at 350 MPa did not completely inactivate surrogate viruses and HuNoVs despite infectivity reductions were observed. At the same

pressure, HuNoV GII.4 Sydney [P16] lost its infectivity for long exposure times (>5 min) in PBS, while retained infectivity in strawberry puree. With regard to moderate (400 MPa) HPP in buffered solution, our data confirm Falcó's findings (Falcóet al., 2023) indicating that 5 min are not sufficient to prevent HuNoV GII.4 Sydney [P16] replication in HIE. In the present study it was proved that also HuNoV GI.3[P13] remains infectious at the same conditions, and that HuNoV GII.4 Sydney [P16] is completely inactivated after 7.5 min treatment. MNV and TV in PBS were inactivated after 7.5 and 5 min, while residual infectivity was detected in strawberry puree also for the largest exposure time tested (7.5 min). These data on MNV inactivation in PBS are barely contrasting as complete inactivation at 400 MPa occurred after 7.5 min and not in 1 or 5 min as in previous reports (Cromeans et al., 2014; Falcó et al., 2023). Infectivity data at 450 MPa for 5 min demonstrated that HuNoV GII.4 Sydney [P16], MNV and TV were completely inactivated (Fig. 2). Cromeans reported that 600 MPa was required for complete TV inactivation in buffered solution (Cromeans et al., 2014). Using porcine gastric mucin-conjugated magnetic beads and RT-qPCR, it was observed that 550 MPa for 2 min determined >2.9 and > 4.0 log reduction of HuNoV GI.1 and HuNoV GII.4, respectively (Huang et al., 2016). We are not the first to report differences among measured inactivation patterns of surrogates and the actual pathogen. It was previously concluded that the inactivation kinetics of TV exposed to HPP appeared quite different from those of the other cultivable surrogates, being more resistant than MNV and FCV (Cromeans et al., 2014). The opposite was reported by Li and colleagues (Li, Ye, Neetoo, Golovan, & Chen, 2013). Accounting for data based on HuNoV replication in HIE, our results indicate that MNV better mimics HPP inactivation of HuNoV GII.4 Sydney [P16] than TV, either in buffered solution and in strawberry puree. As well, differences were observed between the two HuNoV

genogroups tested indicating that there may be more than one inactivation profile for HuNoV. The diverse sensitivity of genogroups might be explained by either the distinctive resistance to HPP inactivation, or it could also result from the different replication rates in the HIE system. However, the former hypothesis is supported by similar findings of previous studies (Huang et al., 2016; Li, Chen, et al., 2013). More generally, our HIE replication results are consistent with a clinical trial that demonstrated 400 MPa HPP as ineffective to completely inactivate HuNoV GI in seeded oysters and resulted in infection among the subjects, while 600 MPa HPP completely prevented participants from the infection (Leon et al., 2011). We found that virus HPP inactivation was enhanced in PBS compared to strawberry puree, since virus replication occurred in strawberry puree samples and not in buffered solution for many combinations of virus, time and pressure exposures. This indicates that the food matrix and its components provided a baroprotective effect, as observed previously (Baert, Debevere, & Uyttendaele, 2009; Balny, Masson, & Heremans, 2002; Falcó et al., 2023; Gross & Jaenicke, 1994; Kingsley & Chen, 2009). Thus, it is not surprising that both time and matrix variables resulted statistically significant to describe virus kinetic inactivation exposed to HPP. The second most relevant aspect of this investigation is the comprehensive comparison of MNV and TV survival patterns to those of infectious HuNoV GII.4 Sydney [P16] in a complex food matrix, such as strawberry puree, exposed to HPP treatments as a control measure. Specifically, experimental data of MNV and TV were fitted to Weibull distribution function as a predictive model and deduced models validated using the HuNoV infectivity dataset. Comparison of survival data was performed by determining the bias factors that resulted lower than 1 for all tested conditions, finally supporting that the deduced models are effective to guarantee the food safety. Bartsch and colleagues assessed the

thermal inactivation of HuNoV in strawberry puree using a capsid integrity assays consisting of a RNase treatment prior to RT-qPCR and compared it with MNV and TV infectivity reductions (Bartsch, Plaza- Rodriguez, Trojnar, Filter, & Johne, 2019). The authors reported that TV infectivity decreased faster than capsid-protected RNA, and concluded that the proposed model needs validation with direct HuNoV infectivity data. The data from this study can be utilized to generate speculative insights into the mechanistic HPP inactivation of HuNoV and its surrogates. In a recent study, a comparison was made among RT-qPCR, viability RT-qPCR, and replication in HIE for HPP-treated HuNoV. The results indicated that various viability RT-qPCRs exhibited no correlation with the loss of infectivity of HPP-treated HuNoV in PBS and strawberry puree. This suggests that pressure treatment does not directly impact RNA and does not completely disrupt capsid integrity (e.g., the nucleic acid) (Wales et al., 2024). This aligns with previous observations where HPP treatments were inefficient at destroying HuNoV capsid, even at 500 to 600 MPa and a 60 min holding time (Fangfei et al., 2012). Nevertheless, HuNoV lost its receptor-binding ability at ≥500 MPa pressure regimes (Huang et al., 2016; Li, Chen, et al., 2013; Ye et al., 2014). Considering these observations and the results in this study, it is plausible to postulate that HPP treatment can alter the structure of the capsid, rendering the virions unable to attach and enter infected host cells, even at lower HPP regimens (5 min at 450 MPa). As far as authors know, this is the first report assessing the performance of predictive models generated with virus surrogates and validated with infectivity HuNoV data by determining the bias factors. These models can be used to suggest reliable pressure/time combinations to inactivate HuNoV in strawberries puree exposed to HPP in industrial food processing settings. Our results also shown that both MNV and TV viruses can be considered as conservative surrogates for HuNoV GII.4 Sydney

[P16] in strawberry puree exposed to HPP. Thus, our findings contribute to the ultimate goal of selecting a representative surrogate to improve public health through a health-based risk assessment framework. Indeed, overestimating pathogen resistance or inactivation will negatively impact risk assessments that finally affect health assessments and safety levels estimations. Ultimately, our data corroborate that the HIE system has significant value for specifically estimating HuNoV infectivity and for validating predictive models based on surrogates.

5. Conclusions

Appropriate holding pressure and exposure time are critical operational parameters of HPP for successfully controlling virus contamination in berry and berry products. By using cell culture methods gold standard for virus infectivity-, we found that commercially acceptable HPP conditions (5 min at 450 MPa) are capable of inactivating infectious HuNoV GII.4 and surrogates in both PBS and strawberry puree. Additionally, we demonstrated that predictive models based on MNV and TV inactivation and validated with experimental HuNoV infectivity data can be used to suggest reliable pressure/time combinations to control HuNoV contamination in strawberries puree. Our work offers a blueprint for moving forward with inactivation studies using the HIE model, which have provided useful practical information on optimum treatments for the best public health outcomes.

Funding

This research was supported by "PREVISION" _(PID2019-105509RJ-I00, MCIN/AEI /10.13039/501100011033) project funded to WR. AM is supported by a predoctoral research grant funded by University of Bari "A. Moro" _(Italy). IF is

supported by a postdoctoral contract grant for the requalification of the Spanish university system from the Ministry of Universities of the Government of Spain, financed by the European Union (NextGeneration EU) (MS21–006). IATA-CSIC is a Centre of Excellence Severo Ochoa (CEX2021–001189-S MCIN/AEI / 10.13039/ 501100011033). The funding sources had no rule in the study design, data collection, analysis of data, writing, or in the decision to publish.

CRediT authorship contribution statement

Annamaria Pandiscia: Writing – review & editing, Writing – original draft, Methodology, Formal analysis, Data curation. **Irene Falcó:** Writing – review & editing, Methodology. **Valentina Terio:** Writing –review & editing, Supervision, Resources. **Antonio Martínez:** Writing – review & editing, Methodology, Formal analysis, Data curation. **Gloria Sánchez:** Writing –review & editing, Supervision. **Dolores Rodrigo:** Writing –review & editing, Formal analysis, Data curation. **Walter Randazzo:** Writing –review & editing, Supervision, Resources, Project administration, Funding acquisition, Formal analysis, Data curation, Conceptualization.

Declaration of competing interest

The authors declare that they have no known competing financial interests or personal relationships that could have appeared to influence the work reported in this paper.

Data availability

Data will be made available on request.

Acknowledgements

Authors would like to thank Prof. Javier Buesa (Department of Microbiology, School of Medicine, University of Valencia, Valencia, Spain) for kindly providing human norovirus-positive faecal samples.

Appendix A. Supplementary data

Supplementary data to this article can be found online at https://doi.org/10.1016/j.ifset.2024.103702.

References

Aadil, R. M., Madni, G. M., Roobab, U., Rahman, U. ur, & Zeng, X.-A. (2019). 1 - Quality Control in Beverage Production: An Overview (A. M. Grumezescu & A. M. B. T.-Q. C. in the B. I. Holban (eds.); pp. 1–38). Academic Press. https://doi.org/https://doi.org/10.1016/B978-0-12-816681-9.00001-1

Baert, L., Debevere, J., & Uyttendaele, M. (2009). The efficacy of preservation methods to inactivate foodborne viruses. International Journal of Food Microbiology, 131(2–3), 83–94. https://doi.org/10.1016/J.IJFOODMICRO.2009.03.007

Balny, C., Masson, P., & Heremans, K. (2002). High pressure effects on biological macromolecules: From structural changes to alteration of cellular processes. Biochimica et Biophysica Acta - Protein Structure and Molecular Enzymology, 1595(1–2), 3–10. https://doi.org/10.1016/S0167-4838(01)00331-4

Bartsch, C., Plaza-Rodriguez, C., Trojnar, E., Filter, M., & Johne, R. (2019). Predictive models for thermal inactivation of human norovirus and surrogates in strawberry puree. Food Control, 96, 87–97. https://doi.org/10.1016/j.foodcont.2018.08.031

Bartsch, C., Szabo, K., Dinh-Thanh, M., Schrader, C., Trojnar, E., & Johne, R. (2016). Comparison and optimization of detection methods for noroviruses in frozen strawberries containing different amounts of RT-PCR inhibitors. Food Microbiology, 60, 124–130. https://doi.org/10.1016/j.fm.2016.07.005

Bower, C. (2007). Postharvest handling, storage, and treatment of freshmarket berries. In Y. Zhaou (Ed.), Berry Fruit: Value-added products for health pro-motion. CRC Press.

Bozkurt, H., Phan-Thien, K.-Y., van Ogtrop, F., Bell, T., & McConchie, R. (2021). Outbreaks, occurrence, and control of norovirus and hepatitis a virus contamination in berries: A review. Critical Reviews in Food Science and Nutrition, 61(1), 116–138. https://doi.org/10.1080/10408398.2020.1719383

Butot, S., Putallaz, T., & Sánchez, G. (2008). Effects of sanitation, freezing and frozen storage on enteric viruses in berries and herbs. International Journal of Food Microbiology, 126(1–2), 30–35. https://doi.org/10.1016/j.ijfoodmicro.2008.04.033

Cannon, J. L., Papafragkou, E., Park, G. W., Osborne, J., Jaykus, L.-A., & Vinjé, J. (2006). Surrogates for the study of norovirus stability and inactivation in the environment: aA comparison of murine norovirus and feline calicivirus. Journal of Food Protection, 69(11), 2761–2765. https://doi.org/10.4315/0362-028x-69.11.2761

Carmona, N., & Randazzo, W. (2023). Passaging human intestinal organoids and monolayers set up. Protocol Exchange. https://doi.org/https://doi.org/10.21203/rs.3.pex-2221/v1

Chen, H., Hoover, D. G., & Kingsley, D. H. (2005). Temperature and treatment time influence high hydrostatic pressure inactivation of feline calicivirus, a norovirus surrogate. Journal of Food Protection, 68(11), 2389–2394. https://doi.org/10.4315/0362-028X-68.11.2389

Codex Alimentarius. (2012). Guidelines on the Application of General Principles of Food Hygiene to the Control of Viruses in Food. Guidelines on the Application of General Principles of Food Hygiene to the Control of Viruses in Food.

Costantini, V., Morantz, E. K., Browne, H., Ettayebi, K., Zeng, X. L., Atmar, R. L., Estes, M. K., & Vinjé, J. (2018). Human Norovirus Replication in Human Intestinal Enteroids as Model to Evaluate Virus Inactivation. Emerging Infectious Diseases, 24(8), 1453–1464. https://doi.org/10.3201/EID2408.180126

Cromeans, T., Park, G. W., Costantini, V., Lee, D., Wang, Q., Farkas, T., Lee, A., & Vinjé, J. (2014). Comprehensive comparison of cultivable norovirus surrogates in response to different inactivation and disinfection treatments. Applied and Environmental Microbiology, 80(18), 5743–5751. https://doi.org/10.1128/AEM.01532-14

Dancho, B. A., Chen, H., & Kingsley, D. H. (2012). Discrimination between infectious and non-

infectious human norovirus using porcine gastric mucin. International Journal of Food Microbiology, 155(3), 222–226. https://doi.org/10.1016/j.ijfoodmicro.2012.02.010

Desdouits, M., Polo, D., Le Mennec, C., Strubbia, S., Zeng, X. L., Ettayebi, K., Atmar, R. L., Estes, M. K., & Le Guyader, F. S. (2022). Use of Human Intestinal Enteroids to Evaluate Persistence of Infectious Human Norovirus in Seawater. Emerging Infectious Diseases, 28(7), 1475–1479. https://doi.org/10.3201/EID2807.220219

DiCaprio, E., Ye, M., Chen, H., & Li, J. (2019). Inactivation of Human Norovirus and Tulane Virus by High Pressure Processing in Simple Mediums and Strawberry Puree . In Frontiers in Sustainable Food Systems (Vol. 3, p. 26). https://www.frontiersin.org/article/10.3389/fsufs.2019.00026

Escudero-Abarca, B. I., Goulter, R. M., Arbogast, J. W., Leslie, R. A., Green, K., & Jaykus, L. A. (2020). Efficacy of alcohol-based hand sanitizers against human norovirus using RNase-RT-qPCR with validation by human intestinal enteroid replication. Letters in Applied Microbiology, 71(6), 605–610. https://doi.org/10.1111/LAM.13393

Estes, M K, Ettayebi, K., Tenge, V. R., Murakami, K., Karandikar, U., Lin, S. C., Ayyar, B. V, Cortes-Penfield, N. W., Haga, K., Neill, F. H., Opekun, A. R., Broughman, J. R., Zeng, X. L., Blutt, S. E., Crawford, S. E., Ramani, S., Graham, D. Y., & Atmar, R. L. (2019). Human Norovirus Cultivation in Nontransformed Stem Cell-Derived Human Intestinal Enteroid Cultures: Success and Challenges. Viruses, 11(7). https://doi.org/10.3390/v11070638

Estes, Mary K., Ettayebi, K., Tenge, V. R., Murakami, K., Karandikar, U., Lin, S. C., Ayyar, B. V., Cortes-Penfield, N. W., Haga, K., Neill, F. H., Opekun, A. R., Broughman, J. R., Zeng, X. L., Blutt, S. E., Crawford, S. E., Ramani, S., Graham, D. Y., & Atmar, R. L. (2019). Human Norovirus Cultivation in Nontransformed Stem Cell-Derived Human Intestinal Enteroid Cultures: Success and Challenges. Viruses, 11(7). https://doi.org/10.3390/V11070638

Ettayebi, K, Crawford, S. E., Murakami, K., Broughman, J. R., Karandikar, U., Tenge, V. R., Neill, F. H., Blutt, S. E., Zeng, X.-L., Qu, L., Kou, B., Opekun, A. R., Burrin, D., Graham, D. Y., Ramani, S., Atmar, R. L., & Estes, M. K. (2016). Replication of human noroviruses in stem cell-derived human enteroids. Science, 353(6306), 1387–1393. https://doi.org/10.1126/science.aaf5211

Ettayebi, Khalil, Crawford, S. E., Murakami, K., Broughman, J. R., Karandikar, U., Tenge, V. R., Neill, F. H., Blutt, S. E., Zeng, X. L., Qu, L., Kou, B., Opekun, A. R., Burrin, D., Graham, D. Y., Ramani, S., Atmar, R. L., & Estes, M. K. (2016). Replication of human noroviruses in stem cell-

derived human enteroids. Science (New York, N.Y.), 353(6306), 1387–1393. https://doi.org/10.1126/SCIENCE.AAF5211

Falcó, I., Randazzo, W., Gómez-Mascaraque, L., Aznar, R., López-Rubio, A., & Sánchez, G. (2017). Effect of (−)-epigallocatechin gallate at different pH conditions on enteric viruses. LWT - Food Science and Technology, 81. https://doi.org/10.1016/j.lwt.2017.03.050

Falcó, Irene, Randazzo, W., Pérez, A., Martínez, A., Rodrigo, D., & Sánchez, G. (2023). High pressure treatment and green tea extract synergistically control enteric virus contamination in beverages. Food Control, 144, 109384. https://doi.org/10.1016/J.FOODCONT.2022.109384

Fangfei, L., Mu, Y., Yuanmei, M., Xinhui, L., Erin, D., Haiqiang, C., Steven, K., John, H., David, K., Jianrong, L., & W., S. D. (2015). A Gnotobiotic Pig Model for Determining Human Norovirus Inactivation by High-Pressure Processing. Applied and Environmental Microbiology, 81(19), 6679–6687. https://doi.org/10.1128/AEM.01566-15

Fangfei, L., Pengwei, H., Hudaa, N., B., G. J., A., N. B., Haiqiang, C., Xi, J., & Jianrong, L. (2012). High-Pressure Inactivation of Human Norovirus Virus-Like Particles Provides Evidence that the Capsid of Human Norovirus Is Highly Pressure Resistant. Applied and Environmental Microbiology, 78(15), 5320–5327. https://doi.org/10.1128/AEM.00532-12

FDA. (2022). FDA Works to Enhance the Safety of Berries. FDA Works to Enhance the Safety of Berries.

Geeraerd, A. H., Valdramidis, V. P., & Van Impe, J. F. (2005). GInaFiT, a freeware tool to assess non-log-linear microbial survivor curves. International Journal of Food Microbiology, 102(1), 95–105. https://doi.org/https://doi.org/10.1016/j.ijfoodmicro.2004.11.038

Govaris, A., & Pexara, A. (2021). Inactivation of Foodborne Viruses by High-Pressure Processing (HPP). In Foods (Vol. 10, Issue 2). https://doi.org/10.3390/foods10020215

Gross, M., & Jaenicke, R. (1994). Proteins under pressure: The influence of high hydrostatic pressure on structure, function and assembly of proteins and protein complexes. European Journal of Biochemistry, 221(2), 617–630. https://doi.org/10.1111/j.1432-1033.1994.tb18774.x

Huang, R., Ye, M., Li, X., Ji, L., Karwe, M., & Chen, H. (2016). Evaluation of high hydrostatic pressure inactivation of human norovirus on strawberries, blueberries, raspberries and in their purees. International Journal of Food Microbiology, 223, 17–24. https://doi.org/10.1016/J.IJFOODMICRO.2016.02.002

Huang, Y., Ye, M., & Chen, H. (2013). Inactivation of Escherichia coli O157:H7 and Salmonella spp. in strawberry puree by high hydrostatic pressure with/without subsequent frozen storage. International Journal of Food Microbiology, 160(3), 337–343. https://doi.org/10.1016/J.IJFOODMICRO.2012.11.008

ISO 15216-1. (2017). Microbiology of food and animal feed—Horizontal method for determination of Hepatitis A Virus and norovirus in food using real-time RT-PCR—Part 1. In Method for quantification.

JEMRA. (2008). Microbiological hazards in fresh fruits and vegetables. Joint FAO/WHO Expert Meetings on Microbiological Risk Assessment (JEMRA). In Microbilogical risk assessment series.

Jones, M. K., Watanabe, M., Zhu, S., Graves, C. L., Keyes, L. R., Grau, K. R., Gonzalez-Hernandez, M. B., Iovine, N. M., Wobus, C. E., Vinjé, J., Tibbetts, S. A., Wallet, S. M., & Karst, S. M. (2014). Enteric bacteria promote human and mouse norovirus infection of B cells. Science, 346(6210), 755–759. https://doi.org/10.1126/science.1257147

Kingsley, D. H., & Chen, H. (2009). Influence of pH, salt, and temperature on pressure inactivation of hepatitis A virus. International Journal of Food Microbiology, 130(1), 61–64. https://doi.org/10.1016/J.IJFOODMICRO.2009.01.004

Kingsley, D. H., Holliman, D. R., Calci, K. R., Chen, H., & Flick, G. J. (2007). Inactivation of a norovirus by high-pressure processing. Applied and Environmental Microbiology, 73(2), 581–585. https://doi.org/10.1128/AEM.02117-06

Koopmans, M. (2008). Progress in understanding norovirus epidemiology. Current Opinion in Infectious Diseases, 21(5), 544–552. https://doi.org/10.1097/QCO.0B013E3283108965

Leon, J S, Kingsley, D. H., Montes, J. S., Richards, G. P., Lyon, G. M., Abdulhafid, G. M., Seitz, S. R., Fernandez, M. L., Teunis, P. F., Flick, G. J., & Moe, C. L. (2011). Randomized, double-blinded clinical trial for human norovirus inactivation in oysters by high hydrostatic pressure processing. Applied and Environmental Microbiology, 77(15), 5476–5482. https://doi.org/10.1128/AEM.02801-10

Leon, Juan S., Kingsley, D. H., Montes, J. S., Richards, G. P., Lyon, G. M., Abdulhafid, G. M., Seitz, S. R., Fernandez, M. L., Teunis, P. F., Flick, G. J., & Moe, C. L. (2011). Randomized, double-blinded clinical trial for human norovirus inactivation in oysters by high hydrostatic pressure

processing. Applied and Environmental Microbiology, 77(15), 5476–5482. https://doi.org/10.1128/AEM.02801-10

Li, D., Butot, S., Zuber, S., & Uyttendaele, M. (2018). Monitoring of foodborne viruses in berries and considerations on the use of RT-PCR methods in surveillance. Food Control, 89, 235–240. https://doi.org/10.1016/j.foodcont.2018.02.024

Li, X., Chen, H., & Kingsley, D. H. (2013a). The influence of temperature, pH, and water immersion on the high hydrostatic pressure inactivation of GI.1 and GII.4 human noroviruses. International Journal of Food Microbiology, 167(2), 138–143. https://doi.org/10.1016/j.ijfoodmicro.2013.08.020

Li, X., Chen, H., & Kingsley, D. H. (2013b). The influence of temperature, pH, and water immersion on the high hydrostatic pressure inactivation of GI.1 and GII.4 human noroviruses. International Journal of Food Microbiology, 167(2), 138–143. https://doi.org/10.1016/J.IJFOODMICRO.2013.08.020

Li, X., Ye, M., Neetoo, H., Golovan, S., & Chen, H. (2013). Pressure inactivation of Tulane virus, a candidate surrogate for human norovirus and its potential application in food industry. International Journal of Food Microbiology, 162(1), 37–42. https://doi.org/10.1016/j.ijfoodmicro.2012.12.016

Nasheri, N., Vester, A., & Petronella, N. (2019). Foodborne viral outbreaks associated with frozen produce. Epidemiology and Infection, 147, e291–e291. https://doi.org/10.1017/S0950268819001791

Overbey, K. N., Zachos, N. C., Coulter, C., Jacangelo, J., & Schwab, K. J. (2021). Recovery of Infectious Human Norovirus GII.4 Sydney From Fomites via Replication in Human Intestinal Enteroids. Frontiers in Cellular and Infection Microbiology, 11. https://doi.org/10.3389/FCIMB.2021.693090

Overbey, K. N., Zachos, N. C., Coulter, C., & Schwab, K. J. (2021). Optimizing Human Intestinal Enteroids for Environmental Monitoring of Human Norovirus. Food and Environmental Virology, 13(4), 470–484. https://doi.org/10.1007/s12560-021-09486-w

Pan, H., Buenconsejo, M., Reineke, K. F., & Shieh, Y. C. (2016). Effect of Process Temperature on Virus Inactivation during High Hydrostatic Pressure Processing of Contaminated Fruit Puree and Juice. Journal of Food Protection, 79(9), 1517–1526. https://doi.org/10.4315/0362-028X.JFP-16-

004

Randazzo, W., Costantini, V., Morantz, E. K., & Vinjé, J. (2020). Human Intestinal Enteroids to Evaluate Human Norovirus GII.4 Inactivation by Aged-Green Tea. Frontiers in Microbiology, 11, 1917. https://doi.org/10.3389/fmicb.2020.01917

Ross, T. (1996). Indices for performance evaluation of predictive models in food microbiology. The Journal of Applied Bacteriology, 81(5), 501–508. https://doi.org/10.1111/j.1365-2672.1996.tb03539.x

Sánchez, G., Aznar, R., Martínez, A., & Rodrigo, D. (2011). Inactivation of human and murine norovirus by high-pressure processing. Foodborne Pathogens and Disease, 8(2), 249–253. https://doi.org/10.1089/FPD.2010.0667

Tong, L., Ding, G., Yang, M., Su, L., Wang, S., Wang, Y., Zheng, L., Zhou, D., & Zhao, F. (2023). High-hydrostatic-pressure inactivation of GI.5 and GII.4 human norovirus and effects on the physical, chemical, and taste characteristics of oyster (Crassostrea virginica). LWT, 176, 114554. https://doi.org/https://doi.org/10.1016/j.lwt.2023.114554

Vahapoglu, B., Erskine, E., Subasi, B. G., & Capanoglu, E. (2021). Recent Studies on Berry Bioactives and Their Health-Promoting Roles. Molecules 2022, Vol. 27, Page 108, 27(1), 108. https://doi.org/10.3390/MOLECULES27010108

Wales, S. Q., Pandiscia, A., Kulka, M., Sánchez, G., & Randazzo, W. (2024). Challenges for estimating human norovirus infectivity by viability RT-qPCR as compared to replication in human intestinal enteroids. International Journal of Food Microbiology, 411, 110507. https://doi.org/10.1016/j.ijfoodmicro.2023.110507

Williams-Woods, J., Rodriguez, R., Marchant, J., Gail Swinford, A., & Burkhardt, W. (2022). FDA BAM Chapter 26: Concentration, Extraction and Detection of Enteric Viruses from Food. In Bacteriological Analytical Manual (BAM). https://www.fda.gov/food/laboratory-methods-food/bam-chapter-26-and-appendices-concentration-extraction-and-detection-enteric-viruses-food

Ye, M., Li, X., Kingsley, D. H., Jiang, X., & Chen, H. (2014). Inactivation of human norovirus in contaminated oysters and clams by high hydrostatic pressure. Applied and Environmental Microbiology, 80(7), 2248–2253. https://doi.org/10.1128/AEM.04260-13

9. LEVERAGING PLASMA-ACTIVATED SEAWATER FOR THE CONTROL OF HUMAN NOROVIRUS AND BACTERIAL PATHOGENS IN SHELLFISH DEPURATION

Shellfish, especially oysters, clams, and mussels, are responsible of several human foodborne viral outbreaks worldwide when consumed raw or undercooked, representing a major concern for public health [2,3,182]. Based on their filter-feeding activity, they can bioaccumulate foodborne pathogens such as enteric viruses, especially HuNoV and HAV and bacteria such as *Vibrio* spp. from contaminated water with human sewage [63,183–191].

According to Reg. EU 2019/627, the harvesting areas of shellfish are classified into three categories—A, B, or C—based on the increasing levels of *E. coli* contamination [192]. Molluscs harvested in areas B and C must undergo depuration processes to ensure compliance with the microbiological criteria outlined in the Reg. (EC) 1441/2007 related to bacterial indicators such as *E. coli* and *Salmonella* spp. [193]. Chlorine, iodophors, UV light and ozone are also employed in the shellfish depuration systems to inactivate foodborne pathogens, but these methods present several drawbacks, and innovative solutions for a complete microbial inactivation are urgently needed [194].

PAW has been applied in various foods matrices demonstrating its antimicrobial activity but there aren't scientific studies exploring the production of Plasma-Activated Seawater (PASW) and its application for seafood depuration [195].

Therefore, in order to introduce a novel non thermal technology able to overcome the limitations of shellfish depuration systems, we investigated the physico-chemical, antibacterial, and antiviral properties of three PASWs against *E. coli* O157, *Salmonella* spp., *V. parahemolyticus*, bacteriophages (MS2 and φ174), cultivable norovirus

surrogates (MNV and TV), and HuNoV using traditional and advanced cell culture techniques. Furthermore, the most effective PASW was assessed for its impact on cytotoxicity and mussel viability, aiming to simulate its practical, real-world applications in shellfish depuration systems.

Article adapted for printing of the PhD thesis. Available online on Foods, MDPI; https://doi.org/10.3390/foods13060850

Leveraging Plasma-Activated Seawater for the Control of Human Norovirus and Bacterial Pathogens in Shellfish Depuration

Annamaria Pandiscia[1,2], Patrizio Lorusso[2], Alessio Manfredi[2], Gloria Sánchez[1], Valentina Terio[2*], and Walter Randazzo[1*]

[1]Department of Preservation and Food Safety Technologies, Institute of Agrochemistry and Food
Technology (IATA-CSIC), Av. Agustín Escardino 7, Paterna, 46980 Valencia, Spain

[2]Department of Veterinary Medicine, University of Bari, Provincial Road to Casamassima Km 3, 70010 Valenzano, Italy

*Correspondence: valentina.terio@uniba.it (V.T.); wrandazzo@iata.csic.es (W.R.)

Abstract: Cold plasma is a promising alternative for water treatment owing to pathogen control and a plethora of issues in the agriculture and food sectors. Shellfish pose a serious risk to public health and are linked to large viral and bacterial outbreaks. Hence, current European regulations mandate a depuration step for shellfish on the basis of their geographical growth area. This study investigated the inactivation of relevant viral and bacterial pathogens of three Plasma-Activated Seawaters (PASWs), and their reactive oxygen and nitrogen species (RONS) composition, as being primarily responsible for microbial inactivation. Specifically, F-specific (MS2) and somatic (φ174) bacteriophage, cultivable surrogate (murine norovirus, MNV, and

Tulane virus, TV), and human norovirus (HuNoV GII.4) inactivation was determined using plaque counts and infectivity assays, including the novel human intestinal enteroid (HIE) model for HuNoV. Moreover, the kinetic decay of *Escherichia coli*, *Salmonella* spp., and *Vibrio parahaemolyticus* was characterized. The results showed the complete inactivation of phages (6–8 log), surrogates (5–6 log), HuNoV (6 log), and bacterial (6–7 log) pathogens within 24 h while preventing cytotoxicity effects and preserving mussel viability. Nitrites (NO_2^-) were found to be mostly correlated with microbial decay. This research shows that PASWs are a suitable option to depurate bivalve mollusks and control the biohazard risk linked to their microbiological contamination, either viral or bacterial.

Keywords: norovirus; vibrio; bivalve mollusks; inactivation; food safety; bacteriophages; food processing technology; water quality; contamination

DOI: https://doi.org/10.3390/foods13060850

1. Introduction

The global demand for innovative technologies in the food sector is rising, driven by regulatory reviews focusing on sustainability, long-term eco-safety, and human safety, prompting food business operators (FBOs) to seek new technology interventions. Over the last few decades, plasma science and technology has been increasingly investigated to solve the challenges facing by the agriculture and food industry [1–4]. Non-thermal atmospheric plasma, a technology with proven antibacterial effects [5–9], produces plasma-activated water (PAW) upon application to water as a result of the chemical reaction between the ionized gas and the adjacent liquid [10]. The primary factor

responsible for such microbial inactivation is a highly oxidizing environment with reduced pH and reactive oxygen and nitrogen species (RONS), such as hydrogen peroxide (H_2O_2), nitrate (NO_3^-), and nitrite ions (NO_2^-) [4,10–17]. Due to the absence of chemical residues (e.g., trihalomethanes derived from chlorine disinfection) and the absence of a negative environmental impact, along with diversity in its modes of application, PAW has been observed as a sustainable candidate for use as a sanitizer on food surfaces, food preparation surfaces, and processing equipment [18–23]. Low-temperature treatments, the use of air as the working gas, short treatment times, and remarkable antimicrobial efficacy represent the most promising features of applying PAW technology in the food industry. However, challenges such as elevated investment costs, limited knowledge regarding effective doses for various combinations of food matrices and pathogens, and the understudied impact on food quality all present opportunities for future research [1,24].

Based on their high filter-feeding activities, shellfish can bioaccumulate several foodborne pathogens, representing a serious risk to public health since they are often consumed raw or lightly cooked [25]. Epidemiological investigations, microbiological analyses, and scientific evidence frequently confirm the presence of different microbial pathogens in bivalve mollusks, with human norovirus (HuNoV) and *Vibrio* spp. being the etiological agents most often implicated in outbreaks [12]. In Europe, the Rapid Alert System for Food and Feed (RASFF) portal recorded seventy-five notifications of bivalve mollusks contaminated by pathogenic microorganisms in 2023. Among them, HuNoV was linked to more than thirty-five alerts, while *Salmonella* spp. and *Escherichia coli* were reported in ten alerts and *Vibrio* spp. were reported in four [26]. In 2019, a European baseline survey found that 34.5% and 10.8% of oysters from production areas and dispatch centers were contaminated with HuNoV,

respectively [27]. HuNoV causes acute diarrheal gastroenteritis frequently linked to large outbreak sizes with a high number of human cases.

Vibrio spp. cause infections in humans via the oral route through the ingestion of contaminated water or raw or undercooked contaminated seafood (in particular, *Vibrio parahaemolyticus* and *V. cholerae*) [28,29]. *V. parahaemolyticus* is the most common pathogen causing seafood-borne illnesses in many countries, and the strains harboring the tdh (encoding thermostable direct hemolysin) and trh (encoding tdh-related hemolysin) genes are pathogenic in humans [30]. *Vibrio* spp. are one of the zoonotic agents listed in Annex I of Directive 2003/99/EC to be monitored according to the epidemiological situation [31,32]. Moreover, FBOs must control the levels of fecal bacterial indicators such as *E. coli* and *Salmonella* spp. [33]. Salmonellosis is the second most reported zoonosis in humans followed by *Listeria monocytogenes* and Shiga toxin-producing *E. coli* (STEC), including the O157, O26, O103, O146, O145, and O91 serogroups [34]. Considering this risk, the European Union (EU) laid down the criteria for the classification of shellfish harvesting areas and determined the level of post-harvest treatment required before shellfish can be considered suitable for human consumption. The harvesting areas are classified into three sanitary levels (A, B, and C) (EU/2019/627), and current European regulations mandate a depuration process for mollusks harvested in B and C areas, ensuring compliance with the microbiological criteria included in EC Reg. 1441/2007 [33,35]. Specifically, while shellfish from A areas do not undergo depuration (*E. coli* colony-forming units (CFUs) ≤ 230/100 g shellfish in 80% of samples), increased levels of contamination are expected in B (*E. coli* CFUs ≤ 4600/100 g shellfish in 90% of samples) and C areas (*E. coli* CFUs ≤ 46,000/100 g shellfish in 90% of samples), and a depuration step is enforced [36]. Nevertheless, outbreaks still occur, and the scientific community agrees

on the inadequacy of current commercial shellfish depuration processes for HuNoVs and *Vibrio* spp. [25,37,38]. To add complexity to this scenario, the standard procedure to detect HuNoV in bivalve mollusks (ISO 15216-1:2017) [39] relies on molecular methods, which do not provide information on viral infectivity. Indeed, the lack of a reliable propagation model for HuNoV has been a significant roadblock to studying its stability, persistence, and inactivation [40].

To overcome this limitation, bacteriophages (e.g., MS2, and φ174) and cultivable surrogates (e.g., murine norovirus, MNV, and Tulane virus, TV) have been historically used, even though they provide biased data and still represent an indirect estimation for the actual human viral pathogen [41–43]. Specifically, F-specific (e.g., MS2) and somatic (e.g., φ174) bacteriophages have been commonly used as viral surrogates for viral inactivation and as indicators for fecal contamination in Europe and the USA [44,45]. Recently, a novel three dimensional cell culture technique based on stem cell-derived human intestinal enteroids (HIEs) has been described and confirmed to support the replication of HuNoVs [46,47], enabling the first inactivation studies [48–51].

While PAW has been applied in various foods, there are a lack of studies exploring the production of plasma-activated seawater and its application for seafood depuration [52]. Given that electrical conductivity is directly associated with the number of ions generated in solution following plasma treatment, the salinity of seawater presents additional challenges for the production of RONS and maintaining their stability over time. Taking all of these data together, we hypothesized that plasma-activated seawater (PASW) may represent an eco-friendly option to depurate bivalve mollusks and control the biohazard risk linked to their microbiological contamination. As a first step to prove our hypothesis and given that experimental evidence on the efficacy of PASW to control foodborne pathogens is limited, we investigated the physico-chemical,

antibacterial, and antiviral properties of three PASWs activated by different plasma exposures. Specifically, we determined the kinetic in vitro inactivation of *E. coli* O157, *Salmonella* spp., *V. parahemolyticus*, bacteriophages (MS2 and φ174), cultivable norovirus surrogates (MNV and TV), and HuNoV exposed to three different PASWs using traditional and advanced cell culture techniques to define and characterize bacterial and viral inactivation. RONS species were also determined. Ultimately, the most effective PASW was evaluated for its impact on cytotoxicity and mussel viability, simulating real-world applicability.

2. Materials and Methods

2.1. Production and characterization of PASWs

Depurated seawater samples (SW) were collected from the clean seawater reservoir tanks of a commercial depuration center in Bari (Mare Gioioso SRL, Monopoli Bari, Italy). In particular, the depuration center collects seawater from the Adriatic Mediterranean Sea and filters and UV treats it to remove suspended particles and microbial contaminants before using it for mollusk depuration. The SW was collected in Pirex® glassware and transferred to the laboratory. An experimental jet–dielectric barrier discharge (DBD) plasma in a remote configuration was used for the treatments (Renasco S.R.L., Bari, Italy). Specifically, the plasma was ignited in atmospheric air used as the working gas (feed gas) and sustained within the reactor. The jet nozzle was placed at 5 cm from the liquid surface to promote direct contact between the plasma plume and the SW. Plasma was discharged from the plasma generator with an input voltage of 230 V, a total output of 800 watts, and a frequency of 30 kHz. Each batch consisted of 300 mL of SW in a 1000 mL beaker exposed to plasma treatment for 10 (PASW10), 20 (PASW20), or 30 (PASW30) min, obtaining three different PASWs.

SW was used as a control. When higher volumes of PASW were needed (e.g., mussel viability), several batches of 300 mL were prepared, mixed together, and denoted as one batch.

Physico-chemical characterization of PASWs was carried out before and immediately after each plasma treatment. The pH and temperature were monitored using a pH meter (Hanna Instrument, Padova, Italy) and a digital thermometer probe (Fisherbrand™ Traceable™,Waltham, MA, USA), respectively. Electrical conductivity was measured using a portable electrical conductivity probe (Hanna Instrument, HI 8633, Italy). Semi-quantitative test strips were used for hydrogen peroxide (H_2O_2), nitrite (NO_2^-), and nitrate (NO_3^-) (QUANTOFIX, Macherey-Nagel, Milano, Italy) measurements. All inactivation experiments, including bacteria, phages, surrogates, and HuNoV, were carried out at a room temperature of 22 ± 2 ◦C.

2.2. Phage inactivation by PASWs

F-specific (MS2) and somatic (φ174) bacteriophages were initially used to investigate the antiviral effect of PASWs. A double layer plaque assay was used to quantify phages inactivation using the *E. coli* CECT 9198 and *E. coli* WG5 strains as host strains for wild-type MS2 bacteriophage DSM 13767 (DSMZ, Braunschweig, Germany) and φ174 (Bluephage, Barcelona, Spain), respectively [50]. Tryptone soy agar (TSA) (Oxoid, Thermofisher, Madrid, Spain) was used for the lower layers, and semisolid tryptone soy broth (sTSB) (Oxoid, Thermofisher, Madrid, Spain) with 0.5% bacteriological agar (Oxoid, Thermofisher, Madrid, Spain) and 0.04 M magnesium chloride was used for the upper layers. *E. coli* CECT 9198 and *E. coli* WG5 were initially grown in TSB (Oxoid, Thermofisher, Madrid, Spain) at 37 °C until the log phase was reached (optical density, OD = 0.3). Then, a 1 mL ten-fold serial dilution

of phage sample was added to 5 mL sTSB along with 1 mL of *E. coli* host strain (OD = 0.3), mixed, and carefully plated on TSA. The plates were incubated overnight at 37 ◦C and the phage load was determined as plaque-forming units per mL (PFUs/mL). Phage decay was calculated as $\log_{10}$ S (N/N0), where N0 is the titer in the control sample and N is the titer in the plasma-treated one. Phage decay following 24 h exposure to PASW10, PASW20, and PASW30 was investigated for MS2 and φ174. Briefly, 100 µL of 7 log plaque-forming units (PFUs)/mL for MS2 or from 6 log PFUs/mL for φ174 were mixed with 900 µL of each PASW sample. Phage suspensions in phosphate-buffered solution (PBS) pH 7.4 and SW were included as controls.

2.3. Surrogate Inactivation by PASWs

MNV and TV were used as human norovirus surrogates to investigate kinetic inactivation due to exposure to PASWs. MNV (provided by Prof. H. W. Virgin, Washington University School of Medicine, USA) and TV (provided by Prof. Farkas, Louisiana State University, LA, USA) were propagated and assayed respectively in RAW 264.7 and LLC-MK2 (ATCC CCL-7) cells as previously described in [50,54]. Briefly, MNV and TV were cultured in Dulbecco's modified Eagle medium (DMEM, Gibco Life Technologies, Madrid, Spain) supplemented with 10% fetal bovine serum (FBS) and Opti-MEM (Gibco Life Technologies) supplemented with 2% FBS.

Viral decay following exposure to PASW10, PASW20, and PASW30 was investigatedfor each surrogate by collecting samples at 0, 0.5, 1, 3.0, 12, and 24 h to determine their kinetical inactivation. Briefly, 100 µL of 5–6 log 50% tissue culture infectious dose ($TCID_{50}$)/mL was mixed with 900 µL of each PASW sample. Viral suspensions in PBS pH 7.4, PBS pH 5.0, and SW were included as controls. Samples collected at selected time points were neutralized by 1:10 (v/v) dilution in cell culture

media supplemented with 10% FBS. Viral titer was determined using the $TCID_{50}$ assay inoculating 20 µL of 10-fold serial dilutions of MNV or TV prepared in PBS pH 7.4 on eight wells with 70–80% confluent monolayers in 96-well plates. After incubation for 1 h at 37 °C, 180 µL DMEM or Opti-MEM was added. After 2 to 5 days, cells showing cytopathic effect (CPE) were enumerated by visual inspection, and the titer of infectious viruses was determined using the Spearman–Karber method.

2.4. Human Norovirus Inactivation by PASWs

HuNoV GII.4 decay following 24 h exposure to PASW10, PASW20, and PASW30 was investigated using the HIE model. Three-dimensional (3D) HIE derived from human jejunal biopsy (J2 cell line, provided by Prof. Mary K. Estes, Baylor College of Medicine, Houston, TX) and differentiated monolayers were routinely maintained and produced as described by Carmona and Randazzo [55]. The HuNoV GII.4 Sydney [P16]-positive fecal sample (provided by Prof. Buesa, University of Valencia, Valencia, Spain) was de-identified, tested for infectivity in the HIE system, and used for inactivation experiments. The experimental design consisted of exposing 100 µL of 9 log genome copies (GC)/100 µL HuNoV GII.4 to 900 µL of each PASW sample for 24 h. HuNoV suspensions in PBS pH 7.4 and SW were included as controls. Then, each sample was neutralized by mixing 1:10 (v/v) with organoid differentiation medium (ODM) and infected in two sets of 96-well plates with 100% confluent 7–10 day-old differentiated HIE monolayers.

Undifferentiated 3D HIEs and differentiated monolayers were maintained and produced using commercial IntestiCult™ Organoid Medium Human media (STEMCELL Technologies Inc., Vancouver, CO, Canada) as already described [55]. Differentiated HIE monolayers were typically 100% confluent after five to seven days

and used for HuNoV infections. Two sets of 96-well plates with 100% confluent differentiated HIE monolayers were inoculated in triplicate with 100 µL of each HuNoV sample diluted at 1:10 (v/v) in complete media without growth factors (CMGF-) supplemented with 500 µM sodium glycochenodeoxycholate. After 1 h incubation at 37 ◦C, the inoculum was removed, monolayers were washed twice with CMGF-, and 100 µL of ODM was added to each well. For each set of infections, one 96-well plate was immediately frozen at −80 °C (1 hpi) and the second plate was incubated at 37 °C and 5% CO_2 for 48 h (48 hpi) and then frozen. Three technical replicates were included for each sample.

Finally, RT-qPCR was used to determine the amount of HuNoV RNA from HIE monolayers at 1 and 48 hpi to evaluate HuNoV replication. Briefly, viral RNA was extracted using the Maxwell. RSC Instrument (Promega, Madrid, Spain) according to the manufacturer's instructions. Then, it was detected in duplicate via TaqMan RT-qPCR using the RNA UltraSense One-Step quantitative RT-PCR system (Invitrogen, Madrid, Spain) on a LightCycler 480 instrument (Roche Diagnostics, Barcelona, Spain). The primers and probe included in the ISO 15216-1, 2017 were used for detecting HuNoV GII [39]. Ten-fold serial dilutions of synthetic gBlock gene fragments (IDT) were used to build an external standard curve, and HuNoV RNA was quantified as genome equivalents (HuNoV GII: $y = -3.56x + 40.664$, $R = 0.997$). Positive and negative amplification controls were included in each RT-qPCR run, along with the inhibitory amplification control consisting of a 10-fold diluted RNA for each sample.

2.5. Bacterial inactivation by PASWs

The efficacy of PASW was investigated using *E. coli, Salmonella* spp., and *V. parahaemolyticus*. Specifically, *E. coli* O157 and *Salmonella* spp. strains were maintained in sterile glycerol solution at −80 °C in the laboratory collection. The V. parahaemolyticus 17802 reference strain was supplied by ATCC. *E. coli* O157 and *Salmonella* spp. were maintained in tryptone soy broth (TSB, Oxoid, ThermoFisher, Milano, Italy) and Rappaport–Vassiliadis medium (RV, Oxoid, ThermoFisher, Milano, Italy), respectively. *V. parahemolyticus* was grown in TSB medium supplemented with 3% NaCl. Maximum recovery diluent (MRD, Oxoid, ThermoFisher, Milano, Italy) medium was used to prepare ten-fold dilutions, and a plate count assay was used for bacterial titration. Specifically, *E. coli* O157 and *Salmonella* spp. were titrated after 24 h incubation in plate count agar (PCA, Oxoid, ThermoFisher, Milano, Italy) at 37 °C, while *V. parahaemolyticus* was titrated after 24 h incubation in PCA supplemented with 3% NaCl at 41 °C.

Bacterial decay following exposure to PASW30 was investigated for each bacterial species, and samples were collected at 0, 0.5, 1.5, 2.5, 3.5, and 24 h to determine kinetic inactivation. Briefly, 1 mL of 10^6 colony-forming units (CFUs)/mL overnight bacterial suspension was added to 100 mL of PASWs. At each time point, 1 mL of sample was collected, serial dilutions were performed to stop the reaction, and bacterial counts were determined as previously detailed. Bacterial suspensions in PBS pH 7.4 and SW were included as controls.

2.6. *HIE cytotoxicity*

The cytotoxicity effect of PASW10, PASW20, and PASW30 on intestinal epithelial cells obtained from the differentiation of 3D HIE was investigated. The HIE system was maintained as previously described [55]. Each PASW sample was tested undiluted

and diluted at 1:10 (v/v) in CMGF-. HIE monolayers were inoculated with 100 µL of each sample and incubated at 37 °C in a 5% CO_2 incubator for 1 h. Then, monolayers were washed twice with CMGF- and maintained at 37 ◦C and 5% CO_2 for 48 h with ODM. The potential cytotoxicity effect was monitored by visual inspection of monolayers using optical microscopy for the duration of the experiment. Finally, HIE monolayers were infected with HuNoV, and viral replication was assessed as previously described to check for cell functionality after exposure to different PASWs.

2.7. Mussels viability

The effect of PASW30 on live mussels was investigated. Mediterranean mussels (*Mytilus galloprovincialis*) harvested from an A area were purchased from a local market in Bari (Italy). Forty mussels of similar size were selected, excluding under- and oversized mollusks, and transferred into a plastic tank filled with 20 L SW as a control or PASW30 for 24 h. The seawater in the feeding tank was aerated continuously during the experiment to preserve the physiological state of the mussels. The vitality of mussels was monitored every 3 h, checking the opening of their valves and their responsiveness to external stimuli.

2.8. Statitical analyses

All data were compiled from three independent experiments with three technical replicates each. Statistical analyses of data were computed using GraphPad Prism software version 8. A one-way analysis of variance (ANOVA) was performed with a subsequent Tukey's multiple comparison test by assuming a normal data distribution. The statistical results of measurements are shown as the mean value ± standard deviation (SD).p-values < 0.05 were considered statistically significant.

3. Results

3.1. Characterization of PASWs

Physico-chemical characterization of PASW10, PASW20, and PASW30 was carried out to determine the main RONS families generated in SW following the three plasma treatments (Table 1). The concentration of nitrites (NO_2^-) increased according to the duration of the plasma treatments, resulting in PASW10 < PASW20 < PASW30. On the contrary, the content of nitrates (NO_3^-) and peroxides (H_2O_2) was not directly correlated with the duration of the plasma treatment applied to the seawater. However, acidification of seawater samples was observed concomitant to the duration of the plasma treatment, as the pH decreased from 8.13 in SW to 7.95 in PASW10 and 5.00 in PASW30. Electrical conductivity resulted in 47.5 ±1.23 μS/cm on average with no significant differences among the tested PASWs ($p > 0.05$).

Table 1. Physico-chemical characterization of PASWs.

PASW	NO_2^- (mg/L)	NO_3^- (mg/L)	H_2O_2 (mg/L)	pH
SW	0	0	0	8.13 ± 0.31^b
PASW10	5 ± 0.5^b	25 ± 1^a	1 ± 0.2^b	7.95 ± 0.11^b
PASW20	0.5 ± 0.5^a	298 ± 3^b	5 ± 0.3^c	7.73 ± 0.17^b
PASW30	100 ± 0.5^c	310 ± 10^b	0.5 ± 0.1^a	5.00 ± 0.22^a

Different letters indicate significant differences among PASW ($p < 0.05$).

3.2. Phages inactivation by PASWs

MS2 and φ174 phages were exposed to PASW10, PASW20, and PASW30 for 24 h (Figure 1). PBS pH 7.4 and SW served as controls. The results of three independent experiments showed comparable inactivation patterns for both phages. In particular, exposure to PASW10 and PASW20 inactivated both phages by 0.95 to 1.65 log

PFUs/mL. In contrast, PASW30 inactivated MS2 and φ174 phages to undetectable levels within 24 h.

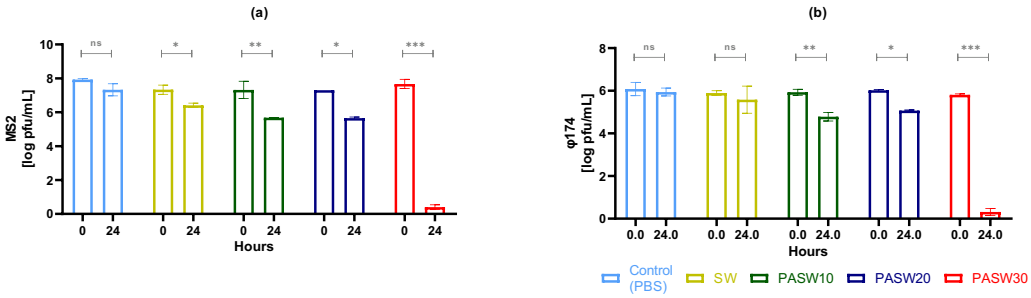

Figure 1. Inactivation of phages in plasma activated seawaters (PASW10, PASW20, PASW30). Phosphate-buffered solution (PBS) and seawater (SW) served as controls. (a) MS2 phage; (b) ϕ174 phage. Error bars indicate SDs; asterisks indicate significant difference between time points for each sample: ns, no significant; *p < 0.05; **p < 0.01; ***p < 0.001.

3.3. Kinetic Inactivation of HuNoV Surrogates

The kinetic inactivation of TV and MNV, serving as surrogates for HuNoV, was investigated, and the results are presented in Figure 2. Specifically, viral suspensions were prepared in PBS pH 7.4, PBS pH 5.0, SW pH 8.2, SW pH 5.0, PASW10, PASW20, and PASW30, and viral titers were monitored at 0 (control), 0.5, 1, 3, 6, or 24 h. In general, the inactivation effect of PASWs on viruses was associated with the intensity of the plasma treatment (PASW10 < PASW20 < PASW30). No statistical differences were noticed among PBS pH 7.4, PBS pH 5.0, SW pH 8.2, and pH 5.0 used as experimental controls for either MNV or TV.

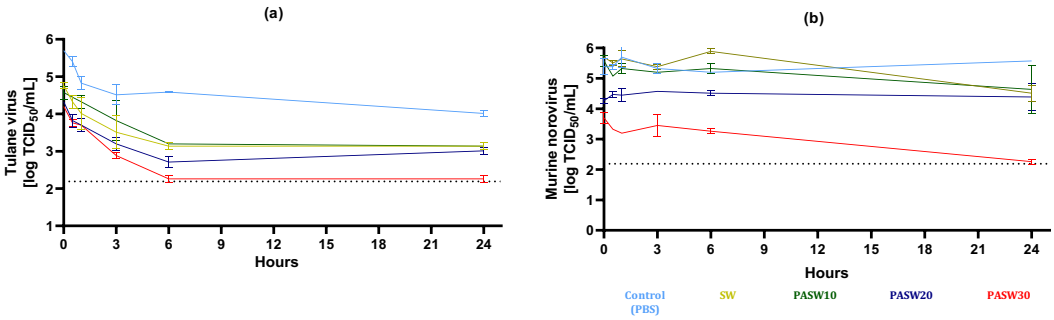

Figure 2. Kinetic inactivation of TV and MNV in plasma activated seawaters (PASW10, PASW20, PASW30). Phosphate-buffered solution (PBS pH 7.4) and seawater (SW) served as con-trols. (a) TV; and (b) MNV.

The titer of TV gradually decreased during 24 h in all samples, including in the PBS and SW controls. PASW10 showed comparable inactivation kinetics to those recorded for SW, indicating a limited effect on TV. However, the inactivation measured in the PASW20 and PASW30 samples was significantly higher, resulting in reductions of 2.99 and 3.44 log $TCID_{50}$/mL after 6 h compared to PBS. This indicates that PASW30 inactivated TV after 6h to non-detectable levels. MNV ended up being kinetically more stable than TV over time (Figure 2b). However, significant MNV decay was observed in PASW30, in which complete inactivation was reached within 24 h. This implied a 3.13 log $TCID_{50}$/mL reduction with respect to the PBS pH 7.4 control. PASW 30 completely inactivated the TV and MNV titers within 24 h.

3.4. Inactivation of HuNoV

HuNoV GII.4 was mixed to PBS pH 7.4, SW, PASW10, PASW20, and PASW30, and samples collected at 0 and 24 h time points. These samples were used to infect HIE monolayers. HuNoV RNA was extracted and quantified from cell supernatant at 0 and 48 hpi to calculated viral replication. The initial HuNoV concentration was 6.1±0.1

log GC/100µL. All samples at time 0, showed replication at comparable extent to the PBS control, reaching titer of 8.4 log GC/100 µL (Figure 3). Samples collected after 24 h in PBS, SW, PASW10, M-PASW, and PASW30 showed different replication rates. Specifically, HuNoV replication decreased by 0.76 and 0.86 log GC/100 µL in SW and PASW10. Inactivation of 1.49 log GC/100 µL was observed in PASW20, and the complete prevention of HuNoV replication was detected in PASW30 (2.37 log GC/100 µL reduction).

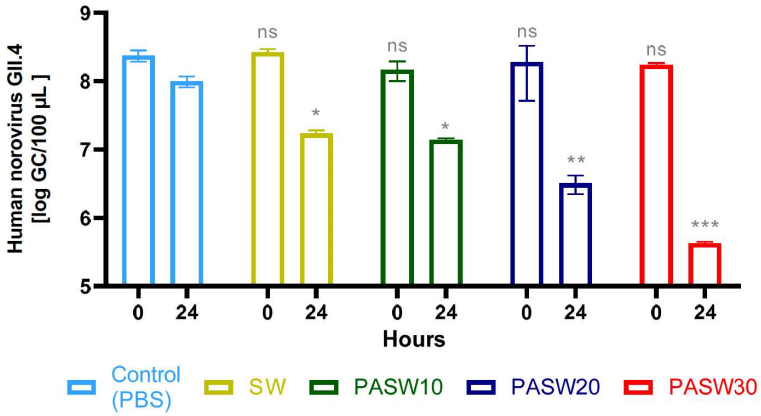

Figure 3. Replication of HuNoV following exposure for 24 h to PASW10, PASW20, and PASW30. Phosphate-buffered solution (PBS pH 7.4) and seawater (SW) served as controls. Error bars indicate SDs; asterisks indicate significant difference for each time exposure point from untreated control (PBS): ns, no significant; *$p < 0.05$; **$p < 0.01$; ***$p < 0.001$.

3.5. Kinetic bacterial inactivation

The kinetic inactivation of three bacterial pathogens exposed to PASW30 for 24 h are shown in Figure 4. The average initial *E. coli* O157, *Salmonella* spp. and V. parahemolyticus load was 6.63±0.09, 6.69±0.01, and 6.79±0.12 log CFU/mL, respectively. No statistically significant reductions of bacterial titers were detected during 24 h in SW. In PASW30, the initial load was statistically reduced by >5 log after 0.5 h. In particular, *E. coli O157*, *Salmonella* spp. and *V. parahemolyticus* were reduced to 1.39

± 0.01, 1.66 ± 0.00, 1.60 ± 0.08 log CFU/ml, respectively. Residual bacterial counts steadily decreased during the following 3.5 h monitoring period, and complete inactivation was reached within 24 h for all the three tested bacteria.

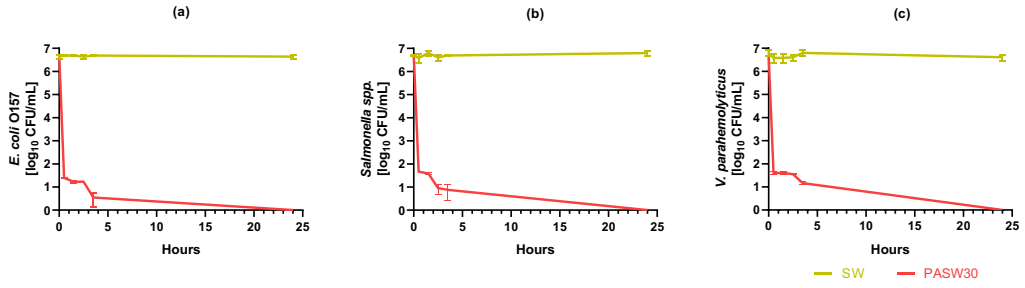

Figure 4. Kinetic bacterial inactivation in plasma activated seawater (PASW30). Untreated seawater (SW) served as control. (a) *E. coli* O157; (b) *Salmonella* spp.; (c) *V. parahemolyticus*.

3.6. HIE citotoxicity

Given the presence of different concentrations of RONS due to the intensity of each plasma treatment in seawater, undiluted and diluted at 1:10 PASWs were tested on HIE monolayers for 1 hour exposure. When tested undiluted, PASWs affected the monolayer integrity, and HuNoV infections were not conducted. On the contrary, no morphological changes of the monolayers structure and uniformity were observed during visual mon-itoring of HIE exposed to PASW10, PASW20 and PASW30 diluted 1:10 in CGMF-. For all tested diluted PASWs, HuNoV replication rates (8.22 ± 0.82 log GC/100 µL) showed no statistical differences ($p>0.05$) compared to the PBS control (8.15 ± 0.75 log GC/100 µL).

3.7. Mussels viability

Given the promising antibacterial and antiviral activity of PASW30, and its significant concentration of RONS, its effect on mussel's viability was investigated in vivo. A total of 40 mussels for each treatment condition (PASW30, and SW) were used in the experiment owing to the need to monitor mortality within 24 h. All mussels in the depuration treatments were observed to open their valves after being left undisturbed, demonstrating their filter feeding activity. However, a total of four mussels perished after 24 h in SW, possibly due to weakness and being in an unfamiliar environment. In PASW30, all mussels survived as tested responsive to external stimuli until 6 h of treatment, even though a total of seven mollusks resulted died at 24 h.

2. Discussion

Current European regulations and commercial depuration processes fail to fully guarantee the microbiological safety of shellfish [12,25–27,38]. Despite there being several studies confirming the effectiveness of PAW in inactivating bacterial pathogens, our study reports novel data on the production of PASW, its efficacy in controlling relevant foodborne viruses and bacteria, and its potential application as a strategy for shellfish depuration.

Our investigation focused on the most relevant pathogens involved in shellfish outbreaks, such as HuNoV and *V. parahemolyticus*, along with additional indicators of microbiological safety (e.g., *E. coli* and phages). Specifically, the DBD plasma device activating SW for 30 min resulted in PASW30, which was able to completely inactivate *E. coli* O157, *Salmonella* spp. and *V. parahemolyticus*, MS2 and φ174 phages, and TV, MNV, and HuNoV within 24 h.

Notably, our experimental design included innovative techniques (e.g., an HIE system) able to robustly inform us about HuNoV infectivity and inactivation. Previous studies

inferred HuNoV decay using molecular methods such as RT-qPCR or viability RT-qPCR, which have not overcome the limitation of the sound correlation of infectivity and molecular assays [56], including for plasma-mediated inactivation [57]. Alternatively, surrogates have been employed, even though their use has been questioned and resulting patterns still need to be correlated with HuNoVs infectivity. Our results indicate that MNV is more stable than TV over time when treated with PASWs (Figure 2). Comparing surrogates with HuNoV GII.4, the viral response to the diverse tested PASWs was qualitatively comparable, with PASW30 being able to completely prevent viral replication in the cell models. In addition, complete inactivation of high titer MS2 and ϕ174 phages (6–8 log PFUs/mL) was observed within 24 h for PASW30 but not for PASW10 or PASW20, providing further evidence of the effectiveness of the treatment in controlling viral contamination. PASW30 was demonstrated to be effective in inactivating bacterial pathogens, namely *E. coli* O157, *Salmonella* spp., and *V. parahemolyticus.* Significant reduction (>5 log) was achieved within the first 30 min of exposure, and complete inactivation was reached within 24 h for all tested bacteria. Comparing the kinetic datasets, bacteria and TV showed consistent inactivation patterns, even though bacterial decay was faster than viral one. Taking these data together, microbial inactivation was associated with the intensity of the plasma treatment (with it being PASW10 < PASW20 < PASW30), and it was time dependent. The physical–chemical characterization of PASWs indicated the production of different concentrations of RONS generated in SW following plasma activation (Table 1). Specifically, nitrites (NO_2^-) increased according to the duration of the plasma treatments, while the content of nitrates (NO_3^-), and peroxides (H_2O_2) was not proportional. Thus, our data suggest that nitrites may be the primary agent responsible for viral inactivation. A comprehensive comparison of our data with the

available literature is difficult as wide differences have been found related to plasma technology (e.g., plasma sources and gas type), type of water (e.g., water, salt water, simulated seawater, and seawater), tested microorganisms, and inactivation conditions [24]. Only a few reports have investigated plasma-activated salt water or seawater, and its use for microbial inactivation [58–63]. Salt concentration affects electrical conductivity, and thus, it is directly related to the number of ions generated in solution during the plasma activation process. This contributes to the production of RONS and other antimicrobial compounds (e.g., singlet oxygen) responsible for microbial inactivation [11,63,64].

Focusing on PASWs, we successfully plasma-activated seawater using actual seawater, with demonstrated antimicrobial activity (Figures 1–4) and characterized by concentrations of NO_3^- similar to a previous study carried out using simulated seawater [63]. Importantly, the NO_3^- concentrations of PASW30 (310 mg/mL) (Table 1) fall within the range reported to avoid adverse effects on clams' and oysters' viability (320 mg/mL) [65]. Our viability assays on mussels provide additional evidence that PASW within the aforementioned limit has a limited impact on mussels' viability. Similar considerations apply to pH as well. Indeed, the decrease in pH in PAW and PASW is attributed to the formation of inorganic acids (e.g., HNO_2 and HNO_3) that contribute to altering microbial and viral stability [66–71], while they can also affect shellfish viability [72]. Thus, PASW is diluted or buffered to prevent premature shellfish mortality [62,63]. However, the pH of PASW tested effectively in our study (PASW30 pH 5) is significantly different from pH < 3 reported previously [57,67]. This discrepancy is likely due to the diverse composition of seawater samples, with natural seawater carrying unidentified elements with buffering capacity (e.g., microalgae, organic matter, trace elements, or minerals) not included in the simulated

seawater used by other authors [62,63]. Regarding antimicrobial activity, the results of this study were compared to previous using PAW, plasma-activated salt water, or simulated PASW since there are no reports on PASW. Campbell and colleagues first reported the reduction of ~3 log CFUs/mL of *E. coli* treated with simulated PASW for 5 min [63]. The authors also reported that *E. coli* reductions were higher in PAW than in PASW produced at the same plasma exposure time, supporting the relevance of the water type in plasma activation as previously discussed. Baek and colleagues observed a reduction > 4 log for *E. coli* O157:H7 after 5 min of exposure to plasma-activated salt water (0.9% NaCl, w/v) [58]. Overall, these results are in accordance with the data obtained in our study where *E. coli* O157 exposed to PASW30 was reduced by >5 log after 30 min (Figure 4a). Yun reported the reduction of >3 log of three different Vibrio strains after 3 h PAWtreatment. In our study, we achieved >5 log *V. parahemolyticus* inactivation after 0.5 h of treatment with PASW30 (Figure 4c), as well as for *Salmonella* spp. In contrast, other authors have reported the even faster inactivation of >5 log *Salmonella* enterica exposed to PAW within 1 min [73]. As we investigated one isolate per studied species, future works should evaluate the effect of PASWs against different strains or isolates of the same species to provide a comprehensive overview of intraspecies sensitivity to this technology.

A comprehensive and quantitative comparison of the viral inactivation measurements of the present study cannot be provided because of the diverse models adopted (e.g., phages, surrogates, and HIE), the different cell systems used, and techniques applied for viral titration (e.g., plaque count vs. $TCID_{50}$ vs. fold RNA increase upon replication), as well as for the experimental design adopted (kinetic vs. endpoint measurements). Still, our dataset provides novel experimental evidence of viral inactivation in SW due to plasma treatments.

Indeed, while reports on viral inactivation of PASW, either salt or simulated SW, are missing, some information is available on viral inactivation using PAW as there is an increasing research interest in the field [74]. For instance, Guo showed that PAW reduced MS2 and ϕ174 phages by >4 log after 4 h of treatment [11]. Furthermore, Wu and colleagues [75] demonstrated that MS2 inactivation was dependent on gas carriers and power levels and achieved it within 3 min under the tested conditions. Enveloped, single-stranded RNA animal viruses have also been tested in water solutions. Interestingly, Newcastle disease virus was completely inactivated after 30 min either in water or salt (0.9% NaCl) water solutions [60]. A significant 4.3 log $TCID_{50}$/100 µL reduction in Feline calicivirus (FCV), acting as a surrogate for human norovirus, was reported after 5 min treatment in sterile water solution, even though weaker reductions of 0.9–2 log $TCID_{50}$/100 µL were recorded in buffered solution [17]. In addition, Pepper mild mottle virus (PMMV) and Tobacco mosaic virus (TMV), non-enveloped plant viruses, have been successfully inactivated by plasma in water, of interest for irrigation water decontamination [76,77]. This study expands the knowledge on the inactivation of the main viral foodborne pathogen, namely HuNoV, using an infectivity assay to assess the efficacy of plasma technology in seawater, which could be exploited in further investigations. Moreover, our data showed the infectivity of HuNoV GII.4 and its surrogates after 24 h in SW. Although the HuNoV, TV, and MNV concentrations were slightly reduced, their infectivity demonstrated after 24 h in SW confirms the experimental evidence on the risk of viral transmissibility through the water cycle [49,78,79]. The mechanism of viral inactivation was not investigated in this study. However, several studies have reported that plasma-mediated virus inactivation is caused by RONS that induce the perforation of viral capsid and a reduction in virus replication [11,71,77,80]. On the other hand, the effect and synergy

of hydrogen peroxide in the inactivation process of plasma treatments is not yet fully elucidated [11,81,82]. Besides the resistance of enteric viruses to slight acid conditions (e.g., pH 4–5) [70], experimentally confirmed in the present study as well, it cannot be excluded that the pH may exert an additive antiviral effect along with RONS. Thus, it would be worth deeply investigating these viral inactivation mechanisms in salt water solutions in future studies. Our study provides evidence to exclude the potential adverse effects of the tested PASW on biological organisms. Indeed, we tested the potential cytotoxicity of PASW on cells using HIE. Diluted 1:1 PASWs were assessed as nontoxic as no structural damage of monolayers was observed, and cell functionality was preserved as HuNoV replication was demonstrated to be supported. Previous studies used HepG2 cell lines or live, immunodeficient mice for similar purposes [76,83]. Besides the different characteristics of activated waters and the biological models used for testing, these studies corroborate the need for assessing the safety of PAW/PASW for its safe use and consumption. Finally, we tested the viability of mussels in PASW30 within 24 h as the first step in employing PASWs in shellfish depuration systems. Interestingly, Campell and colleagues investigated the effective depuration of *E. coli* in bioaccumulated oysters and depurated in PASW for 24 h [62]. The authors reported that 24 h PASW depuration of bioaccumulated oysters reduced total coliforms and *E. coli* by 3.9 and 3.4 logs, respectively, without any negative effect on mollusk viability or quality. Thus, the use of bioaccumulated shellfish with phages or norovirus surrogates and depurated with PASW could represent the next research step to define effective operational procedures of depuration strategies for different bivalve mollusk species.

5. Conclusions

This study proves PASWs to be an efficient technology to inactivate *E. coli* O157, *Salmonella* spp., *V. parahemolyticus*, bacteriophages (MS2 and ϕ174), cultivable norovirus surrogates (MNV and TV), and HuNoV. In particular, PASW activated for 30 min completely inactivated the studied pathogens within 24 h, while preventing cytotoxicity effects and preserving mussel viability. Future studies should validate this antiviral and antibacterial effect of PASWs in bioaccumulated shellfish in a simulated depuration process. Taking all of these results together, this research shows that PASW can be a suitable option to depurate bivalve mollusks and control the biohazard risks linked to microbiological contamination, either viral or bacterial, due to its high efficiency, short treatment period, sustainability, and cost-effectiveness.

Author Contributions: Conceptualization, V.T. and W.R.; methodology, A.P., A.M. and P.L.; formal analysis, A.P.; resources, V.T., G.S. and W.R.; data curation, W.R.; writing—original draft preparation, A.P. and W.R.; writing—review and editing, G.S., V.T, and W.R.; visualization, W.R.; supervision, V.T. and W.R.; project administration, V.T. and W.R.; funding acquisition, V.T. and W.R. All authors have read and agreed to the published version of the manuscript.

Funding: This research was supported by "PREVISION" (PID2019-105509RJ-I00, MCIN/AEI /10.13039/501100011033) project funded to WR. AM was supported by a predoctoral research grant funded by University of Bari "A. Moro" (Italy). IATA-CSIC is a Centre of Excellence Severo Ochoa (CEX2021-001189-S MCIN/AEI / 10.13039/ 501100011033). The funding sources had no role in the study design, data collection, analysis of data, writing, or in the decision to publish.

Institutional Review Board Statement: Not applicable.

Informed Consent Statement: Not applicable.

Data Availability Statement: The original contributions presented in the study are included in the article, further inquiries can be directed to the corresponding authors.

Acknowledgments: The authors acknowledge RENASCO S.R.L. for providing the plasma-activated water and their technical support during the plasma experiments. Mare Gioioso SRL (Bari, Italia) is also acknowledged for providing the seawater samples. The authors acknowledge Tantillo (University of Bari, Italy) for providing the *E. coli* O157 and *Salmonella* spp. strains.

Conflicts of Interest: The authors declare no conflicts of interest.

References

1. Šimončicová, J.; Kryštofová, S.; Medvecká, V.; Ďurišová, K.; Kaliňáková, B. Technical Applications of Plasma Treatments: Current State and Perspectives. *Appl. Microbiol. Biotechnol.* **2019**, *103*, 5117–5129. https://doi.org/10.1007/s00253-019-09877-x.
2. Bourke, P.; Ziuzina, D.; Boehm, D.; Cullen, P.J.; Keener, K. The Potential of Cold Plasma for Safe and Sustainable Food Production. *Trends Biotechnol.* **2018**, *36*, 615–626. https://doi.org/10.1016/j.tibtech.2017.11.001.
3. Zhou, X.; Cai, D.; Xiao, S.; Ning, M.; Zhou, R.; Zhang, S.; Chen, X.; Ostrikov, K.; Dai, X. In Vivo Pen: A Novel Plasma Source for In Vivo Cancer Treatment. *J. Cancer* **2020**, *11*, 2273–2282. https://doi.org/10.7150/jca.38613.
4. Wang, Q.; Salvi, D. Recent Progress in the Application of Plasma-Activated Water (PAW) for Food Decontamination. *Curr. Opin. Food Sci.* **2021**, *42*, 51–60. https://doi.org/10.1016/j.cofs.2021.04.012.
5. Oh, Y.J.; Song, A.Y.; Min, S.C. Inhibition of *Salmonella* Typhimurium on Radish Sprouts Using Nitrogen-Cold Plasma. *Int. J. Food Microbiol.* **2017**, *249*, 66–71. https://doi.org/10.1016/j.ijfoodmicro.2017.03.005.
6. Fernández, A.; Noriega, E.; Thompson, A. Inactivation of *Salmonella* Enterica Serovar Typhimurium on Fresh Produce by Cold Atmospheric Gas Plasma Technology. *Food Microbiol.* **2013**, *33*, 24–29. https://doi.org/10.1016/j.fm.2012.08.007.
7. Choi, S.; Puligundla, P.; Mok, C. Corona Discharge Plasma Jet for Inactivation of *Escherichia coli* O157:H7 and Listeria Monocytogenes on Inoculated Pork and Its Impact on Meat Quality Attributes. *Ann. Microbiol.* **2016**, *66*, 685–694. https://doi.org/10.1007/s13213-015-1147-5.
8. Baier, M.; Görgen, M.; Ehlbeck, J.; Knorr, D.; Herppich, W.B.; Schlüter, O. Non-Thermal Atmospheric Pressure Plasma: Screening for Gentle Process Conditions and Antibacterial Efficiency on Perishable Fresh Produce. *Innov. Food Sci. Emerg. Technol.* **2014**, *22*, 147–157. https://doi.org/10.1016/j.ifset.2014.01.011.

9. Hertwig, C.; Reineke, K.; Ehlbeck, J.; Knorr, D.; Schlüter, O. Decontamination of Whole Black Pepper Using Different Cold Atmospheric Pressure Plasma Applications. *Food Control* **2015**, *55*, 221–229. https://doi.org/10.1016/j.foodcont.2015.03.003.
10. Thirumdas, R.; Kothakota, A.; Annapure, U.; Siliveru, K.; Blundell, R.; Gatt, R.; Valdramidis, V.P. Plasma Activated Water (PAW): Chemistry, Physico-Chemical Properties, Applications in Food and Agriculture. *Trends Food Sci. Technol.* **2018**, *77*, 21–31. https://doi.org/10.1016/j.tifs.2018.05.007.
11. Guo, L.; Xu, R.; Gou, L.; Liu, Z.; Zhao, Y.; Liu, D.; Zhang, L.; Chen, H.; Kong, M.G. Mechanism of Virus Inactivation by Cold Atmospheric-Pressure Plasma and Plasma-Activated Water. *Appl. Environ. Microbiol.* **2018**, *84*, e00726-18. https://doi.org/10.1128/AEM.00726-18.
12. Aboubakr, H.A.; Williams, P.; Gangal, U.; Youssef, M.M.; El-Sohaimy, S.A.A.; Bruggeman, P.J.; Goyal, S.M. Virucidal Effect of Cold Atmospheric Gaseous Plasma on Feline Calicivirus, a Surrogate for Human Norovirus. *Appl. Environ. Microbiol.* **2015**, *81*, 3612–3622. https://doi.org/10.1128/AEM.00054-15.
13. Baert, L.; Debevere, J.; Uyttendaele, M. The Efficacy of Preservation Methods to Inactivate Foodborne Viruses. *Int. J. Food Microbiol.* **2009**, *131*, 83–94. https://doi.org/10.1016/j.ijfoodmicro.2009.03.007.
14. Ahlfeld, B.; Li, Y.; Boulaaba, A.; Binder, A.; Schotte, U.; Zimmermann, J.L.; Morfill, G.; Klein, G. Inactivation of a Foodborne Norovirus Outbreak Strain with Nonthermal Atmospheric Pressure Plasma. *mBio* **2015**, *6*, e02300-14. https://doi.org/10.1128/mBio.02300-14.
15. Bae, S.-C.; Park, S.Y.; Choe, W.; Ha, S.-D. Inactivation of Murine Norovirus-1 and Hepatitis a Virus on Fresh Meats by Atmospheric Pressure Plasma Jets. *Food Res. Int.* **2015**, *76*, 342–347. https://doi.org/10.1016/j.foodres.2015.06.039.
16. Lacombe, A.; Niemira, B.A.; Gurtler, J.B.; Sites, J.; Boyd, G.; Kingsley, D.H.; Li, X.; Chen, H. Nonthermal Inactivation of Norovirus Surrogates on Blueberries Using Atmospheric Cold Plasma. *Food Microbiol.* **2017**, *63*, 1–5. https://doi.org/10.1016/j.fm.2016.10.030.
17. Nayak, G.; Aboubakr, H.A.; Goyal, S.M.; Bruggeman, P.J. Reactive Species Responsible for the Inactivation of Feline Calicivirus by a Two-dimensional Array of Integrated Coaxial Microhollow Dielectric Barrier Discharges in Air. *Plasma Process. Polym.* **2018**, *15*, 1700119. https://doi.org/10.1002/ppap.201700119.
18. Herianto, S.; Shih, M.-K.; Lin, C.-M.; Hung, Y.-C.; Hsieh, C.-W.; Wu, J.-S.; Chen, M.-H.; Chen, H.-L.; Hou, C.-Y. The Effects of Glazing with Plasma-Activated Water Generated by a Piezoelectric Direct Discharge Plasma System on Whiteleg Shrimp (*Litopenaeus vannamei*). *LWT* **2022**, *154*, 112547. https://doi.org/10.1016/j.lwt.2021.112547.
19. Patange, A.; Lu, P.; Boehm, D.; Cullen, P.J.; Bourke, P. Efficacy of Cold Plasma Functionalised Water for Improving Microbiological Safety of Fresh Produce and Wash Water Recycling. *Food Microbiol.* **2019**, *84*, 103226. https://doi.org/10.1016/j.fm.2019.05.010.

20. Andrasch, M.; Stachowiak, J.; Schlüter, O.; Schnabel, U.; Ehlbeck, J. Scale-up to Pilot Plant Dimensions of Plasma Processed Water Generation for Fresh-Cut Lettuce Treatment. *Food Packag. Shelf Life* **2017**, *14*, 40–45. https://doi.org/10.1016/j.fpsl.2017.08.007.
21. Wong, K.S.; Lim, W.T.H.; Ooi, C.W.; Yeo, L.Y.; Tan, M.K. In Situ Generation of Plasma-Activated Aerosols via Surface Acoustic Wave Nebulization for Portable Spray-Based Surface Bacterial Inactivation. *Lab Chip* **2020**, *20*, 1856–1868. https://doi.org/10.1039/D0LC00001A.
22. de Castro Medeiros, L.; de Alencar, F.L.S.; Navoni, J.A.; de Araujo, A.L.C.; do Amaral, V.S. Toxicological Aspects of Trihalomethanes: A Systematic Review. *Environ. Sci. Pollut. Res.* **2019**, *26*, 5316–5332. https://doi.org/10.1007/s11356-018-3949-z.
23. Jenns, K.; Sassi, H.P.; Zhou, R.; Cullen, P.J.; Carter, D.; Mai-Prochnow, A. Inactivation of Foodborne Viruses: Opportunities for Cold Atmospheric Plasma. *Trends Food Sci. Technol.* **2022**, *124*, 323–333. https://doi.org/10.1016/j.tifs.2022.04.006.
24. Rahman, M.; Hasan, M.S.; Islam, R.; Rana, R.; Sayem, A.S.M.; Sad, M.A.A.; Matin, A.; Raposo, A.; Zandonadi, R.P.; Han, H.; et al. Plasma-Activated Water for Food Safety and Quality: A Review of Recent Developments. *Int. J. Environ. Res. Public Health* **2022**, *19*, 6630.
25. Oliveira, J.; Cunha, A.; Castilho, F.; Romalde, J.L.; Pereira, M.J. Microbial Contamination and Purification of Bivalve Shellfish: Crucial Aspects in Monitoring and Future Perspectives—A Mini-Review. *Food Control* **2011**, *22*, 805–816. https://doi.org/10.1016/j.foodcont.2010.11.032.
26. RASFF Window. Available online: https://webgate.ec.europa.eu/rasff-window/screen/search?searchQueries=eyJkYXRlIjp7InN0YXJ0UmFuZ2UiOiIyMDIyLTEyLTMxVDIzOjAwOjAwLjAwMFoiLCJlbmRSYW5nZSI6IjIwMjMtMTItMzBUMjM6MDA6MDAuMDAwWiJ9LCJub3RpZmljYXRpb25TdGF0dXMiOnsibm90aWZpY2F0aW9uU3RhdHVzIjpbWzFdXX0sInByb2R1Y3QiOnsicHJvZHVjdENhdGVnb3J5IjpbWzE4NDMyXV19LCJyaXNrIjp7ImhhemFyZENhdGVnb3J5IjpbWzIxODAxXV19fQ%3D%3D (accessed on 17 January 2024).
27. Analysis of the European Baseline Survey of Norovirus in Oysters. *EFSA J.* **2019**, *17*, e05762. https://doi.org/10.2903/j.efsa.2019.5762.
28. Baker-Austin, C.; Oliver, J.D.; Alam, M.; Ali, A.; Waldor, M.K.; Qadri, F.; Martinez-Urtaza, J. *Vibrio* spp. Infections. *Nat. Rev. Dis. Primers* **2018**, *4*, 1–19. https://doi.org/10.1038/s41572-018-0005-8.
29. Mancini, M.E.; Alessiani, A.; Donatiello, A.; Didonna, A.; D'Attoli, L.; Faleo, S.; Occhiochiuso, G.; Carella, F.; Di Taranto, P.; Pace, L.; et al. Systematic Survey of *Vibrio* spp. and *Salmonella* spp. in Bivalve Shellfish in Apulia Region (Italy): Prevalence and Antimicrobial Resistance. *Microorganisms* **2023**, *11*, 450. https://doi.org/10.3390/microorganisms11020450.
30. Mok, J.S.; Ryu, A.; Kwon, J.Y.; Kim, B.; Park, K. Distribution of *Vibrio* Species Isolated from Bivalves and Bivalve Culture Environments along the Gyeongnam Coast in Korea: Virulence and Antimicrobial

Resistance of *Vibrio parahaemolyticus* Isolates. *Food Control* **2019**, *106*, 106697. https://doi.org/10.1016/j.foodcont.2019.06.023.

31. Directive 2003/99/EC of the European Parliament and of the Council of 17 November 2003 on the monitoring of zoonoses and zoonotic agents, amending Council Decision 90/424/EEC and repealing Council Directive 92/117/EEC. Available online: http://data.europa.eu/eli/dir/2003/99/oj (accessed on 09 March 2024) .
32. European Food Safety Authority; European Centre for Disease Prevention and Control. The European Union One Health 2021 Zoonoses Report. *EFSA J.* **2022**, *20*, e07666. https://doi.org/10.2903/j.efsa.2022.7666.
33. Commission Regulation (EC) No 1441/2007 of 5 December 2007 amending Regulation (EC) No 2073/2005 on microbiological criteria for foodstuffs (Text with EEA relevance). Available online: http://data.europa.eu/eli/reg/2007/1441/oj (accessed on 09 March 2024).
34. European Food Safety Authority; European Centre for Disease Prevention and Control. The European Union One Health 2022 Zoonoses Report. *EFSA J.* **2023**, *21*, e8442. https://doi.org/10.2903/j.efsa.2023.8442.
35. Pavoni, E.; Bertasi, B.; Galuppini, E.; Mangeri, L.; Meletti, F.; Tilola, M.; Carta, V.; Todeschi, S.; Losio, M.-N. Detection of Hepatitis a Virus and Norovirus in Different Food Categories: A 6-Year Survey in Italy. *Food Environ. Virol.* **2022**, *14*, 69–76. https://doi.org/10.1007/s12560-021-09503-y.
36. Commission Implementing Regulation (EU) 2019/627 of 15 March 2019 laying down uniform practical arrangements for the performance of official controls on products of animal origin intended for human consumption in accordance with Regulation (EU) 2017/625 of the European Parliament and of the Council and amending Commission Regulation (EC) No 2074/2005 as regards official controls (Text with EEA relevance). Available online: http://data.europa.eu/eli/reg_impl/2019/627/oj (accessed on 09 March 2024) .
37. Le Mennec, C.; Parnaudeau, S.; Rumebe, M.; Le Saux, J.C.; Piquet, J.C.; Le Guyader, S.F. Follow-Up of Norovirus Contamination in an Oyster Production Area Linked to Repeated Outbreaks. *Food Environ. Virol.* **2017**, *9*, 54–61. https://doi.org/10.1007/s12560-016-9260-6.
38. McLeod, C.; Polo, D.; Le Saux, J.; Le Guyader, F.S. Depuration and Relaying: A Review on Potential Removal of Norovirus from Oysters. *Compr. Rev. Food Sci. Food Saf.* **2017**, *16*, 692–706. https://doi.org/10.1111/1541-4337.12271.
39. *UNI EN ISO 15216-1:2017*; Microbiology of the Food Chain—Horizontal Method for Determination of Hepatitis a Virus and Norovirus Using Real-Time RT-PCR—Part 1: Method for Quantification. International Organization for Standardization, Vernier, Geneva, Switzerland, 2017. Available online: https://www.iso.org/standard/65681.html (accessed on 09 March 2024).

40. Estes, M.K.; Ettayebi, K.; Tenge, V.R.; Murakami, K.; Karandikar, U.; Lin, S.C.; Ayyar, B.V.; Cortes-Penfield, N.W.; Haga, K.; Neill, F.H.; et al. Human Norovirus Cultivation in Nontransformed Stem Cell-Derived Human Intestinal Enteroid Cultures: Success and Challenges. *Viruses* **2019**, *11*, 638. https://doi.org/10.3390/V11070638.

41. Kamarasu, P.; Hsu, H.-Y.; Moore, M.D. Research Progress in Viral Inactivation Utilizing Human Norovirus Surrogates. *Front. Sustain. Food Syst.* **2018**, *2*, 89. https://doi.org/10.3389/fsufs.2018.00089.

42. Cromeans, T.; Park, G.W.; Costantini, V.; Lee, D.; Wang, Q.; Farkas, T.; Lee, A.; Vinjé, J. Comprehensive Comparison of Cultivable Norovirus Surrogates in Response to Different Inactivation and Disinfection Treatments. *Appl. Environ. Microbiol.* **2014**, *80*, 5743–5751. https://doi.org/10.1128/AEM.01532-14.

43. Richards, G.P. Critical Review of Norovirus Surrogates in Food Safety Research: Rationale for Considering Volunteer Studies. *Food Environ. Virol.* **2012**, *4*, 6–13. https://doi.org/10.1007/s12560-011-9072-7.

44. Blondin-Brosseau, M.; Harlow, J.; Doctor, T.; Nasheri, N. Examining the Persistence of Human Coronavirus 229E on Fresh Produce. *Food Microbiol.* **2021**, *98*, 103780. https://doi.org/10.1016/j.fm.2021.103780.

45. Danso, D.; Chow, J.; Streita, W.R. Plastics: Environmental and Biotechnological Perspectives on Microbial Degradation. *Appl. Environ. Microbiol.* **2019**, *85*, e01095-19. https://doi.org/10.1128/AEM.01095-19.

46. Ettayebi, K.; Crawford, S.E.; Murakami, K.; Broughman, J.R.; Karandikar, U.; Tenge, V.R.; Neill, F.H.; Blutt, S.E.; Zeng, X.L.; Qu, L.; et al. Replication of Human Noroviruses in Stem Cell-Derived Human Enteroids. *Science* **2016**, *353*, 1387–1393. https://doi.org/10.1126/SCIENCE.AAF5211.

47. Costantini, V.; Morantz, E.K.; Browne, H.; Ettayebi, K.; Zeng, X.L.; Atmar, R.L.; Estes, M.K.; Vinjé, J. Human Norovirus Replication in Human Intestinal Enteroids as Model to Evaluate Virus Inactivation. *Emerg. Infect. Dis.* **2018**, *24*, 1453–1464. https://doi.org/10.3201/EID2408.180126.

48. Escudero-Abarca, B.I.; Goulter, R.M.; Arbogast, J.W.; Leslie, R.A.; Green, K.; Jaykus, L.A. Efficacy of Alcohol-Based Hand Sanitizers against Human Norovirus Using RNase-RT-QPCR with Validation by Human Intestinal Enteroid Replication. *Lett. Appl. Microbiol.* **2020**, *71*, 605–610. https://doi.org/10.1111/LAM.13393.

49. Desdouits, M.; Polo, D.; Le Mennec, C.; Strubbia, S.; Zeng, X.L.; Ettayebi, K.; Atmar, R.L.; Estes, M.K.; Le Guyader, F.S. Use of Human Intestinal Enteroids to Evaluate Persistence of Infectious Human Norovirus in Seawater. *Emerg. Infect. Dis.* **2022**, *28*, 1475–1479. https://doi.org/10.3201/EID2807.220219.

50. Randazzo, W.; Costantini, V.; Morantz, E.K.; Vinjé, J. Human Intestinal Enteroids to Evaluate Human Norovirus GII.4 Inactivation by Aged-Green Tea. *Front. Microbiol.* **2020**, *11*, 1917. https://doi.org/10.3389/fmicb.2020.01917.

51. Falcó, I.; Randazzo, W.; Pérez, A.; Martínez, A.; Rodrigo, D.; Sánchez, G. High Pressure Treatment and Green Tea Extract Synergistically Control Enteric Virus Contamination in Beverages. *Food Control* **2023**, *144*, 109384. https://doi.org/10.1016/J.FOODCONT.2022.109384.

52. Kulawik, P.; Kumar Tiwari, B. Recent Advancements in the Application of Non-Thermal Plasma Technology for the Seafood Industry. *Crit. Rev. Food Sci. Nutr.* **2019**, *59*, 3199–3210. https://doi.org/10.1080/10408398.2018.1510827.

53. Abedon, S.T.; Yin, J. Bacteriophage Plaques: Theory and Analysis. In *Bacteriophages*; Springer: Berlin/Heidelberg, Germany, 2009; pp. 161–174.

54. Falcó, I.; Randazzo, W.; Rodríguez-Díaz, J.; Gozalbo-Rovira, R.; Luque, D.; Aznar, R.; Sánchez, G. Antiviral Activity of Aged Green Tea Extract in Model Food Systems and under Gastric Conditions. *Int. J. Food Microbiol.* **2019**, *292*, 101–106. https://doi.org/10.1016/j.ijfoodmicro.2018.12.019.

55. Carmona, N.; Randazzo, W. Passaging human intestinal organoids and monolayers set up. *Protoc. Exch.* **2023**. *https://doi.org/10.21203/rs.3.pex-2221/v1*

56. Wales, S.Q.; Pandiscia, A.; Kulka, M.; Sánchez, G.; Randazzo, W. Challenges for Estimating Human Norovirus Infectivity by Viability RT-QPCR as Compared to Replication in Human Intestinal Enteroids. *Int. J. Food Microbiol.* **2024**, *411*, 110507. https://doi.org/10.1016/j.ijfoodmicro.2023.110507.

57. Aboubakr, H.A.; Sampedro Parra, F.; Collins, J.; Bruggeman, P.; Goyal, S.M. În Situ Inactivation of Human Norovirus GII.4 by Cold Plasma: Ethidium Monoazide (EMA)-Coupled RT-QPCR Underestimates Virus Reduction and Fecal Material Suppresses Inactivation. *Food Microbiol.* **2020**, *85*, 103307. https://doi.org/10.1016/j.fm.2019.103307.

58. Baek, K.H.; Yong, H.I.; Yoo, J.H.; Kim, J.W.; Byeon, Y.S.; Lim, J.; Yoon, S.Y.; Ryu, S.; Jo, C. Antimicrobial Effects and Mechanism of Plasma Activated Fine Droplets Produced from Arc Discharge Plasma on Planktonic *Listeria monocytogenes* and *Escherichia coli* O157:H7. *J. Phys. D Appl. Phys.* **2020**, *53*, 124002. https://doi.org/10.1088/1361-6463/ab634d.

59. Oehmigen, K.; Winter, J.; Hähnel, M.; Wilke, C.; Brandenburg, R.; Weltmann, K.; von Woedtke, T. Estimation of Possible Mechanisms of *Escherichia coli* Inactivation by Plasma Treated Sodium Chloride Solution. *Plasma Process. Polym.* **2011**, *8*, 904–913. https://doi.org/10.1002/ppap.201000099.

60. Su, X.; Tian, Y.; Zhou, H.; Li, Y.; Zhang, Z.; Jiang, B.; Yang, B.; Zhang, J.; Fang, J. Inactivation Efficacy of Nonthermal Plasma-Activated Solutions against Newcastle Disease Virus. *Appl. Environ. Microbiol.* **2018**, *84*, e02836-17. https://doi.org/10.1128/AEM.02836-17.

61. Wang, Q.; Salvi, D. Evaluation of Plasma-Activated Water (PAW) as a Novel Disinfectant: Effectiveness on Escherichia Coli and Listeria Innocua, Physicochemical Properties, and Storage Stability. *LWT* **2021**, *149*, 111847. https://doi.org/10.1016/j.lwt.2021.111847.

62. Campbell, V.M.; Hall, S.; Salvi, D. Antimicrobial Effects of Plasma-Activated Simulated Seawater (PASW) on Total Coliform and *Escherichia coli* in Live Oysters during Static Depuration. *Fishes* **2023**, *8*, 396. https://doi.org/10.3390/fishes8080396.

63. Campbell, V.M.; Wang, Q.; Hall, S.G.; Salvi, D. Physicochemical Properties and Antimicrobial Impacts of Plasma-activated Simulated Seawater on *Escherichia coli*. *JSFA Rep.* **2022**, *2*, 228–235. https://doi.org/10.1002/jsf2.46.

64. Olatunde, O.O.; Benjakul, S.; Vongkamjan, K. Dielectric Barrier Discharge Cold Atmospheric Plasma: Bacterial Inactivation Mechanism. *J. Food Saf.* **2019**, *39*, e12705. https://doi.org/10.1111/jfs.12705.

65. Epifanio, C.E.; Srna, R.F. Toxicity of Ammonia, Nitrite Ion, Nitrate Ion, and Orthophosphate to Mercenaria Mercenaria and Crassostrea Virginica. *Mar. Biol.* **1975**, *33*, 241–246. https://doi.org/10.1007/BF00390928.

66. Oehmigen, K.; Hähnel, M.; Brandenburg, R.; Wilke, C.h.; Weltmann, K.-D.; von Woedtke, T.h. The Role of Acidification for Antimicrobial Activity of Atmospheric Pressure Plasma in Liquids. *Plasma Process. Polym.* **2010**, *7*, 250–257. https://doi.org/10.1002/ppap.200900077.

67. Herianto, S.; Hou, C.; Lin, C.; Chen, H. Nonthermal Plasma-activated Water: A Comprehensive Review of This New Tool for Enhanced Food Safety and Quality. *Compr. Rev. Food Sci. Food Saf.* **2021**, *20*, 583–626. https://doi.org/10.1111/1541-4337.12667.

68. Kaushik, N.K.; Bhartiya, P.; Kaushik, N.; Shin, Y.; Nguyen, L.N.; Park, J.S.; Kim, D.; Choi, E.H. Nitric-Oxide Enriched Plasma-Activated Water Inactivates 229E Coronavirus and Alters Antiviral Response Genes in Human Lung Host Cells. *Bioact. Mater.* **2023**, *19*, 569–580. https://doi.org/10.1016/j.bioactmat.2022.05.005.

69. Wolff, A.; Günther, T.; Albert, T.; Johne, R. Effect of Sodium Chloride, Sodium Nitrite and Sodium Nitrate on the Infectivity of Hepatitis E Virus. *Food Environ. Virol.* **2020**, *12*, 350–354. https://doi.org/10.1007/s12560-020-09440-2.

70. Seo, K.; Lee, J.E.; Lim, M.Y.; Ko, G. Effect of Temperature, PH, and NaCl on the Inactivation Kinetics of Murine Norovirus. *J. Food Prot.* **2012**, *75*, 533–540. https://doi.org/10.4315/0362-028X.JFP-11-199.

71. Kaushik, N.; Mitra, S.; Baek, E.J.; Nguyen, L.N.; Bhartiya, P.; Kim, J.H.; Choi, E.H.; Kaushik, N.K. The Inactivation and Destruction of Viruses by Reactive Oxygen Species Generated through Physical and Cold Atmospheric Plasma Techniques: Current Status and Perspectives. *J. Adv. Res.* **2023**, *43*, 59–71. https://doi.org/10.1016/j.jare.2022.03.002.

72. Boulais, M.; Chenevert, K.J.; Demey, A.T.; Darrow, E.S.; Robison, M.R.; Roberts, J.P.; Volety, A. Oyster Reproduction Is Compromised by Acidification Experienced Seasonally in Coastal Regions. *Sci. Rep.* **2017**, *7*, 13276. https://doi.org/10.1038/s41598-017-13480-3.

73. Russell, S. The Effect of Electrolyzed Oxidative Water Applied Using Electrostatic Spraying on Pathogenic and Indicator Bacteria on the Surface of Eggs. *Poult. Sci.* **2003**, *82*, 158–162. https://doi.org/10.1093/ps/82.1.158.

74. Zver, M.; Dobnik, D.; Zaplotnik, R.; Mozetič, M.; Filipić, A.; Primc, G. Non-Thermal Plasma Inactivation of Viruses in Water Solutions. *J. Water Process. Eng.* **2023**, *53*, 103839. https://doi.org/10.1016/j.jwpe.2023.103839.

75. Wu, Y.; Liang, Y.; Wei, K.; Li, W.; Yao, M.; Zhang, J.; Grinshpun, S.A. MS2 Virus Inactivation by Atmospheric-Pressure Cold Plasma Using Different Gas Carriers and Power Levels. *Appl. Environ. Microbiol.* **2015**, *81*, 996–1002. https://doi.org/10.1128/AEM.03322-14.

76. Filipić, A.; Dobnik, D.; Tušek Žnidarič, M.; Žegura, B.; Štern, A.; Primc, G.; Mozetič, M.; Ravnikar, M.; Žel, J.; Gutierrez Aguirre, I. Inactivation of Pepper Mild Mottle Virus in Water by Cold Atmospheric Plasma. *Front. Microbiol.* **2021**, *12*, 618209. https://doi.org/10.3389/fmicb.2021.618209.

77. Hanbal, S.E.; Takashima, K.; Miyashita, S.; Ando, S.; Ito, K.; Elsharkawy, M.M.; Kaneko, T.; Takahashi, H. Atmospheric-Pressure Plasma Irradiation Can Disrupt Tobacco Mosaic Virus Particles and RNAs to Inactivate Their Infectivity. *Arch. Virol.* **2018**, *163*, 2835–2840. https://doi.org/10.1007/s00705-018-3909-4.

78. Shaffer, M.; Huynh, K.; Costantini, V.; Bibby, K.; Vinjé, J. Viable Norovirus Persistence in Water Microcosms. *Environ. Sci. Technol. Lett.* **2022**, *9*, 851–855. https://doi.org/10.1021/acs.estlett.2c00553.

79. Rexin, D.; Rachmadi, A.T.; Hewitt, J. Persistence of Infectious Human Norovirus in Estuarine Water. *Food Environ. Virol.* **2024**. https://doi.org/10.1007/s12560-023-09577-w.

80. Mohamed, H.; Nayak, G.; Rendine, N.; Wigdahl, B.; Krebs, F.C.; Bruggeman, P.J.; Miller, V. Non-Thermal Plasma as a Novel Strategy for Treating or Preventing Viral Infection and Associated Disease. *Front. Phys.* **2021**, *9*, 683118. https://doi.org/10.3389/fphy.2021.683118.

81. Aboubakr, H.A.; Gangal, U.; Youssef, M.M.; Goyal, S.M.; Bruggeman, P.J. Inactivation of Virus in Solution by Cold Atmospheric Pressure Plasma: Identification of Chemical Inactivation Pathways. *J. Phys. D Appl. Phys.* **2016**, *49*, 204001. https://doi.org/10.1088/0022-3727/49/20/204001.

82. Yamashiro, R.; Misawa, T.; Sakudo, A. Key Role of Singlet Oxygen and Peroxynitrite in Viral RNA Damage during Virucidal Effect of Plasma Torch on Feline Calicivirus. *Sci. Rep.* **2018**, *8*, 17947. https://doi.org/10.1038/s41598-018-36779-1.

83. Xu, D.; Cui, Q.; Xu, Y.; Wang, B.; Tian, M.; Li, Q.; Liu, Z.; Liu, D.; Chen, H.; Kong, M.G. Systemic Study on the Safety of Immuno-Deficient Nude Mice Treated by Atmospheric Plasma-Activated Water. *Plasma Sci. Technol.* **2018**, *20*, 044003. https://doi.org/10.1088/2058-6272/aa9842.

10. HUMAN INTESTINAL ENTEROIDS PLATFORM TO ASSESS THE INFECTIVITY OF GASTROENTERITIS VIRUSES IN WASTEWATER

Enteric viruses are known to be highly resilient and undergo conventional sewage treatment processes applied by wastewater treatment plants (WWTPs) such as chlorination and UV radiation [196,197]. As a results, WWTPs often do not completely remove viral particles from sewage leading to the detection of enteric viruses in effluent water samples [198–200].

This poses a risk of high concern for human health since reclaimed water is commonly employed for irrigation of crops or released into water bodies like rivers and lakes [201].

Several food items, particularly shellfish and fresh vegetables, are indeed frequently implicated in waterborne contamination. Shellfish, such as oysters, clams, and mussels, filter large volumes of water and can accumulate viruses present in contaminated water [202]. Similarly, vegetables irrigated with contaminated water, particularly leafy greens like lettuce, spinach, and other crops, eaten raw or minimally processed, can also be contaminated with enteric viruses [203].Therefore, monitoring both the presence and infectivity of human viral pathogens in effluent wastewater can represent and integrated approach to assess the effectiveness of current water reclamation systems and, consequently, to guarantee food safety and public health.

Several scientific studies have employed viability RT-qPCR to estimate the viral infectivity of enteric viruses in water samples [185–189], demonstrating the efficacy of these methods as indicators of viral infectivity, despite some limitations, as highlighted in Chapter 7.

Moreover, cell culture methods represent the gold standard for virus viability testing and have been used to assess viral infectivity in clinical virology, but they face

significant drawbacks when applied to environmental samples [51]. These include co-contamination with multiple viruses, the lack of a robust cell lines for some viruses, especially HuNoV, and the cytotoxic effects of wastewater on cultures [204].

Since 2016, the HIE system has allowed the in vitro cultivation of many HuNoV strains and, secondly, other enteric viruses such as sapovirus, HAstV, HAdV, and RV, representing an efficient cell culture model to assess the viral infectivity[17,205,206]. Nevertheless, as far as we know, no scientific data regarding HuNoV infectivity and simultaneous detection of different gastroenteritis viruses in wastewater samples using the HIE model have been reported yet.

Therefore, we conducted a scientific study with the aim to assess the feasibility of the HIE model to detect replication of co-infections of different human gastroenteritis viruses such as HuNoVs, RV, HAstV and/or HAdV in naturally contaminated wastewater samples. Subsequently, the genotypes of gastroenteritis viruses replicating in HIE from wastewater samples were investigated.

Article adapted for printing of the PhD thesis. Article available online on Water research, ELSEVIER, https://doi.org/10.1016/j.watres.2024.121481

Human intestinal enteroids platform to assess the infectivity of gastroenteritis viruses in wastewater

Noelia Carmona-Vicente [a], **Annamaria Pandiscia** [b,c], Cristina Santiso-Bellón [a], Alba Perez-Cataluña [b], Jesús Rodríguez-Díaz [a,d], Veronica P. Costantini [e], Javier Buesa[a,d], Jan Vinjé [e], Gloria Sánchez [b], Walter Randazzo [b,*]

[a] Department of Microbiology and Ecology, University of Valencia, Valencia, Spain

[b] Department of Preservation and Food Safety Technologies, IATA-CSIC, Valencia, Spain

[c] Department of Veterinary Medicine, University of Bari, Valenzano, Italy

[d] INCLIVA Health Research Institute, Valencia, Spain

[e] National Calicivirus Laboratory, Division of Viral Diseases, Centers for Disease Control and Prevention, Atlanta, Georgia, USA

Highlights

• Enhanced HIE protocols enabled the detection of infectious gastroenteritis viruses.

• Gastroenteritis viruses comparably replicated in single and multiple co-infections.

• Replication of HuNoVs, RV, HAstV, and/or HAdV was observed in 57 % of wastewater.

• Three wastewater samples exhibited replication of HuNoV GI and GII in HIE.

• HIE model confirmed infectivity of various gastroenteritis viruses in wastewater.

ABSTRACT

Fecal-orally transmitted gastroenteritis viruses, particularly human noroviruses (HuNoVs), are a public health concern. Viral transmission risk through contaminated water results underexplored as they have remained largely unculturable until recently and the robust measuring of gastroenteritis viruses infectivity in a single cell line is challenging. This study primarily aimed to test the feasibility of the human intestinal enteroids (HIE) model to demonstrate the infectivity of multiple gastroenteritis viruses in wastewater. Initially, key factors affecting viral replication in HIE model were assessed, and results demonstrated that the reagent-assisted disruption of 3D HIE represents an efficient alternative to syringe pass-through, and the filtering of HuNoV stool suspensions could be avoided. Moreover, comparable replication yields of clinical strains of HuNoV genogroup I (GI), HuNoV GII, rotavirus (RV), astrovirus (HAstV), and adenoviruses (HAdV) were obtained in single and multiple co-infections. Then, the optimized HIE model was used to demonstrate the infectivity of multiple naturally occurring gastroenteritis viruses from wastewater. Thus, a total of 28 wastewater samples were subjected to (RT)-qPCR for each virus, with subsequent testing on HIE. Among these, 16 samples (57 %) showed replication of HuNoVs (n = 3), RV (n = 5), HAstV (n = 8), and/or HAdV (n = 5). Three samples showed HuNoV replication, and sequences assigned to HuNoV GI.3[P13] and HuNoV GII.4[P16] genotypes. Concurrent replication of multiple gastroenteritis viruses occurred in 4 wastewater samples. By comparing wastewater concentrate and HIE supernatant sequences, diverse HAstV and HAdV genotypes were identified in 4 samples. In summary, we successfully employed HIE to demonstrate the presence of multiple infectious human gastroenteritis viruses, including HuNoV, in naturally contaminated wastewater samples.

Keywords: Viral infectivity; Human norovirus; Cell culture; Virus isolation; Environmental contamination; Enteric virus

DOI: *https://doi.org/10.1016/j.watres.2024.121481*

1. Introduction

Human gastroenteritis viruses are an important cause of morbidity and mortality in humans of all ages with acute gastroenteritis worldwide. They include rotavirus (RV), human norovirus (HuNoV), human astrovirus (HAstV), sapovirus and human adenovirus (HAdV) (Chatterjee et al., 2004; GBD 2015, 2016; GBD 2016, 2018; Qi et al., 2018; Valcarce et al., 2021). These viruses are excreted at high concentrations (up to 1012 viruses/g feces) by infected individuals and transmitted to other humans via the fecal-oral route (Haramoto et al., 2018). Given the high persistence of these viruses in wastewater and their high transmissibility, their presence in drinking water or irrigated foods could pose substantial public health risks. Many foodborne virus outbreaks have been linked to produce or bivalve molluscs contaminated by fecally impacted waters (EFSA and ECDC, 2022). Traditionally, detection of gastroenteritis viruses in environmental samples relies on molecular methods and realtime polymerase chain reaction (PCR) detection methods are widely used. However, for viruses such as HuNoV, the lack of a robust cell culture method to determine viral infectivity hampered assessing public health risks (Condit, 2013; Gerba et al., 2018; Hamza et al., 2011). A major breakthrough was the successful replication of HuNoV in non-transformed stem cell-derived human intestinal enteroids (HIEs) (Costantini et al., 2018; Desdouits et al., 2022; Ettayebi et al., 2021; Ettayebi et al., 2016; Randazzo et al., 2020). In addition to HuNoV, the HIE model has also been successfully

employed to demonstrate replication of sapovirus, HAstV, HAdV, and RV (Euller-Nicolas et al., 2023; Holly and Smith, 2018; Kolawole et al., 2019; Saxena et al., 2016). As recently estimated with the HIE model, HuNoVs retain their infectivity for 7 to 28 days in tap, surface and seawater (Desdouits et al., 2022; Kennedy et al., 2023; Shaffer et al., 2022), which is a relevant data to implement prevention and control strategies for viral infections transmitted through contaminated waters (Pandiscia et al., 2024). However, experimental evidence for HuNoV infectivity and simultaneous detection of different gastroenteritis viruses in wastewater samples using the HIE model has not been reported. This study aimed to assess the feasibility of the HIE model to detect replication of co-infections of different human gastroenteritis viruses in naturally contaminated wastewater samples. To this end, a protocol for passaging HIE and differentiate HIE monolayers was optimized, single and concurrent replication of diverse gastroenteritis virus in optimized HIE model assessed, and finally it was applied to evaluate viral infectivity in wastewater. Thus, this HIE platform could contribute to a deeper comprehension of viral behaviour in wastewater, with relevant implications for public health and environmental safety.

2. Material and methods

2.1. Wastewater sampling and concentration

A total of twenty-eight wastewater grab samples were collected between June and August 2022 from eleven urban wastewater treatment plants across Spain with equivalent inhabitant values ranging from 60,600 to 1900,800. The samples were transferred on ice to the laboratory, and processed within 24 h. Briefly, 200 mL of each wastewater sample was centrifuged at 4654 × *g* for 30 min to remove larger particles. The viral particles were then concentrated from the supernatants using

Centricon Plus-70 centrifugal filter devices with a cut-off of 10 kDa (Millipore, the Netherlands) and repeated centrifugation steps at 1500 × *g* for 15 min. The concentrate (1–2 mL) was serially filtered through 5 µm, 1.2 µm, 0.8 µm, and 0.45 µm polyvinylidene fluoride (PVDF) filters, and diluted 1:10 in infection media for immediate infection of the HIE monolayers, while remaining aliquots were stored at -80 °C.

2.2. Gastroenteritis viruses used in the study

Forty-two gastroenteritis virus-positive stool specimens (IDs: S1-S42) were tested on HIE, including 35 HuNoV-positive specimens, 3 human rotavirus-positive specimens, 2 cell-adapted rotavirus strains (Ito and Wa), a HAdV-positive specimen, and a HAstV-positive specimen (Table 1). Fecal specimens were stored at –80 °C until testing.

Table 1. Human enteric viruses tested for replication on jejunal HIEs.

Sample ID	Virus	Genogroup / Genotype / Strain	Collection Date[a]	Patient	Mean RNA/DNA copies/µL	Virus RNA/DNA increase (log10)[b]
1	Human norovirus	GI.4	2011		2.20×10^6	
2		GI [P2]	2018		3.13×10^5	
3		GI [P7]	2018		1.74×10^7	
4		GI.3[P13]	2022 May	Pediatric, 2y 4m, female	1.44×10^7	1.03
5		GI	2019		1.13×10^6	
6		GI	2017		2.73×10^5	
7		GI	2016		4.88×10^7	
8		GI	2011		3.11×10^5	
9		GI	2013		1.17×10^7	
10		GI	2011		2.14×10^5	
11		GI	2014		2.47×10^6	

12		GI			1.73×10^7	
13		GI			1.21×10^7	
14		GI			1.28×10^7	
15		GI			2.59×10^8	
16		GI			3.03×10^7	
17		GI.3	2018	Pediatric, 1m 6 d, female	4.99×10^6	
18		GI.3	2019	Pediatric, 2y 3m, male	9.35×10^5	
19		GI.3	2020	Adult, 45y, male	4.40×10^7	
20		GI.4			1.07×10^7	
21		GI.4	2018	Pediatric, 1y 3m, male	3.33×10^5	
22		GI.4	2019	Pediatric, 1y 8m, female	9.66×10^7	
23		GI.7	2020	Pediatric, 1y 9m, male	3.09×10^7	
24		GI.1		Adult, 62y	9.44×10^6	
25		GI.1		Adult, 96y, male	2.24×10^7	
26		GI.1	2020	Pediatric, 4y 5m, female	7.22×10^5	
27		GI.1	2020	Adult, 63y, female	6.05×10^6	
28		GII.3 [P12]	2021 Oct	Pediatric, 1y 7m, female	1.16×10^8	3.44
29		GII.3 [P12]	2021 Sept	Pediatric, 1y 9m, female	1.44×10^7	2.12
30		GII.4 [P31]	2021 Sept	Pediatric, 2y, male	1.37×10^7	4.63
31		GII.4 [P31]	2021 Sept	Pediatric, 1y 28d, male	2.65×10^7	3.90
32		GII.4 Sydney			2.51×10^7	3.29
33		GII.4 Sydney			3.56×10^8	2.79
34		GII.4 Sydney			2.24×10^7	3.28
35		GII.4 Sydney [P16]	2021 Oct	Pediatric, 10m, male	1.07×10^8	3.33
36	Human rotavirus	G9 [P8]	2019 May		3.14×10^8	1.00
37		G9 [P8]	2019 June	Pediatric, 6y 6m, female	1.47×10^8	1.24
38		G9 G12 [P8]	2019 June	Pediatric, 5y, male	2.15×10^7	2.05
39		G1 [P8]		Wa, cell culture adapted strain	3.23×10^8	2.26
40		G3 [P8]		Ito, cell culture adapted strain	8.88×10^8	2.85
41	Human adenovirus		2022 May	Pediatric, 1 year, male	7.94×10^{10}	3.69
42	Human astrovirus		2022 May	Pediatric, 4 years, male	2.79×10^9	3.24

[a] When month was not available, only year of collection is reported.

[b] Virus RNA/DNA increase at 48 hpi expressed as log_{10} fold increase. For each fecal filtrate, data represent highest mean viral RNA/DNA increase among 1:10, 1:100, 1:10,00 and 1:10,000 dilutions tested in tree replicates each.

2.3. Optimization of the human intestinal enteroid model for viral replication

Three-dimensional (3D) HIE derived from human jejunal biopsy (J2 cell line) were provided by Dr. Mary K. Estes (Baylor College of Medicine, Houston, TX). The impact of three key experimental variables on viral replication was investigated to optimize the HIE for environmental studies: (i) mechanical vs reagent-assisted disruption of 3D HIE cells prior to passaging and single cell seeding; (ii) preparation of viral suspensions with or without filtering steps, and (iii) single vs multiple viral replication. The experiments to assess (i) and (ii) were conducted using HuNoV in a round robin test involving two different laboratories. Two alternative procedures for disrupting and passaging 3D HIE were compared. The originally reported passage of 3D undifferentiated HIE using 2× pipetting steps with a 25Gx5/8 syringe (Ettayebi et al., 2016; Zou et al., 2019) was compared to incubation with Gentle Cell Dissociation Reagent (STEMCELL Technologies, BC, Canada) (Carmona and Randazzo, 2023). Three HuNoV-positive stool samples from hospitalized children with acute gastroenteritis (ID: S34 for HuNoV GII.4 Sydney; ID:S28 for HuNoV GII.3 [P12]; ID:S35 for HuNoV GII.4 Sydney [P16]) were diluted to 10 % in sterile phosphate-buffered saline and divided into portions used to compare two alternative procedures for preparing viral suspensions. An aliquot of each sample was vortexed for 30 s, and the supernatant was recovered after centrifugation at 1500 × *g* for 1 min (unfiltered samples). Alternatively, 10 % fecal suspensions were serially filtered through PVDF filters with pore sizes of 5 μm, 1.2 μm, 0.8 μm, and 0.45 μm, as originally described (Ettayebi et al., 2016). HuNoV GI.3[P13] (Sample ID: S4) and GII.4 Sydney [P16]

(Sample ID: S35), human RV G9 G12 [P8] (Sample ID: S38), HAdV (Sample ID: S41), and HAstV (Sample ID: S42) were inoculated into HIE monolayers alone (single infections) or concomitantly (multiple infections including all the five pathogens) and the rate of replication was determined after 48-hour post-infection (hpi).

2.4. HIE infection

Undifferentiated 3D HIEs and differentiated monolayers were routinely maintained and produced using commercial IntestiCult™ Organoid Growth Medium (Human) as described (Carmona and Randazzo, 2023). To determine the infectivity of human gastroenteritis viruses, (RT)-qPCR was used to quantify viral RNA/DNA from HIE monolayers at 1 and 48 hpi (Costantini et al., 2018; Ettayebi et al., 2016). For this purpose, two sets of 96-well plates with 100 % confluent 7–10 day-old-differentiated HIE monolayers were inoculated in triplicate with 100 µl of fecal suspension (diluted at 1:10, 1:100, 1:1000, and 1:10,000) or wastewater concentrate diluted at 1:10 in infection media supplemented with 500 µM sodium glycochenodeoxycholate. Infections were performed in triplicate (technical replicates), and experiments repeated at least twice. For each set of infections, one 96-well plate was immediately frozen at -80 °C at 1 hpi and the second plate was incubated at 37 °C and 5 % CO_2 for 48 h and then frozen (48 hpi). Cytotoxicity was monitored for all infections by visual/microscopic inspection of HIE monolayers.

2.5. Extraction, detection, and quantification of gastroenteritis viruses

Total nucleic acid was extracted from wastewater concentrates, and from supernatants and cell lysates of infected HIEs using the Maxwell® RSC Instrument (Promega, Spain) and the Maxwell RSC Pure Food GMO and authentication kit (Promega)

(Perez-Cataluña et al., 2021). The viral genomes were detected and quantified using TaqMan RT-qPCR with the RNA UltraSense One-Step quantitative RT-PCR system (Invitrogen, MA, USA) for RNA viruses, and the Premix Ex TaqTM kit (Takara Bio Inc., Japan) for HAdV on a LightCycler 480 instrument (Roche Diagnostics, Germany) (see Supplemental section S1 and Table S1 for details).

2.6. Gastroenteritis virus genome amplification, and sequence analyses

Sixteen wastewater samples that demonstrated replication on HIE at 48 hpi for at least one human gastroenteritis virus were chosen for sequence analysis. Briefly, viral genomes extracted from the wastewater inocula used for HIE infections and the supernatants of infected HIE at 48 hpi were used as templates to generate viral amplicons. Complementary DNAs were synthesized, amplified and semi-nested PCR assays were performed to obtain PCR products for Sanger sequencing (Aladin et al., 2010; Belliot et al., 2001, 1997; Beuret et al., 2002; Gentsch et al., 1992; Gouvea et al., 1990; Iturriza-Gómara et al., 2004, 2001, 2000; Kojima et al., 2002; Mena and Gerba, 2009; Pina et al., 1998). All sequences that passed the quality and control checks were deposited into GenBank with accession numbers OR252328 for HuNoV GI, OR252346 and OR252347 for HuNoV GII, from OR260001 to OR260015 for RV, from OR260023 to OR260032 for HAstV, and from OR260016 to OR260022 for HAdV. Phylogenetic trees were built using viral sequences obtained from previous wastewater (Santiso-Bellón et al., 2020) and clinical (Navarro-Lleó et al., 2022) surveillance studies in Spain, as well as reference clinical sequences retrieved from GenBank (see Supplemental Section S2 and Table S2 for details).

3. Results

3.1. Human gastroenteritis virus replication in optimized human intestinal enteroid model

Based on the integration of data from multiple experiments, we observed that reagent-assisted disruption of 3D HIE using GCDR was an efficient alternative to syringe pass-through. The optimized protocol allowed (i) efficient passage of the J2 HIE line from P17 to >P43, (ii) induced differentiation without affecting cell differentiation or monolayer formation, and (iii) supported replication of various genetically distinct gastroenteritis viruses. The concentration of the number of single cells for monolayer set up was reduced to 10^4 cells/mL from the initial 10^6 cells/mL, resulting in a 3D dome: differentiated monolayer ratio of 1:6 and improved overall efficiency. However, at HIE passage higher than 30, a ratio of 1:4 was required to obtain monolayers. In a round robin test, six samples were tested in two different laboratories. Results demonstrated that HuNoV positive stool suspensions showed similar levels of viral replication in either GCDR or syringe pass-through derived monolayers (Fig. 1). There were no statistical differences between the two monolayers preparation methods based on 1 hpi data, while two out of six samples (Filtered ID:S34 diluted 1:100, and unfiltered ID:S35 diluted 1:1000) showed statistically significant differences in viral replication after 48 hpi (Fig. 1). Moreover, replication rates of unfiltered and filtered HuNoV GII.4 Sydney [P16] fecal suspensions showed no statistical differences (Fig. 1).

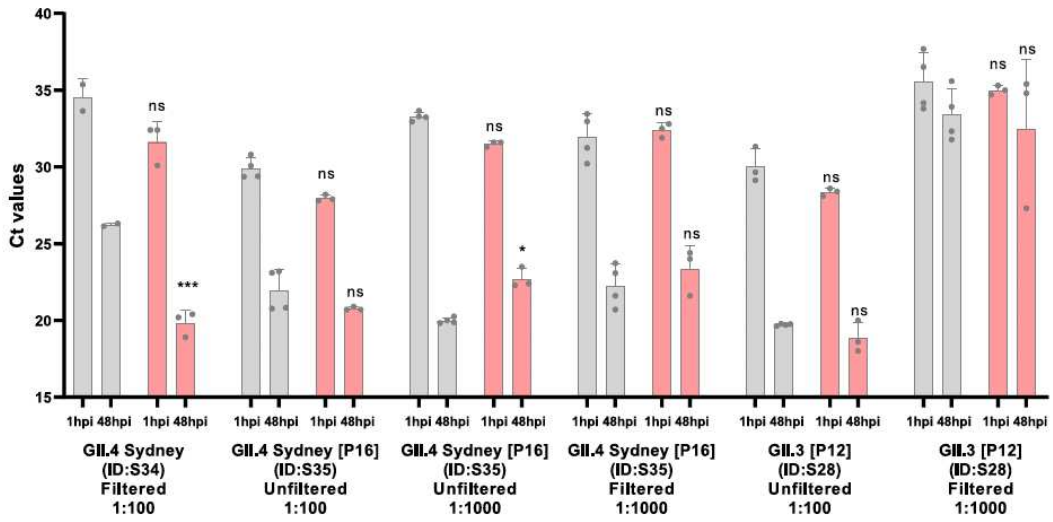

Fig. 1. Replication of human norovirus from either filtered or unfiltered fecal suspensions in human intestinal enteroids maintained and differentiated according to reagent-assisted disruption (grey bars, Lab 1) or syringe pass-through (red bars, Lab 2). Data represent Ct values of 3 replicates for each experiment. Specimens ID according to Table 1. For each sample and each infection time point, 1-way analysis of variance followed by Dunnett's test was performed. P-values of 1 hpi and 48 hpi infections in Lab2 are compared with those of Lab1: ns, not significant, $*p < 0.05$, $***p < 0.001$. hpi, hours postinfection.

A total of 40 stool suspensions and two rotavirus cell-adapted strains were tested for viral infectivity in HIE (Table 1). Only one HuNoV GI sample (ID:S4) replicated on HIE exhibiting a 1.03 $\log_{10}$ RNA increase. All HuNoV GII samples successfully replicated on HIE showing an average of 3.35 $\log_{10}$ RNA increase (Table 1). Among different HuNoV GII variants, GII.4 showed 3.54 $\log_{10}$ RNA increase on average, which resulted higher than GII.3 [P12] (2.78 $\log_{10}$ RNA). HIEs did not support virus replication of the majority of HuNoV GI positive stool samples, and the increase in yields for HuNoV GI (ID:S4) was significantly lower than that observed for GII HuNoVs. All three rotavirus-positive stool suspensions replicated on HIE with a mean 1.43 $\log_{10}$ RNA increase. Wa and Ito cell-culture adapted strains showed higher replication (2.26 and 2.85 $\log_{10}$ RNA increase, respectively) than rotavirus-positive

specimen (1.00–2.05 log_{10} RNA increase). Furthermore, both HAstV and HAdV samples successfully replicated, showing 3.24 and 3.69 log_{10} DNA/RNA increase, respectively. Single and multiple viral (co)-infections on HIEs were performed using HuNoV GI, HuNoV GII.4, rotavirus, HAdV, and HAstV (Fig. 2). The results demonstrated the successful and concurrent replication of multiple gastroenteritis viruses present in the same sample on HIE monolayers. At 1 hpi, viral attachment was not affected when single or multiple viruses were inoculated. The titer of attached virus (1 hpi) ranged between 2.32 (HuNoV GII) and 3.49 (rotavirus) log_{10} genome copies (GC)/well. Moreover, the replication yields at 48 hpi for HuNoV GI, HuNoV GII, RV, and HAdV showed no statistical differences between single and multiple (co)-infections. Replication in single and multiple infections was deemed as statistically significant for HAstV ($p = 0.004$), even though the differences in titer resulted in 0.16 log_{10}. HuNoV GII showed the highest replication rate (3.48 log_{10}), followed by HAdV (2.96 log_{10}) and HAstV (2.77 log_{10}), while HuNoV GI showed the lowest (0.65 log_{10}) (Fig. 2).

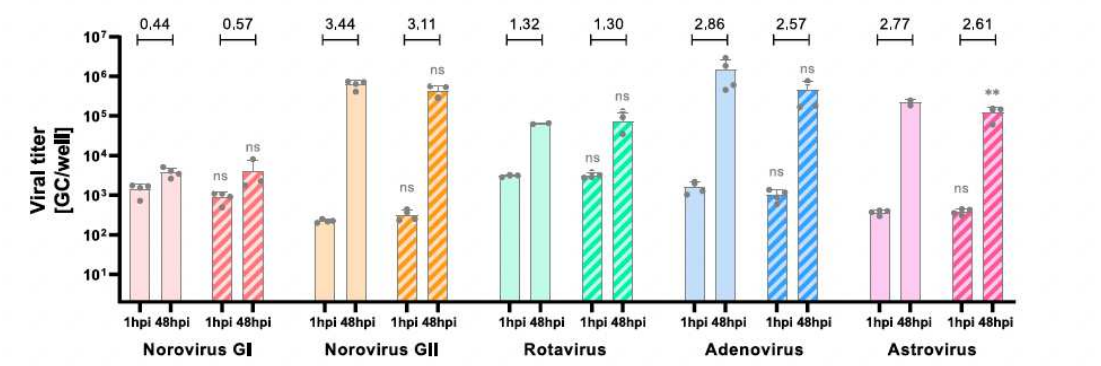

Fig. 2. Comparison of human gastroenteritis virus replication in human intestinal enteroids (HIEs) infected by single (plain bars) versus multiple (striped bars) viral pathogens. Multiple co-infections included HuNoV GI.3[P13] (ID: S4) and GII.4 Sydney [P16] (ID: S35), human RV G9 G12 [P8] (ID: S38), HAdV (ID: S41), and HAstV (ID: S42). The log_{10} increase of each virus in single and multiple

infections is provided on top of each set of bars. For each virus, a 1-way analysis of variance followed by Dunnett's test was performed. The P-values obtained from multiple infections were compared with those from single infections: ns, not significant, $^{**}p = 0.04$. hpi, hours postinfection.

3.2. Replication of multiple gastroenteritis viruses from wastewater samples on HIE

Initially, a subset of 6 samples was used to validate the concentration procedure of virus from wastewater samples in terms of viral recovery efficiency and cytotoxicity on HIE monolayers. Centricon concentration with or without additional PVDF filters increased HuNoV GI, HuNoV GII and RV RNA titers by up to 2 $\log_{10}$ GC/L compared to direct extraction from unconcentrated wastewater (data not shown). Furthermore, the Centricon concentration coupled with PVDF filtering procedure showed the lowest cytotoxicity and thus selected for concentrating 28 wastewater samples. Among the 28 wastewater samples analysed by (RT)-qPCR, 24 (86 %) tested positive for all five targeted gastroenteritis viruses. Two samples did not contain HuNoV GI or HAdV (Fig. 3A). The mean viral load in the wastewater samples was 5.08±1.49 $\log_{10}$ GC/L for HuNoV GI, 8.07±0.42 $\log_{10}$ GC/L for HuNoV GII, 8.28±0.66 log10 GC/L for RV, 6.88±0.76 $\log_{10}$ GC/L for HAstV, and 7.64±2.23 $\log_{10}$ GC/L for HAdV. HIE monolayers were infected with each of the 28 concentrated wastewater samples. Specific cut-off criteria were adopted to designate a wastewater sample as infectious: (i) no cytotoxic effect on monolayers at 48 hpi, (ii) at least a 3-fold RNA/DNA increase in HIEs culture (Desdouits et al., 2022), and (iii) quantifiable viral load at both 1 hpi and 48 hpi with statistically significant difference between time points. Sixteen of 28 wastewater samples (57 %) showed viral replication that met these criteria (Fig. 3B). Single infectious viruses were detected in 12 wastewater samples. Infectious RV, HAstV, and HAdV were detected in Sample 2, while Samples 8, 11 and 22 showed replication of two different gastroenteritis viruses (HuNoV GI/HAstV, HuNoV

GI/RV, HAstV/HAdV, respectively) (Fig. 3B). Sample 2 had the highest replication yields with increases of 4.37 for HAstV and 3.42 $\log_{10}$ for HAdV. In contrast, 1.01 to 1.33 $\log_{10}$ increases were detected for HuNoV GI and GII in Sample 7, 8, or 11. RV increased from 1.02 (Sample 11) to 1.40 $\log_{10}$ (Sample 2), HAstV from 1.04 (Sample 19) to 4.37 $\log_{10}$ (Sample 11), and HAdV from 1.03 (Sample 8) to 3.42 $\log_{10}$ (Sample 2). No significant correlation could be established between the viral load detected by RT-qPCR in wastewater samples and successful viral replication on HIEs. For example, wastewater samples with lower HAstV titers (5.74 $\log_{10}$ GC/L) showed successful replication in HIEs, while samples with higher titers (8.85 $\log_{10}$ GC/L) did not. Similarly, HuNoV GI detected at levels of 5.86±0.16 (Sample 8) and 6.10±0.03 $\log_{10}$ GC/L (Sample 11) successful replicated in HIEs with 1.33 and 1.27 $\log_{10}$ increases, respectively. However, other samples did not exhibit replication in HIEs despite having comparable viral titers. Likewise, HuNoV GII viruses detected at 8.59±0.01 $\log_{10}$ GC/L in wastewater (Sample 7) yielded a replication rate of 1.01 $\log_{10}$ in HIEs, while samples at higher concentrations did not. Upon ranking all wastewater samples according to initial viral load, successful replication of either HuNoV GI or GII in HIEs occurred in samples within the first quartile of the ranked list (>5.08 $\log_{10}$ GC/L for HuNoV GI, and >8.32 $\log_{10}$ GC/L for HuNoV GII). In other words, those wastewater samples with higher HuNoV loads tended to result in successful replication in the HIE system. Unlike HuNoV, the successful replication of RV, HAstV, and HAdV in the HIE system did not exhibit a consistent pattern based on their viral load in wastewater samples.

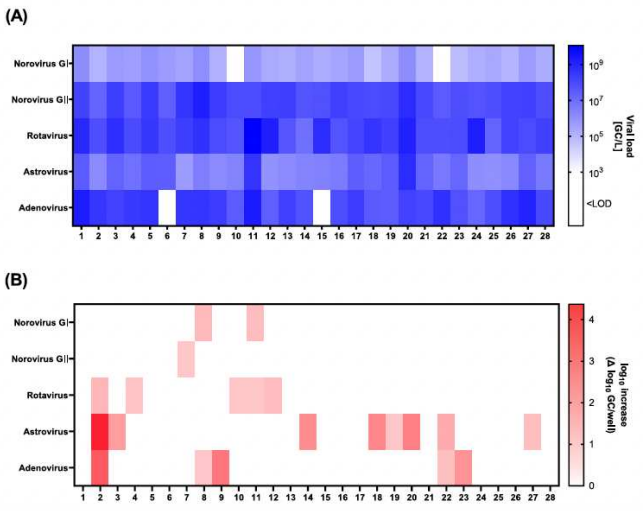

Fig. 3. Heat map of gastroenteritis virus concentrations in influent wastewater samples (A) and viral replication from these samples on human intestinal enteroids (B).

3.3. Genotypes of gastroenteritis viruses replicating in HIE from wastewater

Confirmation of viral replication in HIE infected with wastewater samples was achieved by comparing viral sequences from wastewater nucleic acid and supernatants and cell lysates from HIEs (Table 2). However, in some positive samples the genotype could not be determined. A HuNoV GI.3[P13] was detected from Sample 8 infected HIEs, while HuNoV GII.4 Sydney [P16] was detected from both wastewater and HIEs from Sample 7 (Figures S1, S2). The capsid sequences from wastewater and HIEs in Sample 7 were identical while the polymerase sequences showed 99.5 % identity. RV G3 was detected in wastewater and HIEs from Sample 11 and Sample 12, while RV G9 was found in HIEs from Sample 4 and in wastewater coupled with G12 from Sample 10 (Figure S3). Notably, G12 sequence was 100 % similar with a Spanish clinical sequence (ESPv148) and 96 % similar with sequences from a previous Spanish wastewater surveillance study (R5 and R15). While G9 genotypes clustered with previous sequences from Spanish wastewater samples, G3 did not. For the VP4 gene, P[8] was the only genotype obtained from all RV positive samples and all sequences

clustered together (Figure S3D). All HAstV sequences belonged to group A of the MAstV-1 genus (Figure S4). HAstV-4 was identified in wastewater and HIEs from Sample 2 and Sample 3, while HAstV-8 was found in wastewater and HIEs from Sample 20. Intriguingly, both Sample 18 and Sample 22 displayed HAstV-8 sequences in wastewater, while HAstV-1 sequences were obtained from the corresponding HIE supernatants. Four sequences from wastewater and three from HIE samples were successfully assigned to human mastadenovirus F or C species (Figure S5). Specifically, sequences from wastewater showed 100 % similarity with HAdV-41 (Sample 8, Sample 22) or 96 % similarity with HAdV-40 (Sample 9). The sequence from wastewater Sample 23 shared 99 % identity with HAdV-5 belonging to Human mastadenovirus C species. All three sequences from HIE supernatants clustered with HAdV-41 (Sample 2, Sample 9, and Sample 23).

Table 2. Genotypes of enteric viruses in wastewater samples replicating in HIE.

Sample			**RV**			
ID	**Type**	**HuNoV**	**VP7**	**VP4**	**HAstV**	**HAdV**
2	WW			P[8]	HAstV-4	ND
	HIEs			P[8]	HAstV-4	HAdV-41
3	WW				HAstV-4	
	HIEs				HAstV-4	
4	WW		ND	P[8]		
	HIEs		G9	P[8]		
7	WW	GII.4[P16]				
	HIEs	GII.4[P16]				
8	WW	ND				HAdV-41

	HIEs	GI.3[P13]				ND
9	WW					HAdV-40
	HIEs					HAdV-41
10	WW		G9+G12	P[8]		
	HIEs		ND	P[8]		
11	WW	ND	G3			
	HIEs	ND	G3			
12	WW		G3	P[8]		
	HIEs		G3	P[8]		
14	WW				ND	
	HIEs				ND	
18	WW				HAstV-8	
	HIEs				HAstV-1	
19	WW				ND	
	HIEs				ND	
20	WW				HAstV-8	
	HIEs				HAstV-8	
22	WW				HAstV-8	HAdV-41
	HIEs				HAstV-1	ND
23	WW					HAdV-5
	HIEs					HAdV-41
27	WW				ND	
	HIEs				ND	

Abbreviations: WW, wastewater; HIEs, human intestinal enteroids; ND, not determined (either the sequence was not identified or the genotype assigned based upon available sequence).

3.Discussion

The detection of infectious viruses in wastewater holds crucial public health implications as understanding their dynamics and persistence is imperative for assessing potential risks and refining reclamation procedures to safely discharge and reuse water resources. Our data demonstrate the successful replication of multiple gastroenteritis viruses in HIE monolayers from urban wastewater samples. By using the HIE model it was demonstrated that HuNoV remained infectious for between 7 and 35 days in artificially spiked tap water, creek and seawater samples (Desdouits et al., 2022; Kennedy et al., 2023; Shaffer et al., 2022), but there is no information on wastewater. We showed replication of HuNoV GI.3[P13], GII.4 Sydney [P16], RV G3, G9 and P[8], HAstV-1, -4, and -8, and HAdV-41 genotypes, all of which are predominant among the Spanish population (Navarro-Lleoó et al., 2022; Perez-Ortín et al., 2019; Vu et al., 2019). Concomitant detection of infectious HuNoV GI and GII, RV, HAstV and HAdV from wastewater samples demonstrates that HIEs can support replication of a wide diversity of human infectious gastroenteritis viruses present in a single wastewater sample. We used optimized methodologies for testing viral infectivity in wastewater samples including the use of GCDR to disrupt 3D HIE for passaging and setting up cell monolayers. Our data also suggest that the serial filtration steps for stool suspension preparation as in the original publication of Ettayebi may not be necessary (Ettayebi et al., 2016), as reported recently (Overbey et al., 2021). The viral load of gastroenteritis viruses in our samples was comparable to those reported in previous studies (Farkas et al., 2018; Haramoto et al., 2018; Santiso-Bellón et al., 2020). This indicates that the Centricon-filtering procedure effectively recovers viral particles while maintaining their infectivity. These implemented methodologies are essential for matching the HIE model with the specific needs of food and

environmental virology laboratories. Another relevant aspect of our study is the establishment of a biobank of infectious gastroenteritis virus-positive fecal specimens that show successful replication on HIEs. As reported previously, HuNoV GII.4 viruses exhibit higher replication yields compared to other genotypes (Costantini et al., 2018; Ettayebi et al., 2021), while the majority of GI noroviruses failed to replicate (Costantini et al., 2018; Ettayebi et al., 2016). This discrepancy in replication success could be attributed to the lower mean concentrations of GI in stools compared to GII (Ettayebi et al., 2021), to the loss of infectious particles due to long period storage, and to other unknown factors in the stool or media supplements required for successful infection (Estes et al., 2019; Murakami et al., 2020). Concurrent infections were also studied using the HIE model. Similar replication rates were observed in both single- and multiple- (co)infections (Fig. 2), strengthening the hypothesis that the HIE model can simultaneously show replication of multiple viruses from stool samples and contaminated wastewater. Cell culture systems have been used to detect infectious gastroenteritis viruses from environmental samples. However, a single cell culture system capable of replicating multiple viruses, including HuNoV, has been lacking. Continuous Caco-2 cell line has been used to isolate RV, HAdV, HAstV, coxsackieviruses, reovirus, and poliovirus, while Buffalo green monkey (BGM) cell line was selected by the United States Environmental Protection Agency for detecting human enteroviruses in water (Gerba and Betancourt, 2019). In contrast, HIEs, which maintain relevant *in vivo* features, are able to support the replication of a wider variety of gastroenteritis viruses (Euller-Nicolas et al., 2023; Giobbe et al., 2021; Pe˜na-Gil et al., 2023; Zhao et al., 2021). In our study, not all viruses detected in wastewater samples replicated in the HIE model (Fig. 3). Importantly, the absence of replication does not necessarily indicate that a sample is non-infectious, as there may still be

infectious viral particles present at levels below the limit of detection of the HIE assay (103–4 GC/well). Additional factors, such as model preferences for certain viruses or disturbances caused by physical and chemical substances (e.g., unspecific binding, undetected cytotoxicity), may have also influenced the observed replication rates. False-negative outcomes carry significant implications for public health responses. Therefore, it is imperative to ensure quality assurance and quality control procedures, representative sampling approaches, effective virus concentration, and clear guidelines for data interpretation before the HIE platform can be considered for wastewater monitoring and/or water reuse purposes. To this end, interlaboratory comparisons studies utilizing standardized reference materials and protocols to achieve results' reliability should be prioritized. Diverse fold increases for HuNoV GII, HAstV, and HAdV were observed in fecal compared to wastewater samples (Sample 7, 8, and 19 respectively), suggesting the presence of defective and non-infectious viral particles. However, the infectious particle-to-genomic copies ratio for each virus could not be estimated using the HIE model, as viral load in wastewater and viral replication did not correlate. In addition, sequence analyses of HAstV and HAdV for paired samples demonstrated that genotypes that replicated in HIEs differed from those detected in wastewater (Samples 18 and 22 for HAstV, and Samples 9 and 23 for HAdV). This suggests that either the majority genotype present in wastewater may not be infectious, or that minority genotypes could replicate with higher efficiency in the HIE system. The HIE was instrumental for enriching the Sample 8 for subsequent sequence analysis. Indeed, HuNoV GI was identified in wastewater by RT-qPCR (Fig. 3a), but typing was unsuccessful. However, it was possible to genotype the RNA from the supernatant as HuNoV GI.3[P13] following replication on HIEs (Table 2). HuNoV GII genotypes are more frequently detected in wastewater compared to GI genotypes,

and they are usually found at higher titers (Ekundayo et al., 2021; Fumian et al., 2019; Huang et al., 2022; Mabasa et al., 2022; Tao et al., 2015). This lower prevalence and concentration of HuNoV GI compared to GII creates a bias in understanding the genotypes circulating among the population. Similar occurrence patterns were observed in a previous study conducted in the same Spanish region as the current study. In that study, GII.2 was present at 40 %, GII.6 at 8.6 %, and GII.17 at 5.7 %, alongside GI.2 (6.25 %) and GI.4 (6.25 %), while 87.5 % of GI could not be genotyped (Santiso-Bellón et al., 2020). We intentionally did not spike wastewater samples with a recovery control to avoid saturating the binding sites of HIE monolayers. This limited the direct estimation of the efficiency of the concentration protocol. Another limitation is the occurrence of cytotoxicity attributed to wastewater in a considerable proportion of monolayers, estimated to be around 20 %, which resulted in the exclusion of those monolayers from the study. Future experiments should benchmark the HIE model with continuous cell lines, such as Caco-2 or BGM, to provide a comprehensive assessment of the efficiency of the overall method for detecting infectious virus from environmental water samples, as recently demonstrated for nonculture-adapted RV clinical strains (Peña-Gil et al., 2023). Additionally, the HIE platform ideally needs testing with a broader range of gastroenteritis virus strains and combinations of genotypes. Moreover, next-generation sequencing (NGS) technology should be coupled with viral infectivity data in the HIE system to study the relationship between viral detection and infectivity at the genotype/variant level. Additionally, it would be crucial to challenge the sensitivity of the HIE system with effluent wastewater. Understanding the behaviour and persistence of infectious viruses in effluent wastewater is essential for assessing potential risks and ensuring the safety of water reuse applications.

5. Conclusions

The HIE model has demonstrated its robustness for studying single and concurrent replication of naturally occurring viruses from wastewater. Therefore, the HIE model provides a unified platform for culturing human gastroenteritis viruses, potentially enabling the isolation of a greater diversity of viruses, that has to date been unattainable with standard cell lines. Besides the limitation of the HIE model, the advancements of this study will contribute significantly to our understanding of viral infectivity in wastewater and its implication for public health and environmental safety.

Disclaimer

The findings and conclusions in this article are those of the authors and do not necessarily represent the official position of the CDC.

CRediT authorship contribution statement

Noelia Carmona-Vicente: Methodology, Investigation. **Annamaria Pandiscia:** Methodology, Investigation **Cristina Santiso-Bellón**: Methodology, Investigation. **Alba Perez- Cataluña:** Writing – review & editing. **Jesús Rodríguez-Díaz:** Writing – review & editing, Investigation. **Veronica P. Costantini:** Writing -review & editing, Validation, Methodology, Investigation, Formal analysis. **Javier Buesa:** Writing – review & editing, Supervision, Investigation. **Jan Vinjé:** Writing – review & editing, Validation, Investigation. **Gloria Sánchez:** Writing – review & editing, Resources, Conceptualization. **Walter Randazzo:** Writing – review & editing, Writing – original draft, Supervision, Resources, Project administration, Investigation, Funding acquisition, Conceptualization.

Declaration of competing interest

The authors declare that they have no known competing financial interests or personal relationships that could have appeared to influence the work reported in this paper.

Data availability

Data will be made available on request.

Funding

The study was supported by PREVISION project (reference no. PID2019-105509RJ-I00) funded by the Spanish Ministry of Science, Innovation and Universities and AEI/FEDER, UE to WR and MCEC WATER (PID2020-116789RBC42 AEI/FEDER, UE) to GS. AM is supported by a predoctoral research grant funded by University of Bari “A. Moro” _(Italy). The contract of AP-C is part of the grant IJC2020-045382- I, financed by MCIN/AEI/10.13039/501100011033, and by the European Union "NextGenerationEU/PRTR". C.S-B. is recipient of PRE2018- 083315 FPI predoctoral grant (MICIN/AEI/10.13039/501100011033 and “ESF Investing in your future”). Wastewater samples were collected as part of the Spanish COVID-19 wastewater monitoring programme (VATar COVID-19) funded by the Spanish Ministry for the Ecological Transition and the Demographic Challenge and the Spanish Ministry of Health. IATA-CSIC is a Centre of Excellence Severo Ochoa (CEX2021- 001189-S MCIU/AEI/10.13039/501100011033).

Acknowledgements

The authors are thankful to Prof. Susana Guix (University of Barcelona, Spain) and Prof. Simona De Grazia (University of Palermo, Italy) for providing some HuNoV GI samples. The authors thank the Príncipe Felipe Research Center Foundation (CIPF) (CIPF, Valencia, Spain) for providing sequencing service.

Supplementary materials Supplementary material associated with this article can be found, in the online version, at doi:10.1016/j.watres.2024.121481.

References

Aladin, F., Nawaz, S., Iturriza-G´omara, M., Gray, J., 2010. Identification of G8 rotavirus strains determined as G12 by rotavirus genotyping PCR: updating the current genotyping methods. J. Clin. Virol. Off. Publ. Pan Am. Soc. Clin. Virol. 47, 340–344. https://doi.org/10.1016/j.jcv.2010.01.004.

Belliot, G.M., Fankhauser, R.L., Monroe, S.S., 2001. Characterization of "Norwalk-likeviruses" and astroviruses by liquid hybridization assay. J. Virol. Methods 91,119–130. https://doi.org/10.1016/s0166-0934(00)00254-8.

Belliot, G.M., Laveran, H., Monroe, S.S., 1997. Detection and genetic differentiation of human astroviruses: phylogenetic grouping varies by coding region. Arch. Virol. 142, 1323–1334. https://doi.org/10.1007/s007050050163.

Beuret, C., Kohler, D., Baumgartner, A., Lüthi, T., 2002. Norwalk-like virus sequences in mineral waters: one-year monitoring of three brands. Appl. Environ. Microbiol. 68, 1925–1931. https://doi.org/10.1128/AEM.68.4.1925-1931.2002.

Carmona, N., Randazzo, W., 2023. Passaging human intestinal organoids and monolayers set up. Protoc. Exch. https://doi.org/10.21203/rs.3.pex-2221/v1.

Chatterjee, N.K., Moore, D.W., Monroe, S.S., Glass, R.I., Cambridge, M.J., Kondracki, S. F., Morse, D.L., 2004. Molecular epidemiology of outbreaks of viral gastroenteritis in New York State, 1998–1999. Clin. Infect. Dis. 38, S303–S310. https://doi.org/10.1086/381600.

Condit, R.C., 2013. Principles of virology. Fields Virology, 6th ed. Wolters Kluwer Health Adis (ESP), Department of Molecular Genetics and Microbiology, University of Florida, Gainesville, FL,

United States.

Costantini, V., Morantz, E.K., Browne, H., Ettayebi, K., Zeng, X.L., Atmar, R.L., Estes, M.K., Vinje, J., 2018. Human Norovirus replication in human intestinal enteroids as model to evaluate virus inactivation. Emerg. Infect. Dis. 24, 1453–1464. https://doi.org/10.3201/EID2408.180126.

Desdouits, M., Polo, D., Le Mennec, C., Strubbia, S., Zeng, X.L., Ettayebi, K., Atmar, R.L.,Estes, M.K., Le Guyader, F.S., 2022. Use of human intestinal enteroids to evaluate persistence of infectious human norovirus in seawater. Emerg. Infect. Dis. 28, 1475–1479. https://doi.org/10.3201/EID2807.220219.

EFSA, ECDC, 2022. The European Union One Health 2021 Zoonoses Report. EFSA J. 20,e07666. https://doi.org/10.2903/j.efsa.2022.7666.

Ekundayo, T.C., Igere, B.E., Oluwafemi, Y.D., Iwu, C.D., Olaniyi, O.O., 2021. Human norovirus contamination in water sources: a systematic review and meta-analysis.Environ. Pollut. 291, 118164 https://doi.org/10.1016/j.envpol.2021.118164.

Estes, M.K., Ettayebi, K., Tenge, V.R., Murakami, K., Karandikar, U., Lin, S.C., Ayyar, B. V., Cortes-Penfield, N.W., Haga, K., Neill, F.H., Opekun, A.R., Broughman, J.R., Zeng, X.L., Blutt, S.E., Crawford, S.E., Ramani, S., Graham, D.Y., Atmar, R.L., 2019. Human norovirus cultivation in nontransformed stem cell-derived human intestinal enteroid cultures: success and challenges. Viruses 11. https://doi.org/10.3390/v11070638.

Ettayebi, K., Crawford, S.E., Murakami, K., Broughman, J.R., Karandikar, U., Tenge, V.R., Neill, F.H., Blutt, S.E., Zeng, X.-L., Qu, L., Kou, B., Opekun, A.R., Burrin, D., Graham, D.Y., Ramani, S., Atmar, R.L., Estes, M.K., 2016. Replication of human noroviruses in stem cell-derived human enteroids. Science (80-.) 353, 1387–1393. https://doi.org/10.1126/science.aaf5211.

Ettayebi, K., Tenge, V.R., Cortes-Penfield, N.W., Crawford, S.E., Neill, F.H., Zeng, X.-L., Yu, X., Ayyar, B.V., Burrin, D., Ramani, S., Atmar, R.L., Estes, M.K., 2021. New insights and enhanced human norovirus cultivation in human intestinal enteroids.mSphere 6. https://doi.org/10.1128/mSphere.01136-20.

Euller-Nicolas, G., Le Mennec, C., Schaeffer, J., Zeng, X.-L., Ettayebi, K., Atmar, R.L., Le Guyader, F.S., Estes, M.K., Desdouits, M., 2023. Human sapovirus replication in human intestinal enteroids. J. Virol. 97 https://doi.org/10.1128/JVI.00383-23.

Farkas, K., Marshall, M., Cooper, D., McDonald, J.E., Malham, S.K., Peters, D.E., Maloney, J.D.,

Jones, D.L., 2018. Seasonal and diurnal surveillance of treated and untreated wastewater for human enteric viruses. Environ. Sci. Pollut. Res. 25, 33391–33401. https://doi.org/10.1007/s11356-018-3261-y.

Fumian, T.M., Fioretti, J.M., Lun, J.H., dos Santos, I.A.L., White, P.A., Miagostovich, M. P., 2019. Detection of norovirus epidemic genotypes in raw sewage using next generation sequencing. Environ. Int. 123, 282–291. https://doi.org/10.1016/j. envint.2018.11.054.

GBD 2015, 2016. Global, regional, and national life expectancy, all-cause mortality, and cause-specific mortality for 249 causes of death, 1980–2015: a systematic analysis for the Global Burden of Disease Study 2015. Lancet 388, 1459–1544. https://doi. org/10.1016/S0140-6736(16)31012-1.

GBD 2016, 2018. Estimates of the global, regional, and national morbidity, mortality, and aetiologies of diarrhoea in 195 countries: a systematic analysis for the Global Burden of Disease Study 2016. Lancet Infect. Dis. 18, 1211–1228. https://doi.org/ 10.1016/S1473-3099(18)30362-1.

Gentsch, J.R., Glass, R.I., Woods, P., Gouvea, V., Gorziglia, M., Flores, J., Das, B.K., Bhan, M.K., 1992. Identification of group A rotavirus gene 4 types by polymerase chain reaction. J. Clin. Microbiol. 30, 1365–1373. https://doi.org/10.1128/ jcm.30.6.1365-1373.1992.

Gerba, C.P., Betancourt, W.Q., 2019. Assessing the occurrence of waterborne viruses in reuse systems: analytical limits and needs. Pathog. (Basel, Switzerland) 8. https://doi.org/10.3390/pathogens8030107.

Gerba, C.P., Betancourt, W.Q., Kitajima, M., Rock, C.M., 2018. Reducing uncertainty in estimating virus reduction by advanced water treatment processes. Water Res. 133, 282–288. https://doi.org/10.1016/j.watres.2018.01.044.

Giobbe, G.G., Bonfante, F., Jones, B.C., Gagliano, O., Luni, C., Zambaiti, E., Perin, S., Laterza, C., Busslinger, G., Stuart, H., Pagliari, M., Bortolami, A., Mazzetto, E., Manfredi, A., Colantuono, C., Di Filippo, L., Pellegata, A.F., Panzarin, V., Thapar, N., Li, V.S.W., Eaton, S., Cacchiarelli, D., Clevers, H., Elvassore, N., De Coppi, P., 2021.SARS-CoV-2 infection and replication in human gastric organoids. Nat. Commun. 12,6610. https://doi.org/10.1038/s41467-021-26762-2.

Gouvea, V., Glass, R.I., Woods, P., Taniguchi, K., Clark, H.F., Forrester, B., Fang, Z.Y., 1990. Polymerase chain reaction amplification and typing of rotavirus nucleic acid from stool specimens. J. Clin. Microbiol. 28, 276–282. https://doi.org/10.1128/ jcm.28.2.276-282.1990.

Hamza, I.A., Jurzik, L., Überla, K., Wilhelm, M., 2011. Methods to detect infectious human enteric

viruses in environmental water samples. Int. J. Hyg. Environ. Health 214, 424–436. https://doi.org/10.1016/j.ijheh.2011.07.014.

Haramoto, E., Kitajima, M., Hata, A., Torrey, J.R., Masago, Y., Sano, D., Katayama, H., 2018. A review on recent progress in the detection methods and prevalence of human enteric viruses in water. Water Res. 135, 168–186. https://doi.org/10.1016/ j.watres.2018.02.004.

Holly, M.K., Smith, J.G., 2018. Adenovirus infection of human enteroids reveals interferon sensitivity and preferential infection of goblet cells. J. Virol. 92 https:// doi.org/10.1128/JVI.00250-18.

Huang, Y., Zhou, N., Zhang, S., Yi, Y., Han, Ying, Liu, M., Han, Yue, Shi, N., Yang, L., Wang, Q., Cui, T., Jin, H., 2022. Norovirus detection in wastewater and its correlation with human gastroenteritis: a systematic review and meta-analysis. Environ. Sci. Pollut. Res. 29, 22829–22842. https://doi.org/10.1007/s11356-021- 18202-x.

Iturriza-Gomara, M., Cubitt, D., Desselberger, U., Gray, J., 2001. Amino acid substitution within the VP7 protein of G2 rotavirus strains associated with failure to serotype. J. Clin. Microbiol. 39, 3796–3798. https://doi.org/10.1128/JCM.39.10.3796-3798.2001.

Iturriza-Gomara, M., Green, J., Brown, D.W., Desselberger, U., Gray, J.J., 2000. Diversity within the VP4 gene of rotavirus P[8]strains: implications for reverse transcription PCR genotyping. J. Clin. Microbiol. 38, 898–901. https://doi.org/10.1128/ JCM.38.2.898-901.2000.

Iturriza-Gomara, M., Kang, G., Gray, J., 2004. Rotavirus genotyping: keeping up with an evolving population of human rotaviruses. J. Clin. Virol. 31, 259–265. https://doi.org/10.1016/j.jcv.2004.04.009.

Kennedy, L.C., Costantini, V.P., Huynh, K.A., Loeb, S.K., Jennings, W.C., Lowry, S., Mattioli, M.C., Vinje, J., Boehm, A.B., 2023. Persistence of human norovirus (GII) in surface water: decay rate constants and inactivation mechanisms. Environ. Sci.Technol. 57, 3671–3679. https://doi.org/10.1021/acs.est.2c09637.

Kojima, S., Kageyama, T., Fukushi, S., Hoshino, F.B., Shinohara, M., Uchida, K., Natori, K., Takeda, N., Katayama, K., 2002. Genogroup-specific PCR primers for detection of Norwalk-like viruses. J. Virol. Methods 100, 107–114. https://doi.org/ 10.1016/S0166-0934(01)00404-9.

Kolawole, A.O., Mirabelli, C., Hill, D.R., Svoboda, S.A., Janowski, A.B., Passalacqua, K.D., Rodriguez, B.N., Dame, M.K., Freiden, P., Berger, R.P., Vu, D.-L., Hosmillo, M.,O'Riordan, M.X.D., Schultz-Cherry, S., Guix, S., Spence, J.R., Wang, D., Wobus, C.E.,2019. Astrovirus

replication in human intestinal enteroids reveals multi-cellular tropism and an intricate host innate immune landscape. PLoS Pathog. 15, e1008057 https://doi.org/10.1371/journal.ppat.1008057.

Mabasa, V.V., van Zyl, W.B., Ismail, A., Allam, M., Taylor, M.B., Mans, J., 2022. Multiple novel human norovirus recombinants identified in wastewater in pretoria, South Africa by next-generation sequencing. Viruses. https://doi.org/10.3390/v14122732.

Mena, K.D., Gerba, C.P., 2009. Waterborne adenovirus. Rev. Environ. Contam. Toxicol. 198, 133–167. https://doi.org/10.1007/978-0-387-09647-6_4. Murakami, K., Tenge, V.R., Karandikar, U.C., Lin, S.-C., Ramani, S., Ettayebi, K., Crawford, S.E., Zeng, X.-L., Neill, F.H., Ayyar, B.V., Katayama, K., Graham, D.Y.,Bieberich, E., Atmar, R.L., Estes, M.K., 2020. Bile acids and ceramide overcome the entry restriction for GII.3 human norovirus replication in human intestinal enteroids. Proc. Natl. Acad. Sci. U.S.A. 117, 1700–1710. https://doi.org/10.1073/pnas.1910138117.

Navarro-Lleó, N., Santiso-Bellón, C., Vila-Vicent, S., Carmona-Vicente, N., Gozalbo-Rovira, R., Carcamo-Calvo, R., Rodríguez-Díaz, J., Buesa, J., 2022. Recombinant noroviruses circulating in Spain from 2016 to 2020 and proposal of two novel genotypes within genogroup I. Microbiol. Spectr. 10, e02505–e02521. https://doi.org/10.1128/spectrum.02505-21.

Overbey, K.N., Zachos, N.C., Coulter, C., Schwab, K.J., 2021. Optimizing human intestinal enteroids for environmental monitoring of human norovirus. Food Environ. Virol. 13, 470–484. https://doi.org/10.1007/s12560-021-09486-w.

Pandiscia, A., Lorusso, P., Manfredi, A., Sánchez, G., Terio, V., Randazzo, W., 2024. Leveraging plasma-activated seawater for the control of human norovirus and bacterial pathogens in shellfish depuration. Foods https://doi.org/10.3390/foods13060850.

Peña-Gil, N., Randazzo, W., Carmona-Vicente, N., Santiso-Bell´on, C., C´arcamo-C´alvo, R.,Navarro-Lle´o, N., Monedero, V., Yebra, M.J., Buesa, J., Gozalbo-Rovira, R., Rodríguez-Díaz, J., 2023. Culture of human rotaviruses in relevant models shows differences in culture-adapted and nonculture-adapted strains. Int. J. Mol. Sci. https://doi.org/10.3390/ijms242417362.

Perez-Cataluña, A., Cuevas-Ferrando, E., Randazzo, W., Falcò, I., Allende, A., Sánchez, G., 2021. Comparing analytical methods to detect SARS-CoV-2 in wastewater. Sci. Total Environ. 758, 143870 https://doi.org/10.1016/j. scitotenv.2020.143870.

Perez-Ortín, R., Santiso-Bellón, C., Vila-Vicent, S., Carmona-Vicente, N., Rodríguez-Díaz, J., Buesa,

J., 2019. Rotavirus symptomatic infection among unvaccinated and vaccinated children in Valencia, Spain. BMC Infect. Dis. 19, 998. https://doi.org/10.1186/s12879-019-4550-x.

Pina, S., Puig, M., Lucena, F., Jofre, J., Girones, R., 1998. Viral pollution in the environment and in shellfish: human adenovirus detection by PCR as an index of human viruses. Appl. Environ. Microbiol. 64, 3376–3382. https://doi.org/10.1128/AEM.64.9.3376-3382.1998.

Qi, R., Huang, Y.-T., Liu, J.-W., Sun, Y., Sun, X.-F., Han, H.-J., Qin, X.-R., Zhao, M., Wang, L.-J., Li, W., Li, J.-H., Chen, C., Yu, X.-J., 2018. Global prevalence of asymptomatic norovirus infection: a meta-analysis. EClinicalMedicine 2–3, 50–58. https://doi.org/10.1016/j.eclinm.2018.09.001.

Randazzo, W., Costantini, V., Morantz, E.K., Vinje, J., 2020. Human intestinal enteroids to evaluate human norovirus GII.4 inactivation by aged-green tea. Front. Microbiol. 11, 1917. https://doi.org/10.3389/fmicb.2020.01917.

Santiso-Bellón, C., Randazzo, W., Perez-Cataluña, A., Vila-Vicent, S., Gozalbo-Rovira, R., Munoz, C., Buesa, J., Sánchez, G., Díaz, J.R., 2020. Epidemiological surveillance of norovirus and rotavirus in sewage (2016–2017) in Valencia (Spain). Microorganisms 8. https://doi.org/10.3390/microorganisms8030458.

Saxena, K., Blutt, S.E., Ettayebi, K., Zeng, X.-L., Broughman, J.R., Crawford, S.E., Karandikar, U.C., Sastri, N.P., Conner, M.E., Opekun, A.R., Graham, D.Y., Qureshi, W., Sherman, V., Foulke-Abel, J., In, J., Kovbasnjuk, O., Zachos, N.C., Donowitz, M., Estes, M.K., 2016. Human intestinal enteroids: a new model to study human rotavirus infection, host restriction, and pathophysiology. J. Virol. 90, 43–56. https://doi.org/10.1128/JVI.01930-15.

Shaffer, M., Huynh, K., Costantini, V., Bibby, K., Vinje, J., 2022. Viable norovirus persistence in water microcosms. Environ. Sci. Technol. Lett. 9, 851–855. https://doi.org/10.1021/acs.estlett.2c00553.

Tao, Z., Xu, M., Lin, X., Wang, H., Song, L., Wang, S., Zhou, N., Zhang, D., Xu, A., 2015. Environmental surveillance of genogroup I and II noroviruses in Shandong Province, China in 2013. Sci. Rep. 5, 17444. https://doi.org/10.1038/srep17444.

Valcarce, M.D., Kambhampati, A.K., Calderwood, L.E., Hall, A.J., Mirza, S.A., Vinje, J., 2021. Global distribution of sporadic sapovirus infections: a systematic review and meta-analysis. PLoS ONE 16. https://doi.org/10.1371/journal.pone.0255436.

Vu, D.L., Sabrina, A., Aregall, N., Michl, K., Rodriguez Garrido, V., Goterris, L., Bosch, A., Pinto,

R.M., Guix, S., 2019. Novel human astroviruses: prevalence and association with common enteric viruses in undiagnosed gastroenteritis cases in Spain. Viruses 11. https://doi.org/10.3390/v11070585.

Zhao, X., Li, C., Liu, X., Chiu, M.C., Wang, D., Wei, Y., Chu, H., Cai, J.-P., Hau-Yee Chan, I., Kak-Yuen Wong, K., Fuk-Woo Chan, J., Kai-Wang To, K., Yuen, K.Y., Zhou, J., 2021. Human intestinal organoids recapitulate enteric infections of enterovirus and coronavirus. Stem Cell Rep. 16, 493–504. https://doi.org/10.1016/ j.stemcr.2021.02.009.

Zou, W.Y., Blutt, S.E., Crawford, S.E., Ettayebi, K., Zeng, X.-L., Saxena, K., Ramani, S., Karandikar, U.C., Zachos, N.C., Estes, M.K., 2019. Human Intestinal Enteroids: New Models to Study Gastrointestinal Virus Infections BT - Organoids: Stem Cells, Structure, and Function, in: Turksen, K. (Ed.), . Springer New York, New York, NY, pp. 229–247. https://doi.org/10.1007/7651_2017_1.

11. CONCLUSIONS

The microbiological safety and quality of high-risk foods, particularly minimally processed and ready-to-eat products, remain significant concerns in the food industry. With increasing consumer demand for these foods, the risk of contamination by foodborne pathogens, especially HuNoV poses a significant threat for public health. While thermal treatments are effective in reducing microbial hazards, they often compromise the nutritional and sensory qualities of food. Non-thermal technologies, including HPP and PAW, represent promising alternatives that do not adversely affect food quality.

The four original research articles described in this PhD thesis demonstrated that HPP and PASW are promising technologies for mitigating the virological hazards posed by HuNoV in food matrices. Our findings support the integration of these non-thermal treatments into food safety strategies, particularly for high-risk foods such as shellfish and berries, which are susceptible to HuNoV contamination.

In particular, our studies revealed a critical limitation in using RT-qPCR as the sole indicator of viral inactivation, highlighting its inability to reliably assess viral infectivity (Chapter 7). By comparing viability RT-qPCR with replication in HIE, we found that replication in HIE was a more robust assay for assessing HuNoV infectivity after thermal and HPP treatments. However, we also showed that viability RT-qPCR can still be used to determine the inactivation of HuNoV but only at extreme thermal (95 °C) and pressure (450 MPa) conditions.

Additionally, we expanded our understanding of the reduction in infectivity of various HuNoV strains (HuNoV GI.3[P13], HuNoV GII.4 Sydney [P16]), as well as HuNoV surrogates (MNV and TV), using HPP under different pressure conditions and exposure times, both in PBS and in strawberry puree (Chapter 8). Our data indicate

that commercially feasible HPP conditions (5 minutes at 450 MPa) are effective in inactivating infectious HuNoV GII.4 and its surrogates in both PBS and strawberry puree. Furthermore, the development of predictive models based on the inactivation of HuNoV surrogates (e.g., MNV and TV) provided valuable guidelines for optimizing pressure-time combinations to control HuNoV contamination, particularly in berry purees. These findings contribute to the development of evidence-based strategies for improving food safety and protecting public health.

In addition, the scientific work, conducted to evaluate the antimicrobial efficacy of PASW (Chapter 9), showed that it is an efficient and sustainable technology for inactivating a range of pathogens, including *E. coli* O157, S*almonella* spp, *V. parahemolyticus*, HuNoV and its surrogates. Looking ahead, the future perspective of our scientific research involves collaborating with the CNR-Institute of Nanotechnology (Bari, Italy) to develop an effective prototype of a shellfish depuration system based on PASW technology, capable to inactivate HuNoV and its surrogates.

Finally, we explored the HIE model for studying the replication of multiple gastroenteritis viruses (HuNoVs, RV, HAstV and/or HAdV) from wastewater samples (Chapter 10). We demonstrated that the HIE system can support the replication of a wide diversity of human infectious gastroenteritis viruses present in a single wastewater sample, contributing valuable insights into viral infectivity to ensure public health and environmental safety.

12. REFERENCES

1. WHO *WHO Estimates of the Global Burden of Foodborne Diseases : Foodborne Disease Burden Epiemiology Reference Group 2007-2015*; World Health Organization, 2015;
2. EFSA *The European Union One Health 2022 Zoonoses Report*; John Wiley and Sons Inc, 2023; Vol. 21;.
3. Olaimat, A.N.; Taybeh, A.O.; Al-Nabulsi, A.; Al-Holy, M.; Hatmal, M.M.; Alzyoud, J.; Aolymat, I.; Abughoush, M.H.; Shahbaz, H.; Alzyoud, A.; et al. Common and Potential Emerging Foodborne Viruses: A Comprehensive Review. *Life* **2024**, *14*, 190, doi:10.3390/life14020190.
4. Trząskowska, M.; Hunt, K.; Rodríguez-Lázaro, D. Risk Assessment of Enteric Viruses along the Food Chain and in the Population. *EFSA Journal* **2022**, *20*, doi:10.2903/j.efsa.2022.e200918.
5. Kendra, J.A.; Tohma, K.; Parra, G.I. Global and Regional Circulation Trends of Norovirus Genotypes and Recombinants, 1995–2019: A Comprehensive Review of Sequences from Public Databases. *Rev Med Virol* **2022**, *32*, doi:10.1002/rmv.2354.
6. Increase in Severe Food-Borne Infections Reported in EU/EEA in 2022 Available online: https://www.ecdc.europa.eu/en/news-events/increase-severe-food-borne-infections-reported-eueea-2022 (accessed on 14 October 2024).
7. RASFF PORTAL.
8. Pexara, A.; Govaris, A. Foodborne Viruses and Innovative Non-Thermal Food-Processing Technologies. *Foods* **2020**, *9*, doi:10.3390/FOODS9111520.
9. Terio, V.; Lorusso, P.; Mottola, A.; Buonavoglia, C.; Tantillo, G.; Bonerba, E.; Di Pinto, A. Norovirus Detection in Ready-To-Eat Salads by Propidium Monoazide Real Time RT-PCR Assay. *Applied Sciences* **2020**, *10*, 5176, doi:10.3390/app10155176.
10. Suffredini, E.; Le, Q.H.; Di Pasquale, S.; Pham, T.D.; Vicenza, T.; Losardo, M.; To, K.A.; De Medici, D. Occurrence and Molecular Characterization of Enteric Viruses in Bivalve Shellfish Marketed in Vietnam. *Food Control* **2020**, *108*, 106828, doi:10.1016/j.foodcont.2019.106828.
11. Bosch, A.; Gkogka, E.; Le Guyader, F.S.; Loisy-Hamon, F.; Lee, A.; van Lieshout, L.; Marthi, B.; Myrmel, M.; Sansom, A.; Schultz, A.C.; et al. Foodborne Viruses: Detection, Risk Assessment, and Control Options in Food Processing. *Int J Food Microbiol* **2018**, *285*, 110–128, doi:10.1016/j.ijfoodmicro.2018.06.001.
12. Chacha, J.S.; Zhang, L.; Ofoedu, C.E.; Suleiman, R.A.; Dotto, J.M.; Roobab, U.; Agunbiade, A.O.; Duguma, H.T.; Mkojera, B.T.; Hossaini, S.M.; et al. Revisiting Non-Thermal Food Processing and Preservation Methods—Action Mechanisms, Pros and Cons: A Technological Update (2016–2021). *Foods* **2021**, *10*, 1430, doi:10.3390/foods10061430.
13. Malik, Y.S.; Verma, A.K.; Kumar, N.; Touil, N.; Karthik, K.; Tiwari, R.; Bora, D.P.; Dhama, K.; Ghosh, S.; Hemida, M.G.; et al. Advances in Diagnostic Approaches for Viral Etiologies of Diarrhea: From the Lab to the Field. *Front Microbiol* **2019**, *10*, doi:10.3389/fmicb.2019.01957.
14. Haramoto, E.; Kitajima, M.; Hata, A.; Torrey, J.R.; Masago, Y.; Sano, D.; Katayama, H. A Review on Recent Progress in the Detection Methods and Prevalence of Human Enteric Viruses in Water. *Water Res* **2018**, *135*, 168–186, doi:10.1016/j.watres.2018.02.004.
15. Randazzo, W.; Vasquez-García, A.; Aznar, R.; Sánchez, G. Viability RT-QPCR to Distinguish between HEV and HAV with Intact and Altered Capsids. *Front Microbiol* **2018**, *9*, 1–8, doi:10.3389/fmicb.2018.01973.
16. Wales, S.Q.; Pandiscia, A.; Kulka, M.; Sanchez, G.; Randazzo, W. Challenges for Estimating Human Norovirus Infectivity by Viability RT-QPCR as Compared to Replication in Human Intestinal Enteroids. *Int J Food Microbiol* **2024**, *411*, 110507, doi:10.1016/j.ijfoodmicro.2023.110507.
17. Ettayebi, K.; Crawford, S.E.; Murakami, K.; Broughman, J.R.; Karandikar, U.; Tenge, V.R.; Neill, F.H.; Blutt, S.E.; Zeng, X.L.; Qu, L.; et al. Replication of Human Noroviruses in Stem Cell-Derived Human Enteroids. *Science* **2016**, *353*, 1387–1393, doi:10.1126/SCIENCE.AAF5211.
18. ICTV Taxon Details.
19. CDC Laboratory Testing for Norovirus.
20. Han, S.; Hyun, S.; Son, J.W.; Song, M.S.; Lim, D.J.; Choi, C.; Park, S.H.; Ha, S. Innovative Nonthermal Technologies for Inactivation of Emerging Foodborne Viruses. *Compr Rev Food Sci Food Saf* **2023**, *22*, 3395–3421, doi:10.1111/1541-4337.13192.

21. Di Martino, B.; Di Profio, F.; Melegari, I.; Sarchese, V.; Cafiero, M.A.; Robetto, S.; Aste, G.; Lanave, G.; Marsilio, F.; Martella, V. A Novel Feline Norovirus in Diarrheic Cats. *Infection, Genetics and Evolution* **2016**, *38*, 132–137, doi:10.1016/j.meegid.2015.12.019.
22. Karst, S.M.; Wobus, C.E.; Lay, M.; Davidson, J.; Virgin, H.W. STAT1-Dependent Innate Immunity to a Norwalk-Like Virus. *Science (1979)* **2003**, *299*, 1575–1578, doi:10.1126/science.1077905.
23. Liu, B.L.; Lambden, P.R.; Günther, H.; Otto, P.; Elschner, M.; Clarke, I.N. Molecular Characterization of a Bovine Enteric Calicivirus: Relationship to the Norwalk-Like Viruses. *J Virol* **1999**, *73*, 819–825, doi:10.1128/JVI.73.1.819-825.1999.
24. Mesquita, J.R.; Barclay, L.; Nascimento, M.S.J.; Vinjé, J. Novel Norovirus in Dogs with Diarrhea. *Emerg Infect Dis* **2010**, *16*, 980–982, doi:10.3201/eid1606.091861.
25. Shen, Q.; Zhang, W.; Yang, S.; Cui, L.; Hua, X. Complete Genome Sequence of a New-Genotype Porcine Norovirus Isolated from Piglets with Diarrhea. *J Virol* **2012**, *86*, 7015–7016, doi:10.1128/JVI.00757-12.
26. Wolf, S.; Williamson, W.; Hewitt, J.; Lin, S.; Rivera-Aban, M.; Ball, A.; Scholes, P.; Savill, M.; Greening, G.E. Molecular Detection of Norovirus in Sheep and Pigs in New Zealand Farms. *Vet Microbiol* **2009**, *133*, 184–189, doi:10.1016/j.vetmic.2008.06.019.
27. Teng, J.L.L.; Martelli, P.; Chan, W.-M.; Lee, H.H.; Hui, S.-W.; Lau, C.C.Y.; Tse, H.; Yuen, K.-Y.; Lau, S.K.P.; Woo, P.C.Y. Two Novel Noroviruses and a Novel Norovirus Genogroup in California Sea Lions. *Journal of General Virology* **2018**, *99*, 777–782, doi:10.1099/jgv.0.001071.
28. Shi, M.; Lin, X.-D.; Chen, X.; Tian, J.-H.; Chen, L.-J.; Li, K.; Wang, W.; Eden, J.-S.; Shen, J.-J.; Liu, L.; et al. The Evolutionary History of Vertebrate RNA Viruses. *Nature* **2018**, *556*, 197–202, doi:10.1038/s41586-018-0012-7.
29. Wu, Z.; Yang, L.; Ren, X.; He, G.; Zhang, J.; Yang, J.; Qian, Z.; Dong, J.; Sun, L.; Zhu, Y.; et al. Deciphering the Bat Virome Catalog to Better Understand the Ecological Diversity of Bat Viruses and the Bat Origin of Emerging Infectious Diseases. *ISME J* **2016**, *10*, 609–620, doi:10.1038/ismej.2015.138.
30. Chhabra, P.; de Graaf, M.; Parra, G.I.; Chan, M.C.-W.; Green, K.; Martella, V.; Wang, Q.; White, P.A.; Katayama, K.; Vennema, H.; et al. Updated Classification of Norovirus Genogroups and Genotypes. *Journal of General Virology* **2019**, *100*, 1393–1406, doi:10.1099/jgv.0.001318.
31. Lee, S.; Liu, H.; Wilen, C.B.; Sychev, Z.E.; Desai, C.; Hykes, B.L.; Orchard, R.C.; McCune, B.T.; Kim, K.-W.; Nice, T.J.; et al. A Secreted Viral Nonstructural Protein Determines Intestinal Norovirus Pathogenesis. *Cell Host Microbe* **2019**, *25*, 845-857.e5, doi:10.1016/j.chom.2019.04.005.
32. Chhabra, P.; Tully, D.C.; Mans, J.; Niendorf, S.; Barclay, L.; Cannon, J.L.; Montmayeur, A.M.; Pan, C.-Y.; Page, N.; Williams, R.; et al. Emergence of Novel Norovirus GII.4 Variant. *Emerg Infect Dis* **2024**, *30*, 163–167, doi:10.3201/eid3001.231003.
33. Vinjé, J. Advances in Laboratory Methods for Detection and Typing of Norovirus. *J Clin Microbiol* **2015**, *53*, 373–381, doi:10.1128/JCM.01535-14.
34. Graziano, V.R.; Wei, J.; Wilen, C.B. Norovirus Attachment and Entry. *Viruses* **2019**, *11*, 495, doi:10.3390/v11060495.
35. Almand, E.A.; Moore, M.D.; Jaykus, L.-A. Virus-Bacteria Interactions: An Emerging Topic in Human Infection. *Viruses* **2017**, *9*, 58, doi:10.3390/v9030058.
36. Cuvry, A.; Gozalbo-Rovira, R.; Strubbe, D.; Neyts, J.; de Witte, P.; Rodríguez-Díaz, J.; Rocha-Pereira, J. The Role of Histo-Blood Group Antigens and Microbiota in Human Norovirus Replication in Zebrafish Larvae. *Microbiol Spectr* **2022**, *10*, doi:10.1128/spectrum.03157-22.
37. Graziano, V.R.; Wei, J.; Wilen, C.B. Norovirus Attachment and Entry. *Viruses* **2019**, *11*, 495, doi:10.3390/v11060495.
38. Zhang, Q.; Zhu, S.; Zhang, X.; Su, L.; Ni, J.; Zhang, Y.; Fang, L. Recent Insights into Reverse Genetics of Norovirus. *Virus Res* **2023**, *325*, 199046, doi:10.1016/j.virusres.2023.199046.
39. Barclay, L.; Cannon, J.L.; Wikswo, M.E.; Phillips, A.R.; Browne, H.; Montmayeur, A.M.; Tatusov, R.L.; Burke, R.M.; Hall, A.J.; Vinjé, J. Emerging Novel GII.P16 Noroviruses Associated with Multiple Capsid Genotypes. *Viruses* **2019**, *11*, 535, doi:10.3390/v11060535.
40. de Graaf, M.; van Beek, J.; Koopmans, M.P.G. Human Norovirus Transmission and Evolution in a Changing World. *Nat Rev Microbiol* **2016**, *14*, 421–433, doi:10.1038/nrmicro.2016.48.
41. Chhabra, P.; de Graaf, M.; Parra, G.I.; Chan, M.C.W.; Green, K.; Martella, V.; Wang, Q.; White, P.A.; Katayama, K.; Vennema, H.; et al. Updated Classification of Norovirus

Genogroups and Genotypes. *Journal of General Virology* **2019**, *100*, 1393–1406, doi:10.1099/JGV.0.001318/CITE/REFWORKS.
42. Navarro-Lleó, N.; Santiso-Bellón, C.; Vila-Vicent, S.; Carmona-Vicente, N.; Gozalbo-Rovira, R.; Cárcamo-Calvo, R.; Rodríguez-Díaz, J.; Buesa, J. Recombinant Noroviruses Circulating in Spain from 2016 to 2020 and Proposal of Two Novel Genotypes within Genogroup I. *Microbiol Spectr* **2022**, *10*, doi:10.1128/spectrum.02505-21.
43. Parra, G.I.; Squires, R.B.; Karangwa, C.K.; Johnson, J.A.; Lepore, C.J.; Sosnovtsev, S. V.; Green, K.Y. Static and Evolving Norovirus Genotypes: Implications for Epidemiology and Immunity. *PLoS Pathog* **2017**, *13*, e1006136, doi:10.1371/journal.ppat.1006136.
44. Vinjé, J. Advances in Laboratory Methods for Detection and Typing of Norovirus. *J Clin Microbiol* **2015**, *53*, 373–381, doi:10.1128/JCM.01535-14.
45. Cates, J.E.; Vinjé, J.; Parashar, U.; Hall, A.J. Recent Advances in Human Norovirus Research and Implications for Candidate Vaccines. *Expert Rev Vaccines* **2020**, *19*, 539–548, doi:10.1080/14760584.2020.1777860.
46. Vega, E.; Barclay, L.; Gregoricus, N.; Shirley, S.H.; Lee, D.; Vinjé, J. Genotypic and Epidemiologic Trends of Norovirus Outbreaks in the United States, 2009 to 2013. *J Clin Microbiol* **2014**, *52*, 147–155, doi:10.1128/JCM.02680-13.
47. Bhavanam, S.; Freedman, S.; Lee, B.; Zhuo, R.; Qiu, Y.; Chui, L.; Xie, J.; Ali, S.; Vanderkooi, O.; Pang, X. Differences in Illness Severity among Circulating Norovirus Genotypes in a Large Pediatric Cohort with Acute Gastroenteritis. *Microorganisms* **2020**, *8*, 1873, doi:10.3390/microorganisms8121873.
48. Kendra, J.A.; Tohma, K.; Parra, G.I. Global and Regional Circulation Trends of Norovirus Genotypes and Recombinants, 1995–2019: A Comprehensive Review of Sequences from Public Databases. *Rev Med Virol* **2022**, *32*, doi:10.1002/rmv.2354.
49. Bartsch, S.M.; O'Shea, K.J.; Lee, B.Y. The Clinical and Economic Burden of Norovirus Gastroenteritis in the United States. *J Infect Dis* **2020**, *222*, 1910–1919, doi:10.1093/infdis/jiaa292.
50. CDC Norovirus Fats and Stats.
51. Randazzo, W.; D'Souza, D.H.; Sanchez, G. Norovirus: The Burden of the Unknown. In; 2018; pp. 13–53.
52. Winder, N.; Gohar, S.; Muthana, M. Norovirus: An Overview of Virology and Preventative Measures. *Viruses* **2022**, *14*, 2811, doi:10.3390/v14122811.
53. Lopman, B.A.; Reacher, M.H.; Vipond, I.B.; Sarangi, J.; Brown, D.W.G. Clinical Manifestation of Norovirus Gastroenteritis in Health Care Settings. *Clinical Infectious Diseases* **2004**, *39*, 318–324, doi:10.1086/421948.
54. ECDC Facts about Norovirus.
55. Atmar, R.L.; Opekun, A.R.; Gilger, M.A.; Estes, M.K.; Crawford, S.E.; Neill, F.H.; Graham, D.Y. Norwalk Virus Shedding after Experimental Human Infection. *Emerg Infect Dis* **2008**, *14*, 1553–1557, doi:10.3201/eid1410.080117.
56. TEUNIS, P.F.M.; SUKHRIE, F.H.A.; VENNEMA, H.; BOGERMAN, J.; BEERSMA, M.F.C.; KOOPMANS, M.P.G. Shedding of Norovirus in Symptomatic and Asymptomatic Infections. *Epidemiol Infect* **2015**, *143*, 1710–1717, doi:10.1017/S095026881400274X.
57. Atmar, R.; Baric, R.; Estes, M.; Kang, C. *Global Burden of Norovirus and Prospects for Vaccine Development Ben Lopman Centers for Disease Control and Prevention Contributors and Reviewers*;
58. ECDC *CommunicableDisease Threats Report*; 2024;
59. Atmar, R.L.; Opekun, A.R.; Gilger, M.A.; Estes, M.K.; Crawford, S.E.; Neill, F.H.; Ramani, S.; Hill, H.; Ferreira, J.; Graham, D.Y. Determination of the 50% Human Infectious Dose for Norwalk Virus. *J Infect Dis* **2014**, *209*, 1016–1022, doi:10.1093/infdis/jit620.
60. Ludwig-Begall, L.F.; Mauroy, A.; Thiry, E. Noroviruses—The State of the Art, Nearly Fifty Years after Their Initial Discovery. *Viruses* **2021**, *13*, 1541, doi:10.3390/v13081541.
61. Lucero, Y.; Matson, D.O.; Ashkenazi, S.; George, S.; O'Ryan, M. Norovirus: Facts and Reflections from Past, Present, and Future. *Viruses* **2021**, *13*, 2399, doi:10.3390/v13122399.
62. Cook, N.; Knight, A.; Richards, G.P. Persistence and Elimination of Human Norovirus in Food and on Food Contact Surfaces: A Critical Review. *J Food Prot* **2016**, *79*, 1273–1294, doi:10.4315/0362-028X.JFP-15-570.
63. Chandran, S.; Gibson, K.E. Improving the Detection and Understanding of Infectious Human Norovirus in Food and Water Matrices: A Review of Methods and Emerging Models. *Viruses* **2024**, *16*, 776, doi:10.3390/v16050776.

64. *Prevention and Control of Microbiological Hazards in Fresh Fruits and Vegetables – Part 4: Specific Commodities*; FAO; WHO;, 2023; ISBN 978-92-5-138101-4.
65. Bozkurt, H.; Phan-Thien, K.-Y.; van Ogtrop, F.; Bell, T.; McConchie, R. Outbreaks, Occurrence, and Control of Norovirus and Hepatitis a Virus Contamination in Berries: A Review. *Crit Rev Food Sci Nutr* **2021**, *61*, 116–138, doi:10.1080/10408398.2020.1719383.
66. Bozkurt, H.; Phan-Thien, K.Y.; van Ogtrop, F.; Bell, T.; McConchie, R. Outbreaks, Occurrence, and Control of Norovirus and Hepatitis a Virus Contamination in Berries: A Review. *Crit Rev Food Sci Nutr* **2021**, *61*, 116–138, doi:10.1080/10408398.2020.1719383.
67. EFSA *The European Union One Health 2019 Zoonoses Report*; 2021; Vol. 19;.
68. Pavoni, E.; Bertasi, B.; Galuppini, E.; Mangeri, L.; Meletti, F.; Tilola, M.; Carta, V.; Todeschi, S.; Losio, M.-N. Detection of Hepatitis A Virus and Norovirus in Different Food Categories: A 6-Year Survey in Italy. *Food Environ Virol* **2022**, *14*, 69–76, doi:10.1007/s12560-021-09503-y.
69. Kamarasu, P.; Hsu, H.-Y.; Moore, M.D. Research Progress in Viral Inactivation Utilizing Human Norovirus Surrogates. *Front Sustain Food Syst* **2018**, *2*, doi:10.3389/fsufs.2018.00089.
70. Cromeans, T.; Park, G.W.; Costantini, V.; Lee, D.; Wang, Q.; Farkas, T.; Lee, A.; Vinjé, J. Comprehensive Comparison of Cultivable Norovirus Surrogates in Response to Different Inactivation and Disinfection Treatments. *Appl Environ Microbiol* **2014**, *80*, 5743–5751, doi:10.1128/AEM.01532-14.
71. Richards, G.P. Critical Review of Norovirus Surrogates in Food Safety Research: Rationale for Considering Volunteer Studies. *Food Environ Virol* **2012**, *4*, 6–13, doi:10.1007/s12560-011-9072-7.
72. Wobus, C.E.; Thackray, L.B.; Virgin, H.W. Murine Norovirus: A Model System To Study Norovirus Biology and Pathogenesis. *J Virol* **2006**, *80*, 5104–5112, doi:10.1128/JVI.02346-05.
73. Cannon, J.L.; Papafragkou, E.; Park, G.W.; Osborne, J.; Jaykus, L.-A.; Vinjé, J. Surrogates for the Study of Norovirus Stability and Inactivation in the Environment: A Comparison of Murine Norovirus and Feline Calicivirus. *J Food Prot* **2006**, *69*, 2761–2765, doi:10.4315/0362-028X-69.11.2761.
74. Wobus, C.E.; Karst, S.M.; Thackray, L.B.; Chang, K.-O.; Sosnovtsev, S. V; Belliot, G.; Krug, A.; Mackenzie, J.M.; Green, K.Y.; Virgin, H.W. Replication of Norovirus in Cell Culture Reveals a Tropism for Dendritic Cells and Macrophages. *PLoS Biol* **2004**, *2*, e432, doi:10.1371/journal.pbio.0020432.
75. Farkas, T.; Sestak, K.; Wei, C.; Jiang, X. Characterization of a Rhesus Monkey Calicivirus Representing a New Genus of *Caliciviridae*. *J Virol* **2008**, *82*, 5408–5416, doi:10.1128/JVI.00070-08.
76. Tian, P.; Yang, D.; Quigley, C.; Chou, M.; Jiang, X. Inactivation of the Tulane Virus, a Novel Surrogate for the Human Norovirus. *J Food Prot* **2013**, *76*, 712–718, doi:10.4315/0362-028X.JFP-12-361.
77. Farkas, T.; Cross, R.W.; Hargitt, E.; Lerche, N.W.; Morrow, A.L.; Sestak, K. Genetic Diversity and Histo-Blood Group Antigen Interactions of Rhesus Enteric Caliciviruses. *J Virol* **2010**, *84*, 8617–8625, doi:10.1128/JVI.00630-10.
78. Blondin-Brosseau, M.; Harlow, J.; Doctor, T.; Nasheri, N. Examining the Persistence of Human Coronavirus 229E on Fresh Produce. *Food Microbiol* **2021**, *98*, doi:10.1016/j.fm.2021.103780.
79. Danso, D.; Chow, J.; Streit, W.R. Plastics: Environmental and Biotechnological Perspectives on Microbial Degradation. *Appl Environ Microbiol* **2019**, *85*, doi:10.1128/AEM.01095-19.
80. Jiang, S.C.; Bischel, H.N.; Goel, R.; Rosso, D.; Sherchan, S.P.; Whiteson, K.L.; Yan, T.; Solo-Gabriele, H.M. Integrating Virus Monitoring Strategies for Safe Non-Potable Water Reuse. *Water (Basel)* **2022**, *14*, 1187, doi:10.3390/w14081187.
81. Hata, A.; Hanamoto, S.; Shirasaka, Y.; Yamashita, N.; Tanaka, H. Quantitative Distribution of Infectious F-Specific RNA Phage Genotypes in Surface Waters. *Appl Environ Microbiol* **2016**, *82*, 4244–4252, doi:10.1128/AEM.00621-16.
82. Ettayebi, K.; Crawford, S.E.; Murakami, K.; Broughman, J.R.; Karandikar, U.; Tenge, V.R.; Neill, F.H.; Blutt, S.E.; Zeng, X.-L.; Qu, L.; et al. Replication of Human Noroviruses in Stem Cell–Derived Human Enteroids. *Science (1979)* **2016**, *353*, 1387–1393, doi:10.1126/science.aaf5211.
83. Lou, F.; Neetoo, H.; Chen, H.; Li, J. High Hydrostatic Pressure Processing: A Promising Nonthermal Technology to Inactivate Viruses in High-Risk Foods. *Annu Rev Food Sci Technol* **2015**, *6*, 389–409, doi:10.1146/annurev-food-072514-104609.

84. Gómez-López, V.M.; Jubinville, E.; Rodríguez-López, M.I.; Trudel-Ferland, M.; Bouchard, S.; Jean, J. Inactivation of Foodborne Viruses by UV Light: A Review. *Foods* **2021**, *10*, 3141, doi:10.3390/foods10123141.
85. Ahmed, H.; Maunula, L.; Korhonen, J. Reduction of Norovirus in Foods by Nonthermal Treatments: A Review. *J Food Prot* **2020**, *83*, 2053–2073, doi:10.4315/JFP-20-177.
86. Feng, K.; Divers, E.; Ma, Y.; Li, J. Inactivation of a Human Norovirus Surrogate, Human Norovirus Virus-Like Particles, and Vesicular Stomatitis Virus by Gamma Irradiation. *Appl Environ Microbiol* **2011**, *77*, 3507–3517, doi:10.1128/AEM.00081-11.
87. Sanglay, G.C.; Li, J.; Uribe, R.M.; Lee, K. Electron-Beam Inactivation of a Norovirus Surrogate in Fresh Produce and Model Systems. *J Food Prot* **2011**, *74*, 1155–1160, doi:10.4315/0362-028X.JFP-10-405.
88. Predmore, A.; Sanglay, G.C.; DiCaprio, E.; Li, J.; Uribe, R.M.; Lee, K. Electron Beam Inactivation of Tulane Virus on Fresh Produce, and Mechanism of Inactivation of Human Norovirus Surrogates by Electron Beam Irradiation. *Int J Food Microbiol* **2015**, *198*, 28–36, doi:10.1016/j.ijfoodmicro.2014.12.024.
89. Praveen, C.; Dancho, B.A.; Kingsley, D.H.; Calci, K.R.; Meade, G.K.; Mena, K.D.; Pillai, S.D. Susceptibility of Murine Norovirus and Hepatitis A Virus to Electron Beam Irradiation in Oysters and Quantifying the Reduction in Potential Infection Risks. *Appl Environ Microbiol* **2013**, *79*, 3796–3801, doi:10.1128/AEM.00347-13.
90. Su, X.; Zivanovic, S.; D'Souza, D.H. Inactivation of Human Enteric Virus Surrogates by High-Intensity Ultrasound. *Foodborne Pathog Dis* **2010**, *7*, 1055–1061, doi:10.1089/fpd.2009.0515.
91. Bhullar, M.S.; Patras, A.; Kilanzo-Nthenge, A.; Pokharel, B.; Yannam, S.K.; Rakariyatham, K.; Pan, C.; Xiao, H.; Sasges, M. Microbial Inactivation and Cytotoxicity Evaluation of UV Irradiated Coconut Water in a Novel Continuous Flow Spiral Reactor. *Food Research International* **2018**, *103*, 59–67, doi:10.1016/j.foodres.2017.10.004.
92. Gunter-Ward, D.M.; Patras, A.; S. Bhullar, M.; Kilonzo-Nthenge, A.; Pokharel, B.; Sasges, M. Efficacy of Ultraviolet (UV-C) Light in Reducing Foodborne Pathogens and Model Viruses in Skim Milk. *J Food Process Preserv* **2018**, *42*, doi:10.1111/jfpp.13485.
93. Moon, Y.; Han, S.; Son, J. won; Park, S.H.; Ha, S.-D. Impact of Ultraviolet-C and Peroxyacetic Acid against Murine Norovirus on Stainless Steel and Lettuce. *Food Control* **2021**, *130*, 108378, doi:10.1016/j.foodcont.2021.108378.
94. Park, S.Y.; Ha, S.-D. Ultraviolet-C Radiation on the Fresh Chicken Breast: Inactivation of Major Foodborne Viruses and Changes in Physicochemical and Sensory Qualities of Product. *Food Bioproc Tech* **2015**, *8*, 895–906, doi:10.1007/s11947-014-1452-1.
95. Nasheri, N.; Harlow, J.; Chen, A.; Corneau, N.; Bidawid, S. Survival and Inactivation by Advanced Oxidative Process of Foodborne Viruses in Model Low-Moisture Foods. *Food Environ Virol* **2021**, *13*, 107–116, doi:10.1007/s12560-020-09457-7.
96. Joshi, K.; Mahendran, R.; Alagusundaram, K.; Norton, T.; Tiwari, B.K. Novel Disinfectants for Fresh Produce. *Trends Food Sci Technol* **2013**, *34*, 54–61, doi:10.1016/j.tifs.2013.08.008.
97. Vimont, A.; Fliss, I.; Jean, J. Study of the Virucidal Potential of Organic Peroxyacids Against Norovirus on Food-Contact Surfaces. *Food Environ Virol* **2015**, *7*, 49–57, doi:10.1007/s12560-014-9174-0.
98. Moorman, E.; Montazeri, N.; Jaykus, L.-A. Efficacy of Neutral Electrolyzed Water for Inactivation of Human Norovirus. *Appl Environ Microbiol* **2017**, *83*, doi:10.1128/AEM.00653-17.
99. Jenns, K.; Sassi, H.P.; Zhou, R.; Cullen, P.J.; Carter, D.; Mai-Prochnow, A. Inactivation of Foodborne Viruses: Opportunities for Cold Atmospheric Plasma. *Trends Food Sci Technol* **2022**, *124*, 323–333, doi:10.1016/j.tifs.2022.04.006.
100. Fuzawa, M.; Araud, E.; Li, J.; Shisler, J.L.; Nguyen, T.H. Free Chlorine Disinfection Mechanisms of Rotaviruses and Human Norovirus Surrogate Tulane Virus Attached to Fresh Produce Surfaces. *Environ Sci Technol* **2019**, *53*, 11999–12006, doi:10.1021/acs.est.9b03461.
101. Lin, Y.-C.; Yeh, H.-D. Trihalomethane Species Forecast Using Optimization Methods: Genetic Algorithms and Simulated Annealing. *Journal of Computing in Civil Engineering* **2005**, *19*, 248–257, doi:10.1061/(ASCE)0887-3801(2005)19:3(248).
102. Gallandat, K.; Kolus, R.C.; Julian, T.R.; Lantagne, D.S. A Systematic Review of Chlorine-Based Surface Disinfection Efficacy to Inform Recommendations for Low-Resource Outbreak Settings. *Am J Infect Control* **2021**, *49*, 90–103, doi:10.1016/j.ajic.2020.05.014.
103. Stearns, R.; Freshour, A.; Shen, C. Literature Review for Applying Peroxyacetic Acid and/or Hydrogen Peroxide to Control Foodborne Pathogens on Food Products. *J Agric Food Res* **2022**, *10*, 100442, doi:10.1016/j.jafr.2022.100442.

104. Block, P. The Decomposition Kinetics of Peracetic Acid and Hydrogen Peroxide in Municipal Wastewaters. *Proceedings of the Water Environment Federation* **2016**, *2016*, 555–563, doi:10.2175/193864716819707265.
105. Rahman, S.; Khan, I.; Oh, D. Electrolyzed Water as a Novel Sanitizer in the Food Industry: Current Trends and Future Perspectives. *Compr Rev Food Sci Food Saf* **2016**, *15*, 471–490, doi:10.1111/1541-4337.12200.
106. Rebezov, M.; Saeed, K.; Khaliq, A.; Rahman, S.J.U.; Sameed, N.; Semenova, A.; Khayrullin, M.; Dydykin, A.; Abramov, Y.; Thiruvengadam, M.; et al. Application of Electrolyzed Water in the Food Industry: A Review. *Applied Sciences* **2022**, *12*, 6639, doi:10.3390/app12136639.
107. CDC 2023.
108. Yeargin, T.; Buckley, D.; Fraser, A.; Jiang, X. The Survival and Inactivation of Enteric Viruses on Soft Surfaces: A Systematic Review of the Literature. *Am J Infect Control* **2016**, *44*, 1365–1373, doi:10.1016/j.ajic.2016.03.018.
109. Lisboa, H.M.; Pasquali, M.B.; dos Anjos, A.I.; Sarinho, A.M.; de Melo, E.D.; Andrade, R.; Batista, L.; Lima, J.; Diniz, Y.; Barros, A. Innovative and Sustainable Food Preservation Techniques: Enhancing Food Quality, Safety, and Environmental Sustainability. *Sustainability* **2024**, *16*, 8223, doi:10.3390/su16188223.
110. Govaris, A.; Pexara, A. Inactivation of Foodborne Viruses by High-Pressure Processing (HPP). *Foods* **2021**, *10*, 215, doi:10.3390/foods10020215.
111. Koutsoumanis, K.; Alvarez-Ordóñez, A.; Bolton, D.; Bover-Cid, S.; Chemaly, M.; Davies, R.; De Cesare, A.; Herman, L.; Hilbert, F.; Lindqvist, R.; et al. The Efficacy and Safety of High-pressure Processing of Food. *EFSA Journal* **2022**, *20*, doi:10.2903/j.efsa.2022.7128.
112. Ozaybi, N. High-Pressure Processing of Milk and Dairy Products: Latest Update. *Processes* **2024**, *12*, 2073, doi:10.3390/pr12102073.
113. Abera, G. Review on High-Pressure Processing of Foods. *Cogent Food Agric* **2019**, *5*, 1568725, doi:10.1080/23311932.2019.1568725.
114. Mota, M.J.; Lopes, R.P.; Delgadillo, I.; Saraiva, J.A. Microorganisms under High Pressure — Adaptation, Growth and Biotechnological Potential. *Biotechnol Adv* **2013**, *31*, 1426–1434, doi:10.1016/j.biotechadv.2013.06.007.
115. Lou, F.; Neetoo, H.; Chen, H.; Li, J. High Hydrostatic Pressure Processing: A Promising Nonthermal Technology to Inactivate Viruses in High-Risk Foods. *Annu Rev Food Sci Technol* **2015**, *6*, 389–409, doi:10.1146/annurev-food-072514-104609.
116. Aganovic, K.; Hertel, C.; Vogel, Rudi.F.; Johne, R.; Schlüter, O.; Schwarzenbolz, U.; Jäger, H.; Holzhauser, T.; Bergmair, J.; Roth, A.; et al. Aspects of High Hydrostatic Pressure Food Processing: Perspectives on Technology and Food Safety. *Compr Rev Food Sci Food Saf* **2021**, *20*, 3225–3266, doi:10.1111/1541-4337.12763.
117. European Parliament and Council REGULATION (EC) No 852/2004 OF THE EUROPEAN PARLIAMENT AND OF THE COUNCIL (of 29 April 2004) on the Hygiene of Foodstuff.
118. *Commission Implementing Regulation (EU) 2017/2470 of 20 December 2017 Establishing the Union List of Novel Foods in Accordance with Regulation (EU) 2015/2283 of the European Parliament and of the Council on Novel Foods*; 2015;
119. Regulation (EU) 2015/2283 of the European Parliament and of the Council of 25 November 2015 on Novel Foods, Amending Regulation (EU) No 1169/2011 of the European Parliament and of the Council and Repealing Regulation (EC) No 258/97 of the European Parliament and of the Council and Commission Regulation (EC) No 1852/2001.
120. Huang, H.W.; Hsu, C.P.; Wang, C.Y. Healthy Expectations of High Hydrostatic Pressure Treatment in Food Processing Industry. *J Food Drug Anal* **2020**, *28*, 1–13, doi:10.1016/J.JFDA.2019.10.002.
121. Huang, H.-W.; Hsu, C.-P.; Wang, C.-Y. Healthy Expectations of High Hydrostatic Pressure Treatment in Food Processing Industry. *J Food Drug Anal* **2020**, *28*, 1–13, doi:10.1016/j.jfda.2019.10.002.
122. Bajovic, B.; Bolumar, T.; Heinz, V. Quality Considerations with High Pressure Processing of Fresh and Value Added Meat Products. *Meat Sci* **2012**, *92*, 280–289, doi:10.1016/j.meatsci.2012.04.024.
123. Gómez-Maqueo, A.; Welti-Chanes, J.; Cano, M.P. Release Mechanisms of Bioactive Compounds in Fruits Submitted to High Hydrostatic Pressure: A Dynamic Microstructural Analysis Based on Prickly Pear Cells. *Food Research International* **2020**, *130*, 108909, doi:10.1016/j.foodres.2019.108909.
124. Navarro-Baez, J.E.; Martínez, L.M.; Welti-Chanes, J.; Buitimea-Cantúa, G. V.; Escobedo-Avellaneda, Z. High Hydrostatic Pressure to Increase the Biosynthesis and Extraction of

Phenolic Compounds in Food: A Review. *Molecules* **2022**, *27*, 1502, doi:10.3390/molecules27051502.
125. Pérez-Lamela, C.; Franco, I.; Falqué, E. Impact of High-Pressure Processing on Antioxidant Activity during Storage of Fruits and Fruit Products: A Review. *Molecules* **2021**, *26*, 5265, doi:10.3390/molecules26175265.
126. de Alba, M.; Montiel, R.; Bravo, D.; Gaya, P.; Medina, M. High Pressure Treatments on the Inactivation of Salmonella Enteritidis and the Physicochemical, Rheological and Color Characteristics of Sliced Vacuum-Packaged Dry-Cured Ham. *Meat Sci* **2012**, *91*, 173–178, doi:10.1016/j.meatsci.2012.01.015.
127. Devatkal, S.; Anurag, R.; Jaganath, B.; Rao, S. Microstructure, Microbial Profile and Quality Characteristics of High-Pressure-Treated Chicken Nuggets. *Food Science and Technology International* **2015**, *21*, 481–491, doi:10.1177/1082013214546957.
128. Mengden, R.; Röhner, A.; Sudhaus, N.; Klein, G. High-Pressure Processing of Mild Smoked Rainbow Trout Fillets (Oncorhynchus Mykiss) and Fresh European Catfish Fillets (Silurus Glanis). *Innovative Food Science & Emerging Technologies* **2015**, *32*, 9–15, doi:10.1016/j.ifset.2015.10.002.
129. Kaushik, N.; Kaur, B.P.; Rao, P.S.; Mishra, H.N. Effect of High Pressure Processing on Color, Biochemical and Microbiological Characteristics of Mango Pulp (Mangifera Indica Cv. Amrapali). *Innovative Food Science & Emerging Technologies* **2014**, *22*, 40–50, doi:10.1016/j.ifset.2013.12.011.
130. Pilavtepe-Çelik, M.; Buzrul, S.; Alpas, H.; Bozoğlu, F. Development of a New Mathematical Model for Inactivation of Escherichia Coli O157:H7 and Staphylococcus Aureus by High Hydrostatic Pressure in Carrot Juice and Peptone Water. *J Food Eng* **2009**, *90*, 388–394, doi:10.1016/j.jfoodeng.2008.06.043.
131. Nema, P.K.; Sehrawat, R.; Ravichandran, C.; Kaur, B.P.; Kumar, A.; Tarafdar, A. Inactivating Food Microbes by High-Pressure Processing and Combined Nonthermal and Thermal Treatment: A Review. *J Food Qual* **2022**, *2022*, 1–27, doi:10.1155/2022/5797843.
132. DeWitt, C.A.M.; Nelson, K.A.; Kim, H.J.; Kingsley, D.H. Ultralow Temperature High Pressure Processing Enhances Inactivation of Norovirus Surrogates. *Int J Food Microbiol* **2024**, *408*, 110438, doi:10.1016/j.ijfoodmicro.2023.110438.
133. Bolumar, T.; Orlien, V.; Sikes, A.; Aganovic, K.; Bak, K.H.; Guyon, C.; Stübler, A.; de Lamballerie, M.; Hertel, C.; Brüggemann, D.A. High-pressure Processing of Meat: Molecular Impacts and Industrial Applications. *Compr Rev Food Sci Food Saf* **2021**, *20*, 332–368, doi:10.1111/1541-4337.12670.
134. Kingsley, D.H.; Chen, H. Influence of PH, Salt, and Temperature on Pressure Inactivation of Hepatitis A Virus. *Int J Food Microbiol* **2009**, *130*, 61–64, doi:10.1016/j.ijfoodmicro.2009.01.004.
135. Pan, H.; Buenconsejo, M.; Reineke, K.F.; Shieh, Y.C. Effect of Process Temperature on Virus Inactivation during High Hydrostatic Pressure Processing of Contaminated Fruit Puree and Juice. *J Food Prot* **2016**, *79*, 1517–1526, doi:10.4315/0362-028X.JFP-16-004.
136. Lou, F.; Neetoo, H.; Chen, H.; Li, J. Inactivation of a Human Norovirus Surrogate by High-Pressure Processing: Effectiveness, Mechanism, and Potential Application in the Fresh Produce Industry. *Appl Environ Microbiol* **2011**, *77*, 1862–1871, doi:10.1128/AEM.01918-10.
137. Kingsley, D.H.; Guan, D.; Hoover, D.G.; Chen, H. Inactivation of Hepatitis A Virus by High-Pressure Processing: The Role of Temperature and Pressure Oscillation. *J Food Prot* **2006**, *69*, 2454–2459, doi:10.4315/0362-028X-69.10.2454.
138. Lou, F.; DiCaprio, E.; Li, X.; Dai, X.; Ma, Y.; Hughes, J.; Chen, H.; Kingsley, D.H.; Li, J. Variable High-Pressure-Processing Sensitivities for Genogroup II Human Noroviruses. *Appl Environ Microbiol* **2016**, *82*, 6037–6045, doi:10.1128/AEM.01575-16.
139. Sánchez, G.; Bosch, A. Survival of Enteric Viruses in the Environment and Food. In *Viruses in Foods*; Springer International Publishing: Cham, 2016; pp. 367–392.
140. Seo, K.; Lee, J.E.; Lim, M.Y.; Ko, G. Effect of Temperature, PH, and NaCl on the Inactivation Kinetics of Murine Norovirus. *J Food Prot* **2012**, *75*, 533–540, doi:10.4315/0362-028X.JFP-11-199.
141. Varilla, C.; Marcone, M.; Annor, G.A. Potential of Cold Plasma Technology in Ensuring the Safety of Foods and Agricultural Produce: A Review. *Foods* **2020**, *9*, 1435, doi:10.3390/foods9101435.
142. Yawut, N.; Mekwilai, T.; Vichiansan, N.; Braspaiboon, S.; Leksakul, K.; Boonyawan, D. Cold Plasma Technology: Transforming Food Processing for Safety and Sustainability. *J Agric Food Res* **2024**, *18*, 101383, doi:10.1016/j.jafr.2024.101383.

143. Bourke, P.; Ziuzina, D.; Boehm, D.; Cullen, P.J.; Keener, K. The Potential of Cold Plasma for Safe and Sustainable Food Production. *Trends Biotechnol* **2018**, *36*, 615–626, doi:10.1016/j.tibtech.2017.11.001.
144. Misra, N.N.; Patil, S.; Moiseev, T.; Bourke, P.; Mosnier, J.P.; Keener, K.M.; Cullen, P.J. In-Package Atmospheric Pressure Cold Plasma Treatment of Strawberries. *J Food Eng* **2014**, *125*, 131–138, doi:10.1016/j.jfoodeng.2013.10.023.
145. Thirumdas, R.; Kothakota, A.; Annapure, U.; Siliveru, K.; Blundell, R.; Gatt, R.; Valdramidis, V.P. Plasma Activated Water (PAW): Chemistry, Physico-Chemical Properties, Applications in Food and Agriculture. *Trends Food Sci Technol* **2018**, *77*, 21–31, doi:10.1016/j.tifs.2018.05.007.
146. Sardella, E.; Veronico, V.; Gristina, R.; Grossi, L.; Cosmai, S.; Striccoli, M.; Buttiglione, M.; Fracassi, F.; Favia, P. Plasma Treated Water Solutions in Cancer Treatments: The Contrasting Role of RNS. *Antioxidants* **2021**, *10*, 605, doi:10.3390/antiox10040605.
147. Rahman, M.; Hasan, M.S.; Islam, R.; Rana, R.; Sayem, A.S.M.; Sad, M.A.A.; Matin, A.; Raposo, A.; Zandonadi, R.P.; Han, H.; et al. Plasma-Activated Water for Food Safety and Quality: A Review of Recent Developments. *Int J Environ Res Public Health* 2022, *19*.
148. Oliveira, M.; Fernández-Gómez, P.; Álvarez-Ordóñez, A.; Prieto, M.; López, M. Plasma-Activated Water: A Cutting-Edge Technology Driving Innovation in the Food Industry. *Food Research International* **2022**, *156*, 111368, doi:10.1016/j.foodres.2022.111368.
149. Wong, K.S.; Chew, N.S.L.; Low, M.; Tan, M.K. Plasma-Activated Water: Physicochemical Properties, Generation Techniques, and Applications. *Processes* **2023**, *11*, 2213, doi:10.3390/pr11072213.
150. A. Fridman *Plasma Chemistry*; Cambridge University Press, 2008;
151. Zhang, H.; Ma, D.; Qiu, R.; Tang, Y.; Du, C. Non-Thermal Plasma Technology for Organic Contaminated Soil Remediation: A Review. *Chemical Engineering Journal* **2017**, *313*, 157–170, doi:10.1016/j.cej.2016.12.067.
152. Harikrishna, S.; Anil, P.P.; Shams, R.; Dash, K.K. Cold Plasma as an Emerging Nonthermal Technology for Food Processing: A Comprehensive Review. *J Agric Food Res* **2023**, *14*, 100747, doi:10.1016/j.jafr.2023.100747.
153. Šimončicová, J.; Kryštofová, S.; Medvecká, V.; Ďurišová, K.; Kaliňáková, B. Technical Applications of Plasma Treatments: Current State and Perspectives. *Appl Microbiol Biotechnol* **2019**, *103*, 5117–5129, doi:10.1007/s00253-019-09877-x.
154. Chauvin, J.; Judée, F.; Yousfi, M.; Vicendo, P.; Merbahi, N. Analysis of Reactive Oxygen and Nitrogen Species Generated in Three Liquid Media by Low Temperature Helium Plasma Jet. *Sci Rep* **2017**, *7*, 4562, doi:10.1038/s41598-017-04650-4.
155. Zhou, R.; Zhang, X.; Bi, Z.; Zong, Z.; Niu, J.; Song, Y.; Liu, D.; Yang, S. Inactivation of Escherichia Coli Cells in Aqueous Solution by Atmospheric-Pressure N_2, He, Air, and O_2 Microplasmas. *Appl Environ Microbiol* **2015**, *81*, 5257–5265, doi:10.1128/AEM.01287-15.
156. Kaushik, N.; Mitra, S.; Baek, E.J.; Nguyen, L.N.; Bhartiya, P.; Kim, J.H.; Choi, E.H.; Kaushik, N.K. The Inactivation and Destruction of Viruses by Reactive Oxygen Species Generated through Physical and Cold Atmospheric Plasma Techniques: Current Status and Perspectives. *J Adv Res* **2023**, *43*, 59–71, doi:10.1016/j.jare.2022.03.002.
157. Yamashiro, R.; Misawa, T.; Sakudo, A. Key Role of Singlet Oxygen and Peroxynitrite in Viral RNA Damage during Virucidal Effect of Plasma Torch on Feline Calicivirus. *Sci Rep* **2018**, *8*, 17947, doi:10.1038/s41598-018-36779-1.
158. Chassaing, M.; Bastin, G.; Robin, M.; Majou, D.; Belliot, G.; de Rougemont, A.; Boudaud, N.; Gantzer, C. Free Chlorine and Peroxynitrite Alter the Capsid Structure of Human Norovirus GII.4 and Its Capacity to Bind Histo-Blood Group Antigens. *Front Microbiol* **2021**, *12*, doi:10.3389/fmicb.2021.662764.
159. Wang, Q.; Salvi, D. Recent Progress in the Application of Plasma-Activated Water (PAW) for Food Decontamination. *Curr Opin Food Sci* **2021**, *42*, 51–60, doi:10.1016/j.cofs.2021.04.012.
160. Traylor, M.J.; Pavlovich, M.J.; Karim, S.; Hait, P.; Sakiyama, Y.; Clark, D.S.; Graves, D.B. Long-Term Antibacterial Efficacy of Air Plasma-Activated Water. *J Phys D Appl Phys* **2011**, *44*, 472001, doi:10.1088/0022-3727/44/47/472001.
161. Tsoukou, E.; Bourke, P.; Boehm, D. Temperature Stability and Effectiveness of Plasma-Activated Liquids over an 18 Months Period. *Water (Basel)* **2020**, *12*, 3021, doi:10.3390/w12113021.
162. Guo, L.; Xu, R.; Gou, L.; Liu, Z.; Zhao, Y.; Liu, D.; Zhang, L.; Chen, H.; Kong, M.G. Mechanism of Virus Inactivation by Cold Atmospheric-Pressure Plasma and Plasma-Activated Water. *Appl Environ Microbiol* **2018**, *84*, doi:10.1128/AEM.00726-18.

163. Vlad, I.-E.; Anghel, S.D. Time Stability of Water Activated by Different On-Liquid Atmospheric Pressure Plasmas. *J Electrostat* **2017**, *87*, 284–292, doi:10.1016/j.elstat.2017.06.002.
164. Zver, M.; Dobnik, D.; Zaplotnik, R.; Mozetič, M.; Filipić, A.; Primc, G. Non-Thermal Plasma Inactivation of Viruses in Water Solutions. *Journal of Water Process Engineering* **2023**, *53*, 103839, doi:10.1016/j.jwpe.2023.103839.
165. Nayak, G.; Aboubakr, H.A.; Goyal, S.M.; Bruggeman, P.J. Reactive Species Responsible for the Inactivation of Feline Calicivirus by a Two-dimensional Array of Integrated Coaxial Microhollow Dielectric Barrier Discharges in Air. *Plasma Processes and Polymers* **2018**, *15*, doi:10.1002/ppap.201700119.
166. Wang, F.; Zhang, Q.; An, R.; Lyu, C.; Xu, J.; Wang, D. Reactive Species of Plasma-Activated Water for Murine Norovirus 1 Inactivation. *Food Research International* **2024**, *194*, 114877, doi:10.1016/j.foodres.2024.114877.
167. Guo, L.; Yao, Z.; Yang, L.; Zhang, H.; Qi, Y.; Gou, L.; Xi, W.; Liu, D.; Zhang, L.; Cheng, Y.; et al. Plasma-Activated Water: An Alternative Disinfectant for S Protein Inactivation to Prevent SARS-CoV-2 Infection. *Chemical Engineering Journal* **2021**, *421*, doi:10.1016/J.CEJ.2020.127742.
168. Kaushik, N.K.; Bhartiya, P.; Kaushik, N.; Shin, Y.; Nguyen, L.N.; Park, J.S.; Kim, D.; Choi, E.H. Nitric-Oxide Enriched Plasma-Activated Water Inactivates 229E Coronavirus and Alters Antiviral Response Genes in Human Lung Host Cells. *Bioact Mater* **2023**, *19*, 569–580, doi:10.1016/j.bioactmat.2022.05.005.
169. Liu, D.X.; Liu, Z.C.; Chen, C.; Yang, A.J.; Li, D.; Rong, M.Z.; Chen, H.L.; Kong, M.G. Aqueous Reactive Species Induced by a Surface Air Discharge: Heterogeneous Mass Transfer and Liquid Chemistry Pathways. *Sci Rep* **2016**, *6*, 23737, doi:10.1038/srep23737.
170. Su, X.; Tian, Y.; Zhou, H.; Li, Y.; Zhang, Z.; Jiang, B.; Yang, B.; Zhang, J.; Fang, J. Inactivation Efficacy of Nonthermal Plasma-Activated Solutions against Newcastle Disease Virus. *Appl Environ Microbiol* **2018**, *84*, doi:10.1128/AEM.02836-17.
171. Zimmermann, J.L.; Dumler, K.; Shimizu, T.; Morfill, G.E.; Wolf, A.; Boxhammer, V.; Schlegel, J.; Gansbacher, B.; Anton, M. Effects of Cold Atmospheric Plasmas on Adenoviruses in Solution. *J Phys D Appl Phys* **2011**, *44*, 505201, doi:10.1088/0022-3727/44/50/505201.
172. Bosch, A.; Gkogka, E.; Le Guyader, F.S.; Loisy-Hamon, F.; Lee, A.; van Lieshout, L.; Marthi, B.; Myrmel, M.; Sansom, A.; Schultz, A.C.; et al. Foodborne Viruses: Detection, Risk Assessment, and Control Options in Food Processing. *Int J Food Microbiol* **2018**, *285*, 110–128, doi:10.1016/j.ijfoodmicro.2018.06.001.
173. Leifels, M.; Cheng, D.; Sozzi, E.; Shoults, D.C.; Wuertz, S.; Mongkolsuk, S.; Sirikanchana, K. Capsid Integrity Quantitative PCR to Determine Virus Infectivity in Environmental and Food Applications – A Systematic Review. *Water Res X* **2021**, *11*, 100080, doi:10.1016/j.wroa.2020.100080.
174. Lamhoujeb, S.; Fliss, I.; Ngazoa, S.E.; Jean, J. Evaluation of the Persistence of Infectious Human Noroviruses on Food Surfaces by Using Real-Time Nucleic Acid Sequence-Based Amplification. *Appl Environ Microbiol* **2008**, *74*, 3349–3355, doi:10.1128/AEM.02878-07.
175. Dancho, B.A.; Chen, H.; Kingsley, D.H. Discrimination between Infectious and Non-Infectious Human Norovirus Using Porcine Gastric Mucin. *Int J Food Microbiol* **2012**, *155*, 222–226, doi:10.1016/j.ijfoodmicro.2012.02.010.
176. Raymond, P.; Paul, S.; Guy, R. Impact of Capsid and Genomic Integrity Tests on Norovirus Extraction Recovery Rates. *Foods* **2023**, *12*, 826, doi:10.3390/foods12040826.
177. Randazzo, W.; Khezri, M.; Ollivier, J.; Le Guyader, F.S.; Rodríguez-Díaz, J.; Aznar, R.; Sánchez, G. Optimization of PMAxx Pretreatment to Distinguish between Human Norovirus with Intact and Altered Capsids in Shellfish and Sewage Samples. *Int J Food Microbiol* **2018**, *266*, 1–7, doi:10.1016/j.ijfoodmicro.2017.11.011.
178. Leifels, M.; Jurzik, L.; Wilhelm, M.; Hamza, I.A. Use of Ethidium Monoazide and Propidium Monoazide to Determine Viral Infectivity upon Inactivation by Heat, UV- Exposure and Chlorine. *Int J Hyg Environ Health* **2015**, *218*, 686–693, doi:10.1016/j.ijheh.2015.02.003.
179. Estes, M.K.; Ettayebi, K.; Tenge, V.R.; Murakami, K.; Karandikar, U.; Lin, S.C.; Ayyar, B.V.; Cortes-Penfield, N.W.; Haga, K.; Neill, F.H.; et al. Human Norovirus Cultivation in Nontransformed Stem Cell-Derived Human Intestinal Enteroid Cultures: Success and Challenges. *Viruses* **2019**, *11*, doi:10.3390/V11070638.
180. Alvarenga, V.O.; Brito, L.M.; Lacerda, I.C.A. Application of Mathematical Models to Validate Emerging Processing Technologies in Food. *Curr Opin Food Sci* **2022**, *48*, 100928, doi:10.1016/j.cofs.2022.100928.

181. *UNI EN ISO 15216-1:2017 of the Food Chain - Horizontal Method for Determination of Hepatitis A Virus and Norovirus Using Real-Time RT-PCR - Part 1: Method for Quantification*; 2017;
182. Analysis of the European Baseline Survey of Norovirus in Oysters. *EFSA Journal* **2019**, *17*, doi:10.2903/j.efsa.2019.5762.
183. Pandiscia, A.; Lorusso, P.; Manfredi, A.; Sánchez, G.; Terio, V.; Randazzo, W. Leveraging Plasma-Activated Seawater for the Control of Human Norovirus and Bacterial Pathogens in Shellfish Depuration. *Foods* **2024**, *13*, 850, doi:10.3390/foods13060850.
184. Fu, S.; Wang, Q.; Zhang, Y.; Yang, Q.; Hao, J.; Liu, Y.; Pang, B. Dynamics and Microevolution of Vibrio Parahaemolyticus Populations in Shellfish Farms. *mSystems* **2021**, *6*, doi:10.1128/MSYSTEMS.01161-20.
185. Torresi, M.; Sperandii, A.; Ricci, L.; Prencipe, V.; Migliorati, G.; Pomilio, F. Detection and Characterisation of Potentially Pathogenic Species of Vibrio in the Vibrata River, Abruzzo Region, Italy. *Vet Ital* **2018**, *54*, 125–135, doi:10.12834/VetIt.759.3673.2.
186. Mancini, M.E.; Alessiani, A.; Donatiello, A.; Didonna, A.; D'Attoli, L.; Faleo, S.; Occhiochiuso, G.; Carella, F.; Di Taranto, P.; Pace, L.; et al. Systematic Survey of Vibrio Spp. and Salmonella Spp. in Bivalve Shellfish in Apulia Region (Italy): Prevalence and Antimicrobial Resistance. *Microorganisms* **2023**, *11*, doi:10.3390/microorganisms11020450.
187. Richards, G.P. Shellfish-Associated Enteric Virus Illness: Virus Localization, Disease Outbreaks and Prevention. In *Viruses in Foods*; Springer International Publishing: Cham, 2016; pp. 185–207.
188. Campos, C.J.A.; Lees, D.N. Environmental Transmission of Human Noroviruses in Shellfish Waters. *Appl Environ Microbiol* **2014**, *80*, 3552–3561, doi:10.1128/AEM.04188-13.
189. McLeod, C.; Polo, D.; Le Saux, J.; Le Guyader, F.S. Depuration and Relaying: A Review on Potential Removal of Norovirus from Oysters. *Compr Rev Food Sci Food Saf* **2017**, *16*, 692–706, doi:10.1111/1541-4337.12271.
190. Iritani, N.; Kaida, A.; Abe, N.; Kubo, H.; Sekiguchi, J.-I.; Yamamoto, S.P.; Goto, K.; Tanaka, T.; Noda, M. Detection and Genetic Characterization of Human Enteric Viruses in Oyster-Associated Gastroenteritis Outbreaks between 2001 and 2012 in Osaka City, Japan. *J Med Virol* **2014**, *86*, 2019–2025, doi:10.1002/jmv.23883.
191. Polo, D.; Varela, M.F.; Romalde, J.L. Detection and Quantification of Hepatitis A Virus and Norovirus in Spanish Authorized Shellfish Harvesting Areas. *Int J Food Microbiol* **2015**, *193*, 43–50, doi:10.1016/j.ijfoodmicro.2014.10.007.
192. *COMMISSION IMPLEMENTING REGULATION (EU) 2019/ 627 - of 15 March 2019 - Laying down Uniform Practical Arrangements for the Performance of O fficial Controls on Products of Animal Origin Intended for Human Consumption in Ac cordance with Regulation (EU) 2017/ 625 of the European Parliament and of the Cou ncil and Amending Commission Regulation (EC) No 2074 / 2005 as Regards Official Controls;*
193. *COMMISSION REGULATION (EC) No 1441/2007 of 5 December 2007 Amending Regulation (EC) No 2073/2005 on Microbiological Criteria for Foodstuffs (Text with EEA Relevance);*
194. Fehrenbach, G.W.; Murphy, E.; Pogue, R.; Carter, F.; Clifford, E.; Major, I.; Rowan, N. Pulsed Ultraviolet (PUV) Disinfection of Artificially Contaminated Seawater Seeded with High Levels of Pathogen Disease Indicators as an Alternative for the Shellfish Industry Depuration Systems. *Environmental Science and Pollution Research* **2023**, *30*, 70771–70782, doi:10.1007/s11356-023-27286-6.
195. Kulawik, P.; Kumar Tiwari, B. Recent Advancements in the Application of Non-Thermal Plasma Technology for the Seafood Industry. *Crit Rev Food Sci Nutr* **2019**, *59*, 3199–3210, doi:10.1080/10408398.2018.1510827.
196. Cuevas-Ferrando, E.; Pérez-Cataluña, A.; Falcó, I.; Randazzo, W.; Sánchez, G. Monitoring Human Viral Pathogens Reveals Potential Hazard for Treated Wastewater Discharge or Reuse. *Front Microbiol* **2022**, *13*, doi:10.3389/fmicb.2022.836193.
197. Simmons, F.J.; Xagoraraki, I. Release of Infectious Human Enteric Viruses by Full-Scale Wastewater Utilities. *Water Res* **2011**, *45*, 3590–3598, doi:10.1016/j.watres.2011.04.001.
198. Farkas, K.; Marshall, M.; Cooper, D.; McDonald, J.E.; Malham, S.K.; Peters, D.E.; Maloney, J.D.; Jones, D.L. Seasonal and Diurnal Surveillance of Treated and Untreated Wastewater for Human Enteric Viruses. *Environmental Science and Pollution Research* **2018**, *25*, 33391–33401, doi:10.1007/s11356-018-3261-y.

199. Sano, D.; Amarasiri, M.; Hata, A.; Watanabe, T.; Katayama, H. Risk Management of Viral Infectious Diseases in Wastewater Reclamation and Reuse: Review. *Environ Int* **2016**, *91*, 220–229, doi:10.1016/j.envint.2016.03.001.
200. Ramírez-Castillo, F.; Loera-Muro, A.; Jacques, M.; Garneau, P.; Avelar-González, F.; Harel, J.; Guerrero-Barrera, A. Waterborne Pathogens: Detection Methods and Challenges. *Pathogens* **2015**, *4*, 307–334, doi:10.3390/pathogens4020307.
201. Brouwer, A.F.; Masters, N.B.; Eisenberg, J.N.S. Quantitative Microbial Risk Assessment and Infectious Disease Transmission Modeling of Waterborne Enteric Pathogens. *Curr Environ Health Rep* **2018**, *5*, 293–304, doi:10.1007/s40572-018-0196-x.
202. Randazzo, W.; Khezri, M.; Ollivier, J.; Le Guyader, F.S.; Rodríguez-Díaz, J.; Aznar, R.; Sánchez, G. Optimization of PMAxx Pretreatment to Distinguish between Human Norovirus with Intact and Altered Capsids in Shellfish and Sewage Samples. *Int J Food Microbiol* **2018**, *266*, 1–7, doi:10.1016/j.ijfoodmicro.2017.11.011.
203. López-Gálvez, F.; Truchado, P.; Sánchez, G.; Aznar, R.; Gil, M.I.; Allende, A. Occurrence of Enteric Viruses in Reclaimed and Surface Irrigation Water: Relationship with Microbiological and Physicochemical Indicators. *J Appl Microbiol* **2016**, *121*, 1180–1188, doi:10.1111/jam.13224.
204. Canh, V.D.; Liu, M.; Sangsanont, J.; Katayama, H. Capsid Integrity Detection of Pathogenic Viruses in Waters: Recent Progress and Potential Future Applications. *Science of The Total Environment* **2022**, *827*, 154258, doi:10.1016/j.scitotenv.2022.154258.
205. Costantini, V.; Morantz, E.K.; Browne, H.; Ettayebi, K.; Zeng, X.L.; Atmar, R.L.; Estes, M.K.; Vinjé, J. Human Norovirus Replication in Human Intestinal Enteroids as Model to Evaluate Virus Inactivation. *Emerg Infect Dis* **2018**, *24*, 1453–1464, doi:10.3201/EID2408.180126.
206. Overbey, K.N.; Zachos, N.C.; Coulter, C.; Jacangelo, J.; Schwab, K.J. Recovery of Infectious Human Norovirus GII.4 Sydney From Fomites via Replication in Human Intestinal Enteroids. *Front Cell Infect Microbiol* **2021**, *11*, doi:10.3389/FCIMB.2021.693090.